Subspace based data-driven designs of fault detection systems

von der Fakultät für Ingenieurwissenschaften der

Universität Duisburg-Essen

Abteilung Elektrotechnik und Informationstechnik

zur Erlangung des akademischen Grades eines

Doktor-Ingenieurs

genehmigte Dissertation

von

Amol Subodh Naik

aus

Mumbai, Indien

1. Gutachter: Prof.-Ing. Steven X. Ding
2. Gutachterin: Prof. Sirkka-Liisa Jämsä-Jounela

Tag der Mündlichen Prüfung: 13.12.2010

Acknowledgement

This thesis is incomplete without the effort and support of Prof. Dr.-Ing. Steven. X. Ding, who believed in me and offered me to work in AKS as a research student and then as an academic staff member. His scholarly guidance and insightful discussions have led the foundation of this research work.

I would also like to thank Dr.-Ing. Ping Zhang, who helped me initiate this research, and Dipl.-Ing. Stefan Schneider who has been more of a friend than a colleague. I have extensively worked with M.Sc. Shen Yin. I wish him all the very best for his doctoral studies. I also thank Dr.-Ing. Guojun Yang for his friendly discussions on various topics.

My sincere thanks to Dipl.-Ing. Andreas de Moll, Dipl.-Ing. Georg Nau and Dipl.-Ing. Jonas Esch for wonderful camaraderie. I give my best wishes to M.Sc. Adel Haghani for his research work and sincerely acknowledge his help in various assignments. My thanks to Dr.-Ing. Cristian Chihaia for his help on several occasions pertaining to using software platforms.

The guidance provided by Dipl.-Ing. Eberhard Goldschmidt and Dr.-Ing. Birgit Köppen-Seliger in technical writing and presentation has been invaluable. My acknowledgement will be incomplete without thanking Mrs. Sabine Bay for her help in organizational responsibilities. I would like to mention Dipl.-Ing. Klaus Göbel and Mr. Uwe Janssen for their unfaltering technical support. I extend my gratitude towards M.Sc. Waseem Damlakhi, M.Sc. Abdul Qayyum Khan, M.Sc. Ali Abdo, M.Sc. Jedsada Saijai, and M.Sc. Wei Chen for their timely suggestions, help and assistance.

Finally, I would like to dedicate this work to my parents, Mr. Subodh Naik and Mrs. Nutan Naik. Their unconditional support and unexplainable faith were the only reason for the completion of this work. With the same sentiment, I also dedicate this work to my sister, Mrs. Kavita Beyer-Ogale and to my wife Mrs. Manali Prabhu-Naik.

II

Contents

List of Figures

List of Tables

List of symbols

Mathematical symobols

$\|\|\|\|_2$	2-norm
$\hat{a}$	Estimate of a
a^T	Transpose of a
$a^{\perp}$	Orthogonal complement of a
$a^{\dagger}$	Pseudoinverse of a
$\in$	belongs to
$\mathbf{R}$	Set of real numbers
$\mathbf{R}^n$	Set of n-dimensional real vectors
$\mathbf{R}^{n \times m}$	Set of $n \times m$ dimensional real matrices
$I_{m \times m}$	$m \times m$ identity matrix
$O_{m \times m}$	$m \times m$ zero matrix
λ	Eigenvalue
σ	Singular value
Σ	Matrix of singular values
U	Matrix of left singular vectors
V	Matrix of right singular vectors

Control theoretical symbols

n	Model order
t	Continuous time
k	Discrete time
A	System matrix
B	Input matrix
C	Output matrix
D	Feed-though matrix
E_d	Disturbance matrix
F_d	Disturbance feed-through matrix
E_f	Process fault distribution matrix

F_f	Sensor fault distribution matrix
l	Number of inputs
m	Number of outputs
u	Input signal
y	Output signal
w	Process disturbance
v	Sensor noise
d	Unknown disturbance
f	Fault signal
f_{sen}	Sensor fault
f_{act}	Actuator fault
r	Residual signal
r_{ev}	Evaluated residual signal
Γ_s	Extended observability matrix
$H_{u,s}$	Input distribution matrix
$\Gamma_s^{\perp}$	Left null complement
Y_f	Future output Hankel matrix
U_f	Future input Hankel matrix
Y_p	Past output Hankel matrix
U_p	Past input Hankel matrix
N	Length of sample size
s	Observability index
v_s	Parity vector corresponding to output
ρ_s	Parity vector corresponding to input
L_o	Observer gain
L_{kf}	Kalman filter gain
J_{th}	Threshold value for fault detection
α	Forgetting factor

Statistical symbols

Φ_{aa}	Sample variance of a
Φ_{ab}	Sample covariance of a and b
χ^2	Chi-square distribution

Chapter 1

Introduction

Product quality, economic operation and over-all safety are the most important factors in process design, be it chemical plants, automotive systems or even modern power plants. To ensure safe and economic run of any process, continuous monitoring of it is essential. Any malady must be attended to as soon as possible before the whole process gets affected by it and halts the operation. In a survey in U.S.A., it was found that petro-chemical industry incurs approximately $20 Billion per year due to process abnormalities [103]. But the good news is that these huge losses can be averted by amending the scope for process monitoring [87].

The potential to improve the economy and safety of process operation depends upon good use of instrumentation and monitoring. This requirement has sparked tremendous research efforts in the last few decades in the era that followed modern control theory [56]. Any process monitoring system attempts to track actual process operation with the help of available information. It is then reproduced on graphs, plots or large screen displays whereby deviations from normal operating regions can be easily analyzed and localized for their occurrence.

The success of any process monitoring scheme lies in its design parameters which depend on the application itself. For instance, in a semiconductor manufacturing process, it is important to detect anomaly within the range of nanometers, whereas a nuclear reactor must be observed in real-time and therefore failures must be detected extremely fast, perhaps within nanoseconds. These stringent operational constraints have challenged the design engineers to come up with superior and robust monitoring systems. This chapter attempts to encompass some of the major developments in this field.

1.1   Fault diagnosis

Last three decades have seen tremendous developments in the field of fault detection and diagnosis (FDD). A field that was initially seen as an application area related to signal processing, filter and control system design, now boasts over hundreds of yearly contributions in conferences and in journals. During these years, FDD has expanded to become an independent stream of studies and research [18], [37], [40], [54]. In this section, fault and associated terms are defined and a chronological overview of the developments in the field of FDD is presented.

A **fault** is basically any unwarranted discrepancy from the 'normal' behavior of a plant, where a plant is any static or dynamic, linear or nonlinear, deterministic or stochastic system. A fault diagnosis system, as the name suggests, is a system that 'observes' the plant for its normal behavior. It must bring any discrepancy to the attention of the plant operator, so that a corrective action can be taken, manually or automatically. A complete fault diagnosis system will consist of following three blocks [36]:

Fault detection: detection of undesired malfunctioning of one of the system's functional components

Fault isolation: localization of different faults

Fault identification: estimation of the magnitude and the time of occurrence of the fault

Depending on the functionality, the system is either called FD (fault detection) or FDI (fault detection and isolation, or FDIA (fault detection, isolation, and analysis).

The terms can be explained based on an example of a chemical plant. For instance, three types of faults are most likely to occur in a chemical process:

- **Process parameter changes:** catalyst poisoning, heat exchanger fouling, etc.

- **Sensor faults:** biased pH measurements, analyzer contamination, etc.

- **Actuator faults:** faulty pumps, partial closing of valves, or blocking in pipes, etc.

These faults can not only harm the functional units, but also the entire process through the control loops and feedback systems. Traditionally, an experienced human operator will be required to detect any anomalous
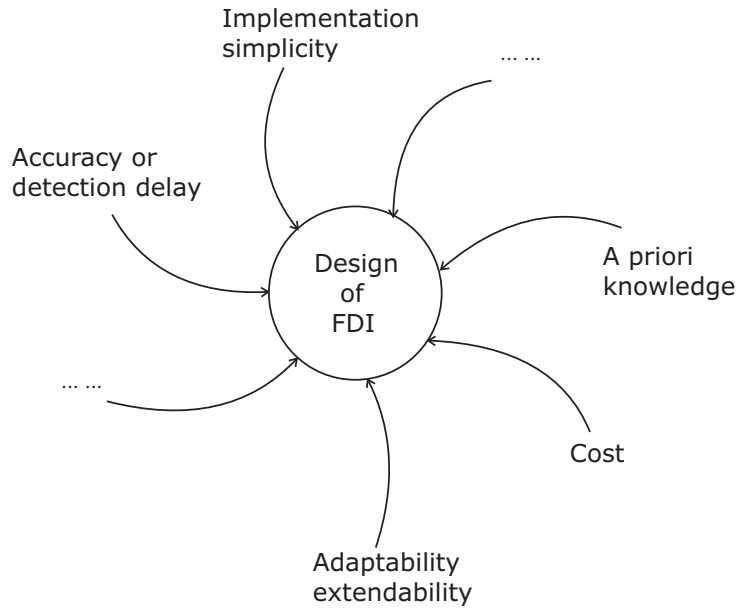
Figure 1.1: Design parameters in FDD

behavior and bring the system back to its normal working condition. But nowadays, FDD systems are capable enough to do the same job with quicker response time. Moreover, these systems do not require process experience for operation and have higher reliability compared to humans. In the next subsections, a few conventional as well as advanced methods of fault detection are described.

1.2 Classification of approaches

A fault in any component of a 'running' system can be detected if it is possible to compare system's actual behavior with its nominal. In technical terms, a 'redundant' device that can perfectly, or even roughly replicate the nominal behavior of the system under consideration is all that is required. There are three most important ways to create 'redundant' system and compare behaviors, namely hardware redundancy, signal processing based, and analytical redundancy [36].

- **Hardware redundancy:** The crucial components in the process are reconstructed using identical hardware. If the operating components fail to deliver the desired performance, the 'stand-by' component is switched in. This approach is extremely reliable and allows direct fault localization and isolation. But its application is restricted to critical

processes such as nuclear reactors, aeroplanes because of higher cost involved in reconstructing.

- **Signal processing based approach:** Measurement signals carry vital information about the actual behavior of the plant. Furthermore, time or frequency domain based tools (processing) can generate important features that are easy to analyze. Typical features of signals for monitoring purpose are its limiting values, statistical moments, power spectra, cepstrum, etc..

- **Analytical redundancy:** The idea behind this approach is to design a model of process. The model can either be quantitative (i.e. based on first principles), qualitative (based on if-then-else rules, decision tree, etc.) or data-driven (process history based). The process behavior can be reconstructed on-line with the help of this model. The difference between estimated and actual behavior gives very good indication of the 'health' of the process.

The selection of a suitable monitoring approach depends upon the application in the first place, the nature of the application, and its criticality. Furthermore, the control architecture requires that the information produced by monitoring system to be fed back in a specific format, so that the system continues to operate despite of the faulty components or is fault-tolerant. There are additional design consideration as well, for instance computation speed, detection delay. A rough sketch of these considerations is shown in Fig.(1.1).

Since the thesis mainly revolves around analytical model-based approach, it is described in details in the following sections. The chronological development in this field is represented in Fig.(1.2).

1.3   Quantitative model-based approach

Broadly, the analytical redundancy based approaches can be divided in three categories: quantitative models, qualitative models, and process history based or so-called data-driven methods [103]. In 1971, Beard [5] and Jones [59] presented the first ever failure detection scheme based on an observer. The contribution spurred rapid development but the thrust always remained on the mathematical knowledge of the process in question [7], [18], [35], [59], [90]. In the 80s, Chow and Willsky presented radically different approach, called parity space [15]. A seemingly simple idea that compresses the model parameters in a vector space which is ultimately used to detect process faults.
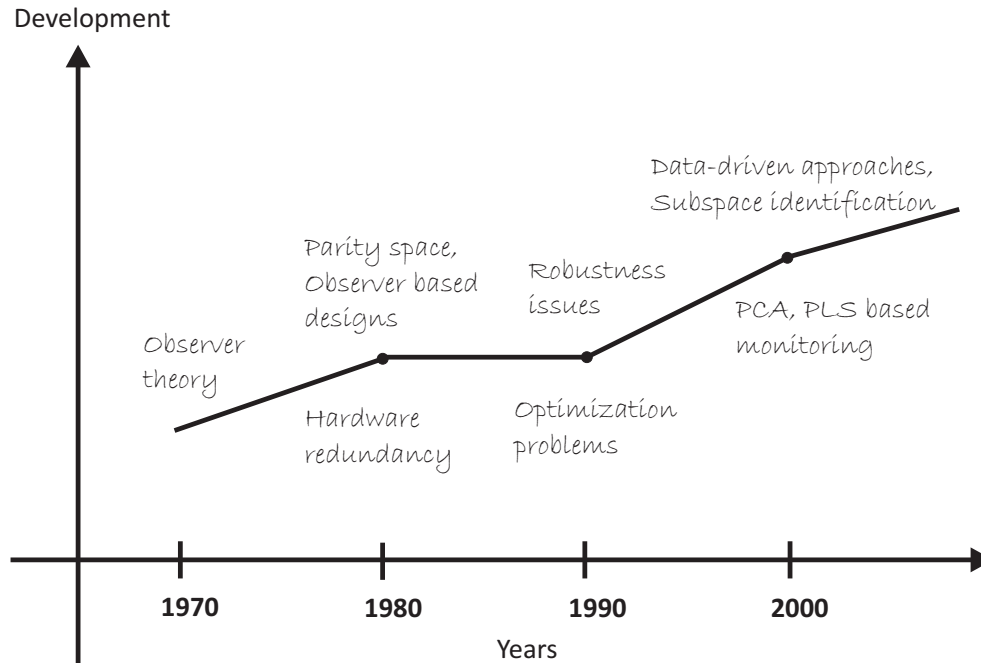
Figure 1.2: Chronology of FDD development

In the 90s, Isermann proposed parametric approach towards design of static and dynamic model building [52], [53].

Based on these three approaches, advanced process diagnostic methods were developed, wherein the issues such as the effect of uncertain model parameters and unnecessary disturbances were handled [30], [35], [41]. Robust fault detection systems were developed parallel to the developments in robust control theory [8], [12]. Optimization of the designs was also addressed as an important issue. For instance, in the 90s, several algorithms were proposed to select filter gains, vector spaces, and various other design parameters of the FD systems [36]. To this end, linear matrix inequality (LMI) based solutions were proven to be very effective solutions, for instance in complex systems such as networked systems [18], [71].

As the processes became more complex, the mathematical modeling of these systems became more clumsy. Therefore, the FDI system could not be designed from just the first principle based modeling alone. Thus an alternative to identify the system based on its data came into the picture [97], [105]. The past decade is mainly dominated by such model identification or data-driven methods to design monitoring schemes. The discussion on this topic is postponed to a separate section the next chapter.
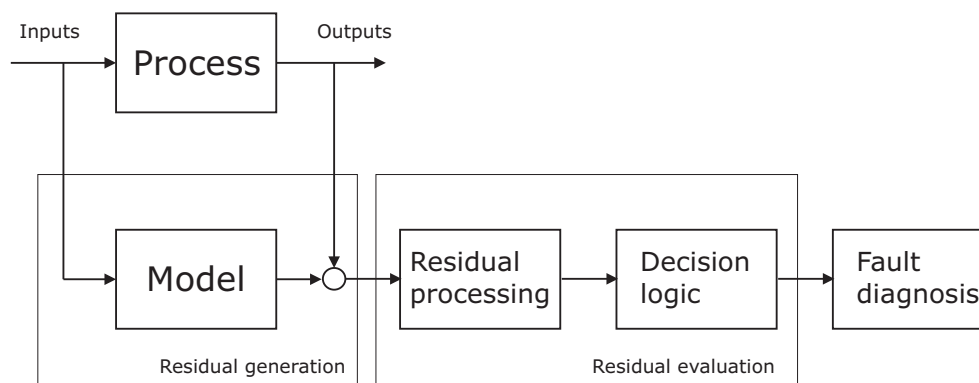
Figure 1.3: Basic model-based FDD scheme

1.4   Qualitative model-based approach

Qualitative models are extensively used for fault diagnosis more than for fault detection. Any diagnostic strategy requires a priori knowledge about the process and an effective search mechanism. The knowledge representation can be classified in two broad classes namely, causal models and abstraction hierarchy. Causal models store information about the process in simple IF-THEN-ELSE rules that mimic human experts. Diagraphs or directed graphs are also used to represent cause-effect relationship within the process.

Basically, the main aim is to design an expert system integrated with an inference engine to correctly indicate process state. Inference engines are designed on topological structure of the entire system or in an abstract sense depending on the symptoms leading to a particular hazard. Conceptually, reliability analysis of a system is also quite similar to failure detection, although done off-line many a times. There, the so called fault-trees are designed that link an event with a possible hazard.

The qualitative models find their applications in large systems that are difficult to model based on first principles. But they suffer from one important drawback. The models are only as good as the knowledge of the perso designing it, and quite often its representation makes it difficult to update or accommodate new rules. Therefore, these models are sometimes referred to as 'shallow' [97]. More discussion on this specialized topic is found in the survey by Venkatasubramanian et al. [104] and the references therein.

1.5 Data-driven approach

Any diagnostic strategy requires reliable *a priori* knowledge about the process. The data-driven approaches make use of this information in terms of process logs, routine measurements, and book-keeping. There are both parametric and nonparametric methods to extract diagnostic information about the process behavior [105]. Depending on the nature of the data, these methods are sometimes also called statistical methods.

Bayesian classifier is possibly the earliest parametric statistical approach which makes use of *a priori* knowledge such as probability density functions. A neural network is also a form of parametric data-driven approach, whereby a weight node is a function of the hidden layers [57], [63]. There are many applications based on these two techniques concerning fault isolation and classification. Integrating process monitoring with quality control, Shewhart [98] came up with an innovative way, where he described that a process under control, which is subjected to its natural variability, remains inside desired performance 'limits.'

Based on it, the so-called Shewhart control charts are developed, which are recognized to be one of the most robust monitoring tools in single variate statistical methods. Page [89] developed a cumulative sum based approach to detect abrupt changes as well as its time of occurrence and magnitude. The popularity of process monitoring led to the founding of an independent stream of studies, called statistical process control which is sometimes intervened with the process monitoring. Under the new stream, statistical analysis based algorithms are extended to large scale plants.

Another faculty of data-driven approaches studies the underlying trends in the data as time-series. The process under control is assumed to have certain probability density function. It changes when the process is disturbed by an unknown parameter or a failure. Based on it, Basseville and Nikiforov [2] developed an on-line change detection method depending on the observations up to the current time. Apart from being simple, these approaches are dedicated ones to detect anomalous behavior and malfunctions [1].

After the success of single variate control charts, efforts were put together to develop multivariate statistical approaches. A major concern with such methods was the compressibility of huge chunks of measured data. Here, the principal component analysis (PCA), arguably the most successful algorithm, developed by Hotelling [49], later extended by Pearson [91], appeared to be extremely suitable for monitoring. See e.g. [26], [34], [65], [93], [117]. Since then, PCA is included in every textbook on process monitoring, and is a standard solution to reduce large dataset without loosing valuable information about process variance.

Similar to PCA, partial least squares (PLS) is also one of the popular approaches in the statistical field. It is also a compression technique, but unlike PCA, PLS correlates most dominant process inputs to the outputs and extracts a parametric model [48], [79], [80]. It has resemblance to the least square solution and hence derives its name. PLS is also extensible to the large-scale, multi-batch processes [39]. For transient behavior, the dynamic versions of both PCA and PLS are also available that take into account serial as well as temporal correlations amongst the measured variables [11], [64], [66].

Combined approach: System identification

The modern day plant architectures have made it almost difficult to run hand in hand with model based control and monitoring tools. It is because of the primary reason that these algorithms require *a priori* knowledge about the process to be represented in a particular form, for instance state space models. Therefore, it becomes the need of the hour to extend and combine peripheries of model-based and statistical tools to accommodate large-scale and complex processes. This issue has gained attention ever since statistical analysis successfully merged with system theory, especially in estimation, filtering, and identification.
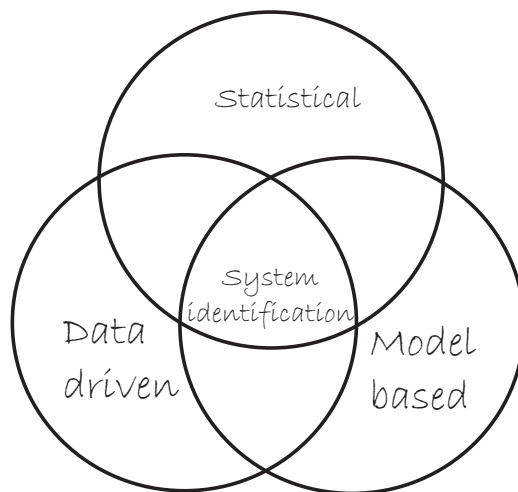
Figure 1.4: System identification: independent research stream

Besides, the first principle based modeling techniques suffer from a major drawback. Usually, if process parameters vary stochastically, the model is uncertain with respect to time. Many industrial systems exhibit this behavior,

thereby limiting the performance of linear or 'linearized' models. As a solution, researchers have recommended combination of statistical approaches to enhance the performance of control and diagnostic algorithms. As an example, in the quantitative model-based FDD approaches, the information engines or decision logic are usually statistical, to reduce the influence of uncertainties.

Relating this concept to the work presented here, the basic idea is to combine process history based approaches with statistical and model based approaches. The aim is to design a compact, identification-oriented FDD system. Moreover, the focus is on the recent advances in consistent subspace based model identification technique, which extracts causal relationship between input and output from measured data. It is also interesting to see its statistical interpretation, wherein the commonality is stressed by the use of tools such as eigenvalue decomposition.
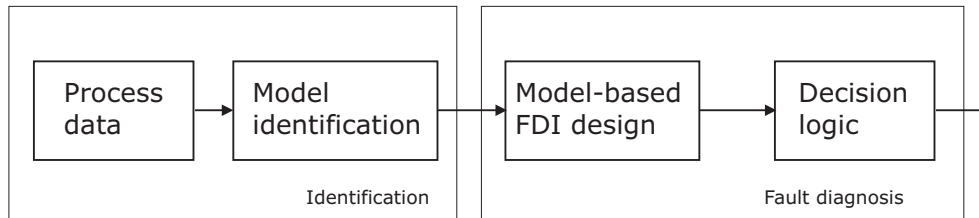
Figure 1.5: Subspace identification based FDD

As a product, the identified model can be used for control or monitoring purpose. See e.g. [60], [86], [94], [101]. The design procedure is shown in the block diagram in Fig.(1.5). This two step approach extends the features of classic model based techniques such as feedback loops, robustness, or sensitivity analysis. For the FDD, the design steps can be further reduced by identifying only what is important. Depending on the application, it can also be called "FDD-oriented identification," which also forms the crux of the work here.

1.6 Motivation and objective

As can be seen from Fig.(1.5), the design of the analytical redundancy based FDD system consists of three steps: (a) identification of model, (b) design of model-based FDD system, (c) on-line implementation of FDD system. But in the work presented here an alternative approach has been taken. It is considering following important issues in the practical situations:

- a complex plant entails tremendous efforts in developing mathematical model for design of control or monitoring systems. The FDD approach that is presented here is motivated by this constraint and attempts to minimize off-line design time.

- modern technical systems consists of several number of sensors and measurement devices, putting severe limitation on the on-line memory storage for further applications and computations. The FDD system must therefore be efficiently designed with minimal computation and storage requirements.

- Often, during the modeling and design stage of control and monitoring systems, knowledge from the plant operators, technicians is required. Also, the implementation of systems needs imparting training on operators and concerned personnel. In the approach presented here, the analytical issues, during both off-line and on-line stages, are simplified so that minimal theoretical knowledge about the plant and mathematical tools is required to specified by the user.

The main assumption held in this study is that the knowledge about the underlying mathematical model of the plant is unavailable or very limited. The objective is to design an efficient fault detection and diagnosis system without identifying the complete mathematical model. The procedure must be restricted to only those parameters which are required by the FDD system. More specifically, the problems that are dealt in this work are stated as follows:

- Assuming that very little knowledge about the plant's mathematical model is available, develop a data-driven design algorithm for efficient fault detection and diagnosis system. While doing so, only the important set of parameters may be identified, without requiring the entire model of the plant.

- Since the plant's parameters are likely to vary around their nominal values, the FDD system must have scope for possible adaptation. The adaptive design must consider on-line storage and computation constraints, especially while dealing with large-scale processes.

- As a part of developing a framework for such FDD-oriented design methodology, the basic algorithm must also solve optimal identification problem. The numerical computation during the design phase must be efficiently implemented considering practical issues.

- The final step of the design work must also include design for bench-mark plant models. The benchmark should be good approximation of complex, large-scale industrial processes.

For the design of the scheme, the data gathered from measurements of various process variables can be used. It is either available as process logs or can be obtained from experimental tests. If a plant simulator is available, then the data gathered from such simulations is also useful. In this case, issues regarding process disturbances and stochastic uncertainties are important and may require special attention.

1.7 Organization of chapters

The chapters are organized assuming that the reader is familiar with linear algebra, control theory, and basic statistical tools. The second chapter provides description of technical systems with notations that are frequently used in the forthcoming chapters. A brief section discusses subspace identification method as its implications are found in the novel data-driven design presented in the third chapter. The most popular model-based fault detection systems such as parity space and diagnostic observers are also discussed therein. The basic idea of statistical process monitoring systems is explained in the concluding section.

In the third chapter, the novel design scheme is introduced that identifies minimal parameter set to design an observer based fault detection system. The closed-loop design of observer is also provided wherein Kalman filter gain is identified only by using the process data. A novel data-driven fault isolation scheme for sensor and actuator is presented. The design method is also extended to soft-sensing application. This part of the work is largely based on earlier publications. See e.g. [19], [20], [83].

Fourth chapter discusses the issue of uncertain parameter variation in plants often due to changes in operating conditions. To deal with it, two adaptive designs of fault detection systems are proposed based on recursive identification. Considering the constraints on on-line computation and memory usage, the algorithm efficiently updates the so-called primary residual generator. A comparative analysis of these algorithms and a demonstrative example are also provided.

In the fifth chapter, optimal identification based design of data-driven fault detection system is studied. To this end, non-orthogonal projection technique is applied to estimate optimal primary residual generator. The algorithm is numerically stabilized and the computation cost is minimized with

the help of QR based decomposition technique. The results are compared with other popular techniques with the help of a demonstrative example.

The sixth chapter provides application aspects of the algorithms developed in chapter 3, 4, and 5. For this task, two industrial plants, Tennessee Eastman process and continuously stirred tank heater are considered. The experiments are carried out under scenarios involving different types of faults such as sensor faults or process parameter deviations. In the last chapter, qualitative summary and future scope of the work is discussed. For simplicity in reading, the organization of chapters is also shown in Fig.(1.6) on the following page.
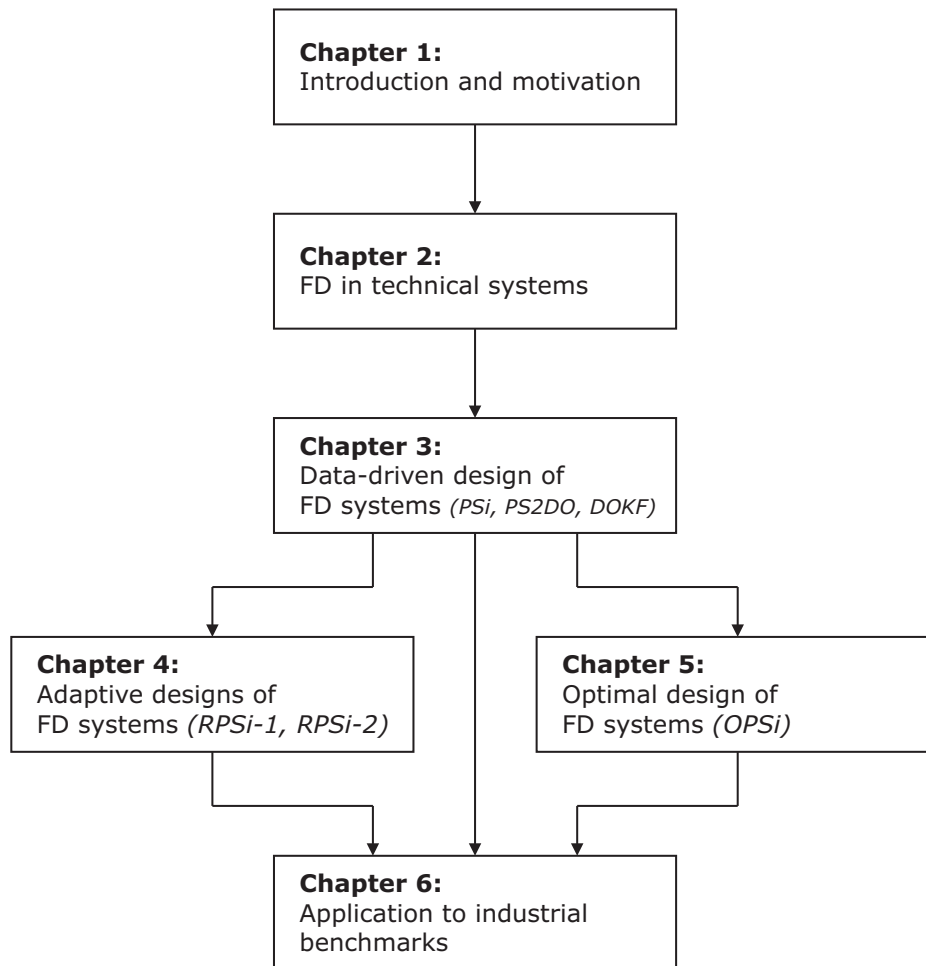
Figure 1.6: Organization of chapters

Chapter 2

Fault diagnosis in technical systems

In broad terms, FDD is basically about process redundancy, i.e. to create a "model" of the process under consideration that can predict its behavior as precisely as possible. Then it is a simple question of comparing the actual values taken from the plant with that from its model. For the technician or plant operator, any significant deviation should suffice to indicate a fault or a failure depending on the nature of abnormality.

The literature on the FDD terminology is abundant [18], [52] and references therein. The most primitive form of detecting a change is by means of limit-checking. The measured outputs, for instance, temperature, pressure, flows are compared with their specified limits and an alarm is set off, if the limits are exceeded. This is a simple and reliable method but suffers many drawbacks. For instance, each measured quantity is observed independently which is extremely difficult for complex processes with hundreds of measurements. To set off an alarm, significant deviation is required, unless technicians are capable enough to anticipate from minute changes [97].

With rapid development in process instrumentation, the task to devise limit-checking based monitoring became infeasible. The mathematical models running on central computer station became easier alternative for fault detection and diagnosis [18], [40]. The most crucial part of this scheme was the modeling for analytical redundancy. These models were developed through rigorous approaches, e.g. via first principles. In the first part of this chapter, the focus is mainly on such model-based FDD schemes, their main features and inter-relations.

Complex industrial processes, such as a petroleum refinery or waste water treatment plant, pose challenging modeling tasks. For these applications often models are directly identified from the plant's historical data. This so-

called training data often consists of sensor and actuator measurements, logs of important events as well as changes in the key process parameters [105]. This approach, which is referred to as process history based, is discussed in the latter part of this chapter.

2.1   Description of technical systems

In this thesis, a linear time invariant (LTI) system is assumed as good starting point for modeling and design phase. The nominal behavior of it in discrete time (DT) is best described by following state space model:

$$x_{k+1} = Ax_k + Bu_k \tag{2.1}$$
$$y_k = Cx_k + Du_k \tag{2.2}$$

where $x \in \mathbf{R}^n$ is the state vector with x_0 as the initial condition of the system, $u \in \mathbf{R}^l$ is the input vector, $y \in \mathbf{R}^m$ is the output vector. The quadruplet $\{A, B, C, D\}$ is a set of real, constant matrices of appropriate dimensions. The transfer function of the model in Eq.(2.1)-(2.2) can be written in Z-domain as:

$$y(z) = G_{yu}(z) u(z) \tag{2.3}$$

where $G_{yu}(z) = C(zI - A)^{-1}B + D$. Note that technical systems are often continuous time systems, but since the work carried out in this thesis deals with discrete or sampled-data systems, the state space model is defined only in the discrete time domain.

In practical situations disturbances due to surrounding environment or cross-interferences due to other technical systems are inevitable. These effects can be incorporated as an additional variable $d \in \mathbf{R}^{k_d}$ in Eq.(2.1) -(2.2). The augmented state space model can be described as:

$$x_{k+1} = Ax_k + Bu_k + E_d d_k \tag{2.4}$$
$$y_k = Cx_k + Du_k + F_d d_k \tag{2.5}$$

where E_d and F_d are known disturbance distribution matrices. As a special case, stochastic disturbances, process and measurement noise can be defined in the following way:

$$x_{k+1} = Ax_k + Bu_k + w_k \tag{2.6}$$
$$y_k = Cx_k + Du_k + v_k \tag{2.7}$$

where matrices $E_d = I_{n \times n}$, $F_d = I_{m \times m}$, and $I_{i \times i}$ is an identity matrix of order i. The stochastic disturbance signals $w \in \mathbf{R}^n, v \in \mathbf{R}^m$ are often white noise sequences with known mean and standard deviation.

Similar to disturbance, a fault can also be introduced in the modeling of the technical systems. As mentioned in the last chapter, there are three types of faults: sensor, actuator, and process faults. The model in Eq.(2.1)-(2.2) can be extended to incorporate them as:

$$x_{k+1} = Ax_k + Bu_k + E_f f_k \tag{2.8}$$
$$y_k = Cx_k + Du_k + F_f f_k \tag{2.9}$$

where $f \in \mathbf{R}^{k_f}$ is the fault vector and E_f, F_f are fault distribution matrices of appropriate sizes. Generally, the faults are either additive or multiplicative changes in the parameters, and can be modeled by choosing proper values for E_f and F_f.

2.2 State space model identification

The processes can be either modeled as static relation between inputs and outputs or as dynamic relations by including internal states. But owing to the complicated structures and insufficient knowledge of the processes, the job of deriving a model has increasingly gotten more involved. To counter this problem, a specialized branch of system theory has, within a short span of time, developed efficient algorithms which extract models from just the training data [75].

There are two most evolved approaches to identify a system. A simple least square based algorithm can extract parametric relationship between input and output data by minimizing mean squared error [51]. On the other hand, recent work based on linear algebra and statistics can identify state space matrices directly from plant's test dataset. A collection of such methods is called subspace identification methods (SIM) [88]. Since the state space matrices are used in variety of problems including robust control and filter designs, it has gained tremendous attention in industrial applications [31], [32].

As a part of the solutions proposed in this thesis, SIM is briefly elaborated in the next subsection. The approach merges linear algebra, system theory and statistical tools to identify state space matrices from data. It avoids nonlinear search for optimized parameters unlike the classical parameter identification. Instead it directly gives the solution set that satisfies the linear dynamic relationship between the inputs and outputs. Its extensibility to multiple input multiple output (MIMO) systems is its most natural advantage.

2.2.1 Subspace identification method (SIM)

Subspace technique formulates the problem of identifying system relevant matrices as: *"Given the input and output data of a linear dynamic process, identify its state space model."* It is assumed that the plant's data is generated by a discrete LTI system described in Eq.(2.1)-(2.2). It is also assumed that the model order n is unknown *a priori*.

The first step in SIM is the identification of state sequence with the help of extended state space models. To do so, Eq.(2.1)-(2.2) are written recursively as follows:

$$
\begin{aligned}
y_{k-s+1} &= Cx_{k-s+1} + Du_{k-s+1} \\
y_{k-s+2} &= Cx_{k-s+2} + Du_{k-s+2} \\
&= CAx_{k-s+1} + CBu_{k-s+1} + Du_{k-s+2},
\end{aligned}
$$

and so on. Continuing in this way, the output equation at k is written as a function of past states and input:

$$
y_k = CA^{s-1}x_{k-s+1} + CA^{s-2}Bu_{k-s+1} + \cdots + CBu_{k-1} + Du_k. \tag{2.10}
$$

To begin with the identification, the input and output data are collected in the following form:

$$
\begin{aligned}
y_{k,s} &= \begin{bmatrix} y_{k-s+1} & y_{k-s+2} & \cdots & y_k \end{bmatrix}^T \in \mathbf{R}^{sm}, \tag{2.11} \\
u_{k,s} &= \begin{bmatrix} u_{k-s+1} & u_{k-s+2} & \cdots & u_k \end{bmatrix}^T \in \mathbf{R}^{sl} \tag{2.12}
\end{aligned}
$$

where s is a user-defined parameter. They are stacked in block Hankel matrices as

$$
\begin{aligned}
Y_f &= \begin{bmatrix} y_{k,s} & y_{k+1,s} & \cdots & y_{k+s-1,s} \end{bmatrix} \in \mathbf{R}^{sm \times N} \tag{2.13} \\
U_f &= \begin{bmatrix} u_{k,s} & u_{k+1,s} & \cdots & u_{k+s-1,s} \end{bmatrix} \in \mathbf{R}^{sl \times N}. \tag{2.14}
\end{aligned}
$$

There are several SIM based algorithms proposed in the literature. Each of the technique has its own competitive advantages and disadvantages. More discussion on this topic can be found in dedicated literature [88]. For the sake of explaining the technique, only the deterministic case presented in [109] is discussed here. Based on recursive equation in (2.10), the so-called extended state space model can be written as:

$$
Y_f = \Gamma_s X_f + H_{u,s} U_f \tag{2.15}
$$

where

$$
\Gamma_s = \begin{bmatrix} C \\ CA \\ \vdots \\ CA^{s-1} \end{bmatrix}, H_{u,s} = \begin{bmatrix} D & 0 & \cdots & 0 \\ CB & D & \cdots & 0 \\ \vdots & \vdots & \ddots & \vdots \\ CA^{s-2}B & \cdots & CB & D \end{bmatrix}.
$$

To remove the effect of the states, Eq.(2.15) is multiplied from both sides by the orthogonal complement of Γ_s.

$$
\Gamma_s^{\perp} Y_f = \Gamma_s^{\perp} H_{u,s} U_f. \tag{2.16}
$$

Note here that this step is similar to the model-based fault detection approach called as parity space method. Rearranging the above equation gives:

$$
\Gamma_s^{\perp} \begin{bmatrix} I & -H_{u,s} \end{bmatrix} Z_f = O \tag{2.17}
$$

where $Z_f = \begin{bmatrix} Y_f^T & U_f^T \end{bmatrix}$. It is decomposed with the help of SVD as follows:

$$
Z_f = \begin{bmatrix} U_1 & U_2 \end{bmatrix} \begin{bmatrix} \Sigma_1 & O \\ O & \Sigma_2 \end{bmatrix} \begin{bmatrix} V_1^T \\ V_2^T \end{bmatrix}. \tag{2.18}
$$

Now, if the inputs satisfy the persistent excitation condition as specified in [109], Σ_1 contains only $sl+n$ nonzero singular values and $\Sigma_2 = O_{(sm-n)\times(sm-n)}$. Therefore, it is easier to show that

$$
\begin{bmatrix} \Gamma_s^{\perp} \\ H_{u,s}^T \Gamma_s^{\perp} \end{bmatrix} = U_2 M \tag{2.19}
$$

where M is any arbitrary regular matrix. If M is chosen as an identity matrix, then

$$
\Gamma_s^{\perp} \begin{bmatrix} I & H_{u,s} \end{bmatrix} = U_2^T. \tag{2.20}
$$

Equation (2.20) suggests that the model parameters are contained in U_2^T because it spans both $\Gamma_s^{\perp}$ and $H_{u,s}$. The state space matrices are extracted as described in the next subsection.

2.2.2   Identification of state space matrices

To identify the state space matrices, only the two subspaces: extended observability space, Γ_s and extended input distribution matrix $H_{u,s}$ are required. It can be extracted as follows:

$$
\Gamma_s = U_{2,y}^{\perp} \tag{2.21}
$$
$$
-U_{2,y}^T H_{u,s} = U_{2,u}^T. \tag{2.22}
$$

Rearrange Eq.(2.21) gives,

$$-U_{2,y}^T = \begin{bmatrix} \Phi_1 & \Phi_2 & \cdots & \Phi_s \end{bmatrix} \tag{2.23}$$

$$U_{2,u}^T = \begin{bmatrix} \Psi_1 & \Psi_2 & \cdots & \Psi_s \end{bmatrix} \tag{2.24}$$

where $\Phi_i \in \mathbf{R}^{(sm-n)\times m}$ is i^{th} block column of Φ and $\Psi_i \in \mathbf{R}^{(sm-n)\times l}$ is i^{th} block column of Ψ. Then Eq.(2.22) becomes

$$\Phi H_{u,s} = \Psi.$$

Considering a single column of $H_{u,s}$,

$$\begin{bmatrix} \Phi_1 & \Phi_2 & \cdots & \Phi_s \\ \Phi_2 & \Phi_3 & \cdots & O \\ \vdots & \vdots & \ddots & \vdots \\ \Phi_s & O & \cdots & O \end{bmatrix} \begin{bmatrix} D \\ CB \\ \vdots \\ CA^{s-2}B \end{bmatrix} = \begin{bmatrix} \Psi_1 \\ \Psi_2 \\ \vdots \\ \Psi_s \end{bmatrix}. \tag{2.25}$$

Equation (2.25) is over-determined, linear system of equation and least square method can be used to solve it to find unknown column vector of $H_{u,s}$.

Then, the state space matrices are identified by first estimating C, which forms the first m rows of $\hat{\Gamma}_s$, where $(\hat{\ })$ denotes estimate.

$$\hat{C} = \hat{\Gamma}_s (1:m,:) \tag{2.26}$$

Estimating A requires only few computational step.

$$\hat{\Gamma}_s (m+1:sm,:) = \hat{\Gamma}_s (1:m(s-1),:) \hat{A}. \tag{2.27}$$

The matrix pair B and D can be extracted by another least squares step, wherein a single column of $H_{u,s}$ is selected as

$$H_{u,s}^1 = \begin{bmatrix} D \\ CB \\ \vdots \\ CA^{s-2}B \end{bmatrix}. \tag{2.28}$$

In the matrix form, it can be expressed as

$$H_{u,s}^1 = \begin{bmatrix} I_{m\times m} & O_{m\times n} \\ O_{m(s-1)\times m} & \hat{\Gamma}_s(1:m(s-1),:) \end{bmatrix} \begin{bmatrix} D \\ B \end{bmatrix}. \tag{2.29}$$

Now, matrices B and D can be estimated as

$$\begin{bmatrix} \hat{D} \\ \hat{B} \end{bmatrix} = \begin{bmatrix} I_{m\times m} & O_{m\times n} \\ O_{m(s-1)\times m} & \hat{\Gamma}_s(1:m(s-1),:) \end{bmatrix}^\dagger H_{u,s}^1. \tag{2.30}$$

Remark: As mentioned earlier, there are several algorithms to determine the subspace of state space matrices. For simplicity in understanding the approach, just one method is described here. It uses robust numerical tools such as SVD to identify state sequence at first. The subspace of state space matrices is then identified with the help of the least squares method. It is also pointed out that the algorithm presented here has intimate connection with the model-based fault diagnosis technique popularly known as parity space method.

2.3 Model-based FD techniques

Model-based techniques for fault detection is an established and thoroughly researched area. It has gained tremendous attention from the industry as well. As the name suggests, a representative process model is the core of model-based FD techniques. Thus full-order state observers, Kalman filters are naturally arising solutions. But the last thirty years of research has brought a lot of insightful and dedicated methods, for instance, diagnostic observers, robust parity space methods. It is impossible to cover the entire spectrum here, but for introduction, only the most important techniques are discussed in this section.

2.3.1 Parity space (PS)

Parity space relation is one of the simplest means to detect abnormal deviations in the behavior of stable linear systems. It is extremely efficient for on-line application and involves just few multiplication and additions. The approach was first proposed by Chow and Willsky [15] back in 1984, but the development still continues to dominate its industrial applications [17], [42], [76].

The parity space based residual generator is originally conceived based on the state space representation of LTI systems. Consider a discrete time system from Eq.(2.1)-(2.2). As explained in the earlier section, the equations can be written in a recursive form up to certain $s > k > 0$, starting from $k - s$. Continuing this way, the output equation at instant k can built up as shown in Eq.(2.10). Extending the result for the state space equations with disturbance, following relation can be written:

$$y_{k,s} = \Gamma_s x_{k-s+1} + H_{u,s} u_{k,s} + H_{d,s} d_{k,s}. \qquad (2.31)$$

where the definitions of $y_{k,s}, u_{k,s}$ and $\Gamma_s, H_{u,s}$ follow from previous section.

The matrix $H_{d,s}$ is defined as

$$H_{d,s} = \begin{bmatrix} F_d & O & \cdots & O \\ CE_d & F_d & \ddots & \vdots \\ \vdots & \ddots & \ddots & O \\ CA^{s-2}E_d & CA^{s-3}E_d & \cdots & F_d \end{bmatrix}.$$

Equation (2.31) is termed as the parity relation. It consists of the information about the process dynamics from the past to the current time instant. The matrices Γ_s and $H_{u,s}$ are formed with the nominal model parameters, i.e. the quadruplet, A, B, C, D.

For the diagnostic purpose, it is important to compare the estimated and the actual system behavior with the help of the so-called residual signal. To do so, the state influence, x_{k-s+1} in Eq.(2.31) needs to be removed. From the basic control theory, it is known that the rank of controllability matrix is equal to the order of the model, i.e.

$$rank\,(\Gamma_s) = n. \tag{2.32}$$

For $s > n$, a non-zero orthogonal complement or the so-called parity space exists. In algebraic way, there is at least one vector $v_s \neq 0$ such that

$$v_s\Gamma_s = 0. \tag{2.33}$$

Equation (2.33) is the fundamental idea behind parity space based residual generation. The subspace belonging to parity space is defined as:

$$P_s = \{v_s|v_s\Gamma_s = 0\}. \tag{2.34}$$

The residual obtained by a parity vector can be described by following equation:

$$r_k = v_s(y_{k,s} - H_{u,s}u_{k,s}). \tag{2.35}$$

In the practical case, it is not possible to exclude the disturbances and faults. Therefore, the residual signal is actually result of all such 'unmodeled' dynamics.

$$r_k = v_s\,(H_{d,s}d_{k,s} + H_{f,s}f_{k,s}) \tag{2.36}$$

where $d_{k,s}$ and $f_{k,s}$ have similar form as that of $y_{k,s}$ and the matrix $H_{f,s}$ is defined similar to $H_{d,s}$. Thus according to Eq.(2.36), if the process is operating under disturbance-free conditions, the residual is simply a function of faults. The robustness technique developed so far deals with enhancing the sensitivity for faults by simultaneously reducing the effect of disturbances.

For more details on robust methods, the readers are referred to [12], [18], [40].

Remark: The design of parity space based residual generator involves finding the left null (orthogonal) complement of Γ_s. Its on-line implementation requires storing past s values of both inputs and outputs and generating residual signal according to Eq.(2.35). This may put some additional restriction in designing FDI scheme for large scale processes. It can be tackled by transforming the residual generator in an equivalent diagnostic observer form [20].

2.3.2 Linear observers

Linear observer for controllers was designed as early as in 70s. Beard [5] and Jones [59] came up with the first ever FDI system based on it. It is commonly known as the fault detection filter (FDF). The construction is very simple and for those who are familiar with the observer theory, it is simply a full-order state observer.

Consider a state space model of discrete LTI system as described in Eq.(2.12)-(2.13). Then, FDF for it can be designed as

$$\hat{x}_{k+1} = A\hat{x}_k + Bu_k + L_o(y_k - \hat{y}_k) \tag{2.37}$$
$$\hat{y}_k = C\hat{x}_k + Du_k \tag{2.38}$$

where the matrix L_o is referred to as the observer gain and it is chosen such that the estimation error, $e = x - \hat{x}$ asymptotically goes to zero.

$$\dot{e}_k = (A - LC)e_k \tag{2.39}$$
$$r_k = Ce_k \tag{2.40}$$

where r is the residual signal and defined as

$$r_k = y_k - \hat{y}_k. \tag{2.41}$$

The design of observer is fundamentally selecting a suitable feedback gain which improves the performance of estimation, prediction or filtering. For FDI, the gain may also improve the sensitivity to faults and increases robustness against deterministic as well as stochastic disturbances. To this end, following generalized model of residual generator is considered:

$$r_k = V(y_k - \hat{y}_k). \tag{2.42}$$

The problem is formulated as optimal selection of the observer gain including the design of a post-filter, V. More details on this type of integrated design of observer based FDI schemes can be found in [18].

2.3.3   Diagnostic observers (DO)

A diagnostic observer is a special type of output observer, in that basically a reduced-order observer dedicated for fault detection purpose. Considering the process model in Eq.(2.41)-(2.42), DO has following form:

$$\dot{z}_k = A_z z_k + B_z u_k + L_z y_k \tag{2.43}$$
$$\hat{y}_k = \bar{c}_z z_k + \bar{d}_z u_k + \bar{g}_z y_k \tag{2.44}$$

where $z \in \mathbf{R}^s$, s denotes order of the observer and it can be lower than model order. For this, the matrices $A_z, B_z, L_z, \bar{c}_z, \bar{d}_z$ and $\bar{g}_z$ together with state transformation matrix, T, must solve following Luenberger equations:

- A_z is stable

- $TA - A_z T = L_z C, B_z = TB - L_z D$

- $C = \bar{c}_z T + \bar{g}_z C, \bar{d}_z = -\bar{g}_z D + D$

The observer error dynamics is then stable, i.e. for $e = Tx - z$,

$$e_{k+1} = A_z e_k, \tag{2.45}$$
$$y_k - \hat{y}_k = \bar{c}_z e_k \tag{2.46}$$

In [19] and their earlier work, modification to the original formulations of DO is suggested. Their a residual signal is defined as shown in Eq.(2.42). Its dynamics can be described:

$$z_{k+1} = A_z z_k + B_z u_k + L_z y_k \tag{2.47}$$
$$r_k = g_z y_k - c_z z_k - d_z u_k \tag{2.48}$$

where $g_z = V(I - \bar{g}_z), c_z = V\bar{c}_z, d_z = V\bar{d}_z$. For the residual generator, only the third condition is redefined as

$$VC - g_z T = 0, d_z = VD.$$

The diagnostic observer based residual generator is thus choosing a suitable 'post-filter' as V with above mentioned design considerations. This observer is extremely efficient for on-line implementation because of the reduced dimensions, scope for feedback, and reduced on-line computation load. The price paid is perhaps more involved off-line design procedure. Ding et al. [19] have further studied the characterization of all possible solutions of Luenberger conditions and this result builds an interesting one-to-one relationship with the solution of the parity space.

2.4   Relation between PS and DO

The diagnostic observer scheme and parity space, two of the most fundamental concepts of fault detection, are interestingly one-to-one compatible. In fact, it implies that the parity space solves the modified Luenberger equations mentioned in section 2.3.3.

The celebrated result in Ding et al. [19] demonstrates that for a given parity space, $v_s = \begin{bmatrix} v_{s,0} & v_{s,1} & \cdots & v_{s,s-1} \end{bmatrix}$, the matrices A_z, L_z, T, g_z and c_z can be obtained as

$$A_z = \begin{bmatrix} 0 & 0 & \cdots & 0 & l_0 \\ 1 & 0 & \ddots & \vdots & l_1 \\ \vdots & \ddots & \ddots & 0 & \vdots \\ 0 & 0 & \cdots & 1 & l_{s-1} \end{bmatrix} \in \mathbf{R}^{s-1 \times s-1}$$

$$T = \begin{bmatrix} v_{s,1} & v_{s,2} & \cdots & v_{s,s-2} & v_{s,s-1} \\ v_{s,2} & v_{s,3} & \cdots & v_{s,s-1} & 0 \\ \vdots & \cdots & \cdots & \vdots & \vdots \\ v_{s,s-1} & 0 & \cdots & \cdots & 0 \end{bmatrix} \begin{bmatrix} C \\ CA \\ \vdots \\ CA^{s-2} \end{bmatrix},$$

$$L_z = - \begin{bmatrix} v_{s,0} \\ v_{s,1} \\ \vdots \\ v_{s,s-2} \end{bmatrix} - \begin{bmatrix} l_0 \\ l_1 \\ \vdots \\ l_{s-1} \end{bmatrix} v_{s,s-1}, c_z = \begin{bmatrix} 0 & \cdots & 0 & 1 \end{bmatrix}, g_z = v_{s,s-1}$$

where the vector $\begin{bmatrix} l_0 & l_1 & \cdots & l_{s-1} \end{bmatrix}^T$ is chosen such that A_z is asymptotically stable. The transformation is two way, that means any observable pair (c_z, A_z) that solves Luenberger equations belongs to the parity space. Thus given matrices A_z, L_z, T, g_z and c_z , one can obtain a parity vector as

$$v_{s,s-1} = v, \begin{bmatrix} v_{s,0} \\ v_{s,1} \\ \vdots \\ v_{s,s-2} \end{bmatrix} = -L_z - \begin{bmatrix} l_0 \\ l_1 \\ \vdots \\ l_{s-1} \end{bmatrix} g_z \tag{2.49}$$

The parity space relation is said to have s-step 'deadbeat' property, i.e. the residual at k^{th} step depends on the input and the output at time $k-s+1$ up to k. The diagnostic observer, on the other hand has no such deadbeat effect. It also has an additional degree of freedom wherein the poles of A_z can be arbitrarily selected. Thus the diagnostic observer is more preferable form of on-line implementation than the parity space based residual generator.

2.5 Statistical process monitoring

The modern process industry is inseparable from statistical process monitoring (SPM). SPM is a specialized branch of statistical data analysis and is extensively involved in developing efficient algorithms to detect faults for consistent, safe and economic process operation. Past few years have seen tremendous growth from simple statistical limit testing to sophisticated time-series analysis. The development has also contributed to various fields such as system identification and model-based fault diagnosis.

In SPM, models are developed directly from the plant's historical data which are applied to detect any abnormal events. The reliability and robustness of such models against plant-wide disturbances are currently the most important challenges in the research. The most attractive feature of SPM is their easy designs and operational simplicity. These issues are elaborated in the next subsection with a specific algorithm.

2.5.1 Principal Component Analysis (PCA)

Principal component analysis or simply PCA, is essentially a data compression method. It reduces large datasets to few but informative components that explain most of the the nominal process variation [105]. The algorithm combines tools from linear algebra (eigenvalue decomposition) and statistical analysis (variance-covariance) to construct a representative model which can be used for monitoring and fault detection purpose.

The existing PCA-based process monitoring algorithms are numerically reliable and stable with minimal programming effort. Because of it, PCA is immensely popular in the process industry [27], [28], [68], [95]. Besides, to detect abnormal behavior, robust multivariate statistical indices are developed. Therefore, from the plant operator's perspective, the task to monitor process health easier with a single time-chart. Furthermore, extensive studies have led to sophisticated tools for fault identification and localization.

As mentioned earlier, the design of PCA-based monitoring is data-driven. It requires representative process data for training, either obtained directly from the plant or from a simulation platform that can replicate process behavior. The training data consists of N samples of m measured variables and is denoted by $X \in \mathbf{R}^{N \times m}$:

$$X = \begin{bmatrix} x_{11} & x_{21} & \cdots & x_{1m} \\ x_{21} & x_{22} & \cdots & x_{2m} \\ \vdots & \vdots & \ddots & \vdots \\ x_{N1} & x_{N2} & \cdots & x_{Nm} \end{bmatrix}. \tag{2.50}$$

From the statistical theory, it is known that the sample covariance of X can be written as:

$$\Phi_{xx} = \frac{1}{N-1} X^T X. \tag{2.51}$$

Next. the crucial step of data compression in PCA is achieved by the eigenvalue (or singular value) decomposition:

$$\Phi_{xx} = V \Delta V^T, \tag{2.52}$$

where V consists of m orthogonal eigenvectors and

$$\Delta = \begin{bmatrix} \lambda_1 & & & \\ & \lambda_2 & & \\ & & \ddots & \\ & & & \lambda_m \end{bmatrix}. \tag{2.53}$$

With the help of Eq.(2.52), it is possible to divide the covariance matrix into two orthogonal subspaces, namely model and residual subspace. The eigenvalues describe the variance in these two subspaces and are arranged in the descending order of their magnitude. Therefore, Eq.(2.52) can be rearranged as:

$$V \Delta V^T = T P^T + \tilde{T} \tilde{P}^T \tag{2.54}$$

where $T, \tilde{T} \in \mathbf{R}^{m \times a}$ and also $P, \tilde{P} \in \mathbf{R}^{a \times m}$ assuming that the model subspace is spanned by the first a largest eigenvalues and eigenvectors. Then, every new measurement is projected to the new a-dimensional subspace as follows:

$$t = P^T x \tag{2.55}$$

where $x \in \mathbf{R}^m$ is the current measurement and $t \in \mathbf{R}^a$ is the projected vector. Note that there are several analytical methods to determine the dimension of principal model space in the design stage. See e.g. [102] for an overview. The projection can be transformed back to original m-dimensional subspace by

$$\hat{x} = P P^T x. \tag{2.56}$$

The difference between x and its approximation $\hat{x}$ is given by

$$E = x - \hat{x}. \tag{2.57}$$

where E is defined as the residual error. It can also be obtained by projecting x directly in the residual space, i.e.

$$E = \left(I - \tilde{P} \tilde{P}^T \right) x. \tag{2.58}$$

For monitoring and fault detection purpose two indices are derived and limit values are calculated [55]. For instance, T^2-statistic can be applied if x is projected onto the model subspace and Q-statistic or SPE (squared prediction error) if x is projected onto the residual space.

Remark: There are other statistical techniques that are frequently used in industrial applications. For instance, independent component analysis (ICA) is used for applications where disturbances are non-Gaussian random sequences [38], [69]. For nonlinear systems support vector machines (SVM) or kernel-based PCA (KPCA) are used these days. See e.g. their applications in [3], [13], [70]. The dynamic version of KPCA is also developed and applied for instance in [14], [58], [111]. These approaches have their own strength and weakness, and the application depend on requirements of the process monitoring systems.

2.6   Relation between SIM and PCA

The aim of the subspace identification algorithm is to extract state space model from the input and output data. The crucial step in this technique is the singular value decomposition (see Eq.(2.18) in subsection 2.2.1) performed on the training dataset. This is also an important step in PCA based process monitoring system (see Eq.(2.52) in subsection 2.5.1). Therefore, in this section a mutual relationship between these two approaches is established [72], [109].

The data matrix X in Eq.(2.50) can be redefined for the system in Eq.(2.1)-(2.2). It consists of measurements from the plant's inputs $u \in \mathbf{R}^l$ and outputs $y \times \mathbf{R}^m$.

$$X = \begin{bmatrix} z_{k-s+1} & z_{k-s+2} & \cdots & z_k \\ z_{k-s+2} & z_{k-s+3} & \ddots & z_{k+1} \\ \vdots & \ddots & \ddots & \vdots \\ z_{k-s+N} & z_{k-s+N+1} & \cdots & z_{k+N-1} \end{bmatrix} \in \mathbf{R}^{N \times s(l+m)}$$

where $z_k = \begin{bmatrix} y_k & u_k \end{bmatrix} \in \mathbf{R}^{(l+m)}$ and s is the number of lagged measurements. Note that this definition of matrix X is similar to that defined in dynamic principal component analysis (DPCA) [66], [97]. Now, if instead of X, eigenvalue decomposition is performed on its transpose and it is divided in two parts as explained in Eq. (2.54), then

$$X^T = PT^T + \tilde{P}\tilde{T}^T \tag{2.59}$$

where $P \in \mathbf{R}^{s(l+m)\times a}$, $\tilde{P} \in \mathbf{R}^{s(l+m)\times(s(l+m)-a)}$ are scoring matrices and $T \in \mathbf{R}^{N\times a}$, $\tilde{T} \in \mathbf{R}^{(s(l+m)-a)\times N}$ are loading matrices. Also, it can be shown that

the number of principal components, a, depends on the order of the model, n. Additionally, if the scores and loading matrices are computed with the help of SVD over X^T, then

$$X^T = \begin{bmatrix} U_m & U_r \end{bmatrix} \begin{bmatrix} \Sigma_m & O \\ O & \Sigma_r \end{bmatrix} \begin{bmatrix} V_m^T \\ V_r^T \end{bmatrix}. \tag{2.60}$$

According to the definitions of the scoring and loading matrices, one can write following relations:

$$P = U_m \Sigma_m, T = V_m, \tilde{P} = U_r \Sigma_r, \tilde{T} = V_r. \tag{2.61}$$

For SIM, it is shown in Eq.(2.20) that the state space model parameters are contained in subspace the spanned by $\Gamma_s^\perp$ and it belongs to $U_2 \in \mathbf{R}^{s(l+m) \times sm-n}$. Therefore, comparing this result with Eq.(2.59), $\Gamma_s^\perp$ can also be expressed as

$$\begin{bmatrix} \Gamma_s^\perp & \Gamma_s^\perp H_{u,s} \end{bmatrix} = M_1 \tilde{P}^T, \tag{2.62}$$

where M_1 is an arbitrary regular matrix. Now, applying the result of SVD in Eq.(2.61),

$$\Gamma_s^\perp = M_2 U_r^T, \Gamma_s^\perp H_{u.s} = M_3 U_r^T \tag{2.63}$$

where M_2, M_3 are also regular matrices. Equation (2.63) implies that the scoring matrix of the residual subspace of PCA model spans the subspace of $\Gamma_s^\perp$. The only constraint is that the number of principal components must reveal the true model order of the system under consideration. This is normally achieved by designing a persistently exciting input signal. More study on this topic can be found in [109], [110].

2.7 Concluding remarks

This chapter covers the major developments and important concepts in the field of model-based fault diagnosis and statistical process monitoring. The technical systems under consideration are assumed as linear discrete time-invariant. They are described taking in account disturbances and faults. It is also explained that if the model is not available, then subspace identification based technique can be applied to extract it, based on just training data.

In the second part of this chapter, the popular model-based FDD approaches such as parity space, linear observers, and diagnostic observers are discussed. Then, the statistical process monitoring is briefly introduced with the help of principal components analysis. Some interesting results such as the relationship between diagnostic observer and parity space, and SIM and PCA are also provided. These analogical relations are also important in dealing with the novel data-driven approach to design FD system discussed in the next chapter.

Chapter 3

Data-driven design of FD systems

Model-based technique is a powerful solution for fault detection, isolation, and diagnosis problem. Modern design of controllers has even integrated it to avert critical failures and stabilize the plant under abnormal events. This is an emerging area called as fault-tolerant control. But as seen from previous chapter, model-based techniques require precisely defined mathematical model of the plant. For complex systems, a way out is identification of the model from the plant's data. The technique is a simpler alternative than to derive model from first principles and offers a compatible model structure for controller and monitoring schemes.

There exists a range of tools to extract model parameters from just the test data, for instance, the subspace identification method (SIM). SIM has gained tremendous attention in the application involving design of controllers, signal processing, or observer-based fault detection. The block diagram in Fig.(3.1) describes the classical subspace identification aided design for observer-based fault detection system. It involves identification of state space matrices from the estimated state sequence. The residual generator is then designed according to the model-based schemes described in the previous chapter.

This procedure can be shortened if the final purpose is well defined in advance. This is often called in the literature as the goal-oriented identification procedure. In this work, identification is exclusively dealt with considering fault diagnosis in complex systems. But the novel data-driven approach presented here is constrained so that only the key components required by the residual generator are identified. This allows the design phase to be shorter, easier and faster. It is principally sketched in Fig.(3.1) parallel to the classical SIM-based approach.
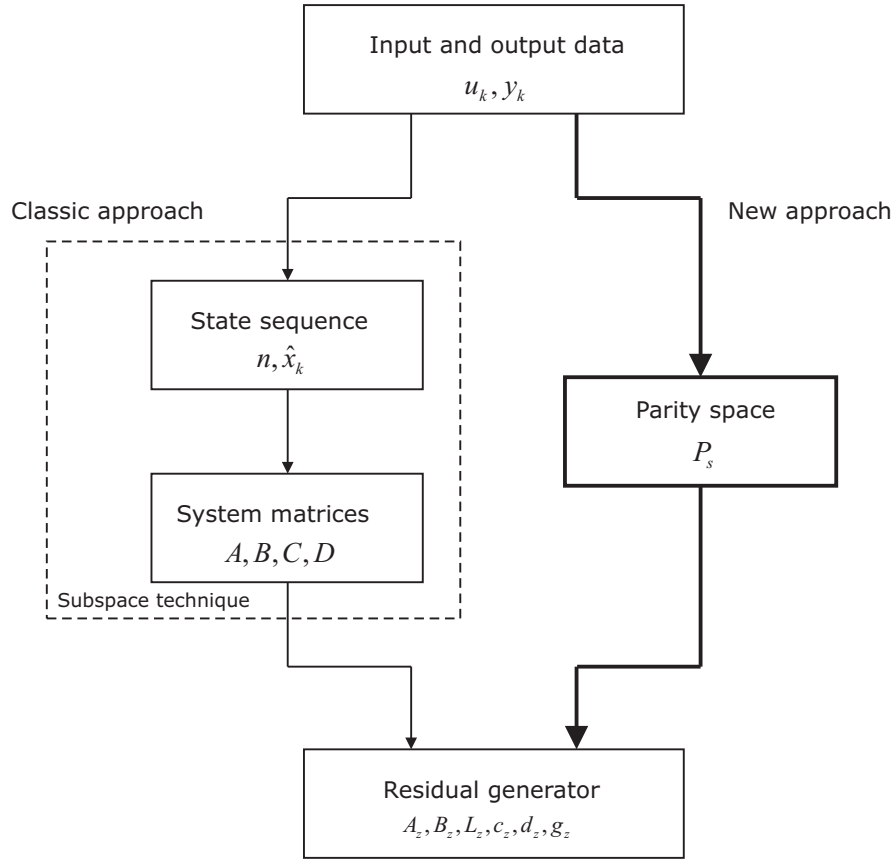
Figure 3.1: Classic vs. new approach

In the proposed design, it is assumed that the mathematical model of the plant under consideration is not available. The input and output are gathered from measurements and are used to identify a parity space based primary residual generator. To improve the performance of it, a closed-loop diagnostic observer is also designed as the secondary form of residual generator. This novel data-driven technique to design fault detection and isolation (FDI) systems has following main features:

- The entire design scheme is based only on the input and output data from the plant under consideration.

- It requires minimal set of identified parameters which simplifies the job of application engineer to select a suitable residual generator.

- The primary residual generator is identified but it is implemented as a closed-loop diagnostic observer with just few additional steps.

- There is no requirement of extra knowledge about modern control theory or observer-based estimation

The motivation behind the proposed work is that although the model-based FDI systems are commonly used in small-scale systems such as automotive, its usage in large-scale processes is very limited. Therefore, this work combines the model-based techniques with statistical analysis and system identification for much wider application range. Also, many technical systems exhibit transient behavior, for instance in reference tracking, instead of static behavior. Therefore, it is important to take in account dynamic models in designing FDI systems.

A further motivation is derived from the state space model identification based on PCA proposed in [109], [110]. It exploits the commonality between SIM and PCA which is mentioned in section 2.6. Although, the proposed work is also based on the same idea, the objective here is to design an observer-based FDI systems. This chapter elaborates the principle idea behind the novel approach, which is also proposed in the publications for instance, [19], [20].

3.1 Mathematical notations and preliminary

The plant under consideration is assumed to have following discrete linear time invariant (DLTI) state space model:

$$
\begin{aligned}
x_{k+1} &= Ax_k + Bu_k + w_k & (3.1)\\
y_k &= Cx_k + Du_k + v_k & (3.2)
\end{aligned}
$$

The model equations are introduced in Eq.(2.1)-(2.2) in the previous chapter. The disturbance signals, $w_k \in \mathbf{R}^n, v_k \in \mathbf{R}^m$, are process and measurement noise having Gaussian distribution with zero mean value and their variance, co-variance have following model:

$$
E\left(\begin{bmatrix} w_i \\ v_i \end{bmatrix} \begin{bmatrix} w_j^T & v_j^T \end{bmatrix} \right) = \begin{bmatrix} Q & S \\ S^T & R \end{bmatrix} \delta_{ij} \qquad (3.3)
$$

where δ_{ij} is Kronecker delta. The matrix quadruplet, $\{A, B, C, D\}$, model order n and noise variances Q, R and S are assumed unknown *a priori*.

To begin with the design procedure, the state space variables are arranged

in the following form:

$$
\begin{aligned}
X_j &= \begin{bmatrix} x_j & x_{j+1} & \cdots & x_{j+N-1} \end{bmatrix} \in \mathbf{R}^{n \times N} \\
U_j &= \begin{bmatrix} u_j & u_{j+1} & \cdots & u_{j+N-1} \end{bmatrix} \in \mathbf{R}^{l \times N} \\
Y_j &= \begin{bmatrix} y_j & y_{j+1} & \cdots & y_{j+N-1} \end{bmatrix} \in \mathbf{R}^{m \times N} \\
W_j &= \begin{bmatrix} w_j & w_{j+1} & \cdots & w_{j+N-1} \end{bmatrix} \in \mathbf{R}^{n \times N} \\
V_j &= \begin{bmatrix} v_j & v_{j+1} & \cdots & v_{j+N-1} \end{bmatrix} \in \mathbf{R}^{m \times N}
\end{aligned}
$$

where N is the length of available data samples. The input and output datasets can be further congregated as the so-called block Hankel structures:

$$
U_p = \begin{bmatrix} U_{i-s} \\ U_{i-s+1} \\ \vdots \\ U_{i-1} \end{bmatrix} \in \mathbf{R}^{sl \times N}, Y_p = \begin{bmatrix} Y_{i-s} \\ Y_{i-s+1} \\ \vdots \\ Y_{i-1} \end{bmatrix} \in \mathbf{R}^{sm \times N}
$$

$$
U_f = \begin{bmatrix} U_i \\ U_{i+1} \\ \vdots \\ U_{i+s-1} \end{bmatrix} \in \mathbf{R}^{sl \times N}, Y_f = \begin{bmatrix} Y_i \\ Y_{i+1} \\ \vdots \\ Y_{i+s-1} \end{bmatrix} \in \mathbf{R}^{sm \times N}
$$

Similarly, the disturbance variables are also gathered in Hankel structures:

$$
W_f = \begin{bmatrix} W_i \\ W_{i+1} \\ \vdots \\ W_{i+s-1} \end{bmatrix} \in \mathbf{R}^{sn \times N}, V_f = \begin{bmatrix} V_i \\ V_{i+1} \\ \vdots \\ V_{i+s-1} \end{bmatrix} \in \mathbf{R}^{sm \times N}.
$$

The subscripts p, f stand for the so-called past and future data. The integer s is user-defined parameter and determines the number of lagged measurements. Usually, $s \gg n$ where n is the expected order of the model. Two more datasets are constructed by concatenating inputs and outputs:

$$
Z_p = \begin{bmatrix} Y_p \\ U_p \end{bmatrix} \in \mathbf{R}^{s(l+m) \times N}, Z_f = \begin{bmatrix} Y_f \\ U_f \end{bmatrix} \in \mathbf{R}^{s(l+m) \times N}. \tag{3.4}
$$

Now, Eq.(3.1) and (3.2) can be brought into familiar extended state space model form explained in the previous chapter:

$$
Y_f = \Gamma_s X_i + H_{u,f} U_f + H_{w,f} W_f + V_f \tag{3.5}
$$

where

$$\Gamma_s = \begin{bmatrix} C \\ CA \\ \vdots \\ CA^{s-1} \end{bmatrix}, H_{u,f} = \begin{bmatrix} D & O & \cdots & O \\ CB & D & \ddots & O \\ \vdots & & \ddots & \ddots & \vdots \\ CA^{s-2}B & CA^{s-1}B & \cdots & D \end{bmatrix}$$

$$H_{w,f} = \begin{bmatrix} O & O & \cdots & O \\ C & O & \ddots & O \\ \vdots & \ddots & \ddots & \vdots \\ CA^{s-2} & \cdots & C & O \end{bmatrix}.$$

Equation (3.5) is the core of the subspace identification techniques as well as the parity space based residual generation. So, according to the definition of parity space from Eq.(2.34):

$$v_s \Gamma_s = 0, v_s = \begin{bmatrix} v_{s,0} & v_{s,1} & \cdots & v_{s,s-1} \end{bmatrix}, \tag{3.6}$$

and the residual generator based on it can be obtained as

$$r_k = v_s \begin{bmatrix} y_{k-s+1} \\ y_{k-s} \\ \vdots \\ y_k \end{bmatrix} - \rho_s \begin{bmatrix} u_{k-s+1} \\ u_{k-s} \\ \vdots \\ u_k \end{bmatrix} \tag{3.7}$$

whereby $v_s \in \Gamma_s^\perp, \rho_s \in \Gamma_s^\perp H_{u,f}$. Therefore, the FDI-oriented identification problem reduces to identifying the two subspaces $\Gamma_s^\perp$ and $\Gamma_s^\perp H_{u,f}$, which will be discussed next.

3.1.1 Identification of primary residual generator

As mentioned earlier, the novel approach involves designing parity space based residual generator as the primary form of the FDI scheme. To this end, Eq.(3.4) is substituted in Eq.(3.5):

$$Z_f = \begin{bmatrix} \Gamma_s & H_{u,s} \\ O & I \end{bmatrix} \begin{bmatrix} X_k \\ U_f \end{bmatrix} + \begin{bmatrix} H_{w,f} W_f + V_f \\ O \end{bmatrix}. \tag{3.8}$$

Here, it is desired to remove the effect of uncorrelated stochastic noise sequences by pre-multiplying Eq.(3.8) with an instrument variable. Assuming that the process and measurement noise are independent and identically distributed (iid), then for large N,

$$\lim_{N \to \infty} \frac{1}{N} \left(H_{w,f} W_f + V_f \right) Z_p^T = O.$$

Thus,

$$Z_f Z_p^T \approx \begin{bmatrix} \Gamma_s & H_{u,s} \\ O & I \end{bmatrix} \begin{bmatrix} X_k \\ U_f \end{bmatrix} Z_p^T. \qquad (3.9)$$

If the input sequences U_p and U_f are chosen such that

$$\begin{aligned} rank\left(Z_f Z_p^T\right) &= rank\left(Z_f\right) \\ &= rank\left(\begin{bmatrix} \Gamma_s & H_{u,s} \\ O & I \end{bmatrix} \begin{bmatrix} X_k \\ U_f \end{bmatrix}\right) \\ &= rank\left(\begin{bmatrix} \Gamma_s & H_{u,s} \\ O & I \end{bmatrix}\right) \\ &= sl + n, \qquad (3.10) \end{aligned}$$

then following relation holds as a consequence of condition (3.10),

$$rank\left(Z_f^\perp\right) = rank\left(\Gamma_s^\perp\right) = sm - n$$

$$\Rightarrow Z_f^\perp \begin{bmatrix} \Gamma_s & H_{u,s} \\ O & I \end{bmatrix} = O. \qquad (3.11)$$

Condition (3.10) has been proven in [109] and [110]. In fact, it ensures that the system is persistently exciting so that the correct model order can be selected. Now, perform SVD on $Z_f Z_p^T$,

$$Z_f Z_p^T = U_z \begin{bmatrix} \Sigma_{z,1} & O \\ O & \Sigma_{z,2} \end{bmatrix} V_z^T \qquad (3.12)$$

where $U_z \in \mathbf{R}^{s(l+m) \times s_f(l+m)}$, and $V_z \in \mathbf{R}^{s(l+m) \times s(l+m)}$. If the system satisfies condition (3.10), then there are exactly $sl + n$ non-zero singular values, i.e.

$$\begin{aligned} rank\left(\Sigma_{z,1}\right) &= rank\left(\begin{bmatrix} \Gamma_s & H_{u,s} \\ O & I \end{bmatrix}\right) \\ &= sl + n. \qquad (3.13) \end{aligned}$$

It implies that $\Sigma_{z,2}$ has exactly $sm - n$ zero singular values. If U_z is divided depending upon the singular values such that

$$U_z = \begin{bmatrix} U_{z,11} & U_{z,12} \\ U_{z,21} & U_{z,22} \end{bmatrix}$$

where $U_{z,11} \in \mathbf{R}^{sm \times sl+n}, U_{z,12} \in \mathbf{R}^{sm \times sm-n}$, and $U_{z,22} \in \mathbf{R}^{sl \times sm-n}$, then

$$\begin{aligned} Z_f^\perp &= P\begin{bmatrix} U_{z,12}^T & U_{z,22}^T \end{bmatrix} \\ &\Rightarrow \Gamma_s^\perp \in PU_{z,12}^T,\ \Gamma_s^\perp H_{u,f} \in PU_{z,22}^T. \qquad (3.14) \end{aligned}$$

Equation (3.14) implies that the parity space is spanned by the subspace of left singular vectors $U_{z,12}$ and $U_{z,22}$. The algorithm to identify the parity space can be summarized in following steps:

Algorithm PSi: Identification of $\Gamma_s^\perp$ and $\Gamma_s^\perp H_{u,s}$

- Generate datasets Z_f and Z_p, construct $Z_f Z_p^T$

- Perform SVD on $Z_f Z_p^T$

- Find $U_{z,12}^T$ and $U_{z,22}^T$ of appropriate dimensions, and select P

- Select $\upsilon_s \in \Gamma_s^\perp$ and $\rho_s \in \Gamma_s^\perp H_{u,f}$ according to Eq.(3.14)

Algorithm PSi directly identifies a subspace belonging to the parity space and in doing so, only the training datasets in the form of Z_f and Z_p are required. In [93], authors have presented an excellent study on the equivalency of this approach with PCA based technique. Extending the discussion, the design of secondary form of residual generator, based on υ_s and ρ_s, is proposed next.

3.1.2 Residual generator based on $\Gamma_s^\perp$ and $\Gamma_s^\perp H_{u,f}$

As seen in section 2.4, the parity space based residual generator has one-to-one relationship with the diagnostic observer (DO). In fact, DO is an infinite impulse response (IIR) filter implementation of the former, which is finite impulse response (FIR) filter [18]. This important result is the basis of this subsection which deals with the design of secondary residual generator.

Consider the two identified vectors υ_s and ρ_s belong to parity space. Based on it, the primary form of residual generator is constructed as:

$$r_k = \begin{bmatrix} \upsilon_0 & \upsilon_1 & \cdots & \upsilon_{s-1} \end{bmatrix} \begin{bmatrix} y_{k-s+1} \\ y_{k-s} \\ \vdots \\ y_k \end{bmatrix} - \begin{bmatrix} \rho_0 & \rho_1 & \cdots & \rho_{s-1} \end{bmatrix} \begin{bmatrix} u_{k-s+1} \\ u_{k-s} \\ \vdots \\ u_k \end{bmatrix}$$

(3.15)

where $\upsilon_i \in \mathbf{R}^m$ and $\rho_i \in \mathbf{R}^l$. Remember that the residual in Eq.(3.15) is a scalar only for the sake of convenience. Multiple vectors belonging to the identified subspace in Eq.(3.14) can be used as a bank of residual generators.

The secondary residual generator can be constructed by using the relationship presented in section 2.4. It requires constructing the matrices

involved in following equations:

$$z_{k+1} = A_z z_k + B_z u_k + L_z y_k \qquad (3.16)$$

$$r_k = c_z z_k + g_z y_k + d_z u_k \qquad (3.17)$$

where

$$
A_z = \begin{bmatrix} 0 & 0 & \cdots & 0 \\ 1 & 0 & \ddots & 0 \\ \vdots & \ddots & \ddots & \vdots \\ 0 & \cdots & 1 & 0 \end{bmatrix} \in \mathbf{R}^{(s-1)\times(s-1)}, B_z = \begin{bmatrix} \rho_{s,0} \\ \rho_{s,1} \\ \vdots \\ \rho_{s,s-2} \end{bmatrix} \in \mathbf{R}^{(s-1)\times l}
$$

$$
L_z = -\begin{bmatrix} \upsilon_{s,0} \\ \upsilon_{s,1} \\ \vdots \\ \upsilon_{s,s-2} \end{bmatrix} \in \mathbf{R}^{(s-1)\times m}, c_z = \begin{bmatrix} 0 & \cdots & 0 & 1 \end{bmatrix} \in \mathbf{R}^{(s-1)}
$$

$$
g_z = -\upsilon_{s,s-1} \in \mathbf{R}^{1\times m}, d_z = \rho_{s,s-1} \in \mathbf{R}^{1\times l}
$$

$$\qquad (3.18)$$

The performance of the observer can be improved by obtaining feedback gain, L_o, from the residual to the states, so that $A_z - c_z L_o$ is stable, i.e.

$$
L_o = \begin{bmatrix} l_1 \\ l_2 \\ \vdots \\ l_{s-1} \end{bmatrix}, A_z - L_o c_z = \begin{bmatrix} 0 & 0 & \cdots & -l_1 \\ 1 & 0 & \ddots & -l_2 \\ \vdots & \ddots & \ddots & \vdots \\ 0 & \cdots & 1 & -l_{s-1} \end{bmatrix}.
$$

Then the closed-loop diagnostic observer has following form:

$$z_{k+1} = A_z z_k + B_z u_k + L_z y_k - L_o r_k \qquad (3.19)$$

$$r_k = c_z z_k + g_z y_k + d_z u_k. \qquad (3.20)$$

The algorithm to design secondary residual generator is summarized on the following page. Note that choosing an appropriate gain L_o, can also improve robustness against stochastic behavior. Therefore, in the next subsection, a method to identify optimal gain with respect to minimal residual variance is presented.

3.1.3   Identification of Kalman gain

For the minimum residual variance, i.e. to obtain Kalman gain, the variance and covariance of the process and disturbance signals are required. To this

---

Algorithm PS2DO: Based on $v_s \in \Gamma_s^\perp$ and $\rho_s \in \Gamma_s^\perp H_{u,s}$

- Construct A_z, B_z, L_z, c_z, g_z, d_z according to result in Eq.(3.18)

- Design L_o such that $A_z - c_z L_o$ has eigenvalues inside the unit circle

- Construct the residual generator according to Eqs.(3.19)-(3.20)

---

end, the error dynamics of the observer in Eq.(3.16)-(3.17) is written as:

$$e_{k+1} = A_z e_k + T w_k - L_z v_k \tag{3.21}$$
$$r_k = c_z e_k + g_z v_k \tag{3.22}$$

It is important to estimate variance and covariance of following quantities:

$$\bar{w}_k = T w_k - L_z v_k, \bar{v} = g_z v_k$$

Let $\alpha_s \in \Gamma_s^\perp$, then from the result in section 2.4 and Eq.(3.18),

$$\left(\begin{bmatrix} \alpha_s H_{s,0} & \cdots & \alpha_s H_{s,j} \end{bmatrix} \begin{bmatrix} U_{i+s-j} \\ \vdots \\ U_{i+s} \end{bmatrix} - \begin{bmatrix} \alpha_{s,0} & \cdots & \alpha_{s,j} \end{bmatrix} \begin{bmatrix} Y_{i+s-j} \\ \vdots \\ Y_{i+s} \end{bmatrix} \right) \bar{Z}_p^T =$$
$$\frac{1}{N} Q_{i+s-j,i+s} = \left(\begin{array}{c} B_{z,1} U_{i+s-j} - \alpha_{s,0} C X_{i+s-j} + \\ \cdots + B_{z,j} U_{i+s} - \alpha_{s,j} C X_{i+s} \end{array} \right) \bar{Z}_p^T, j = 0, \cdots, s-1$$
$$\tag{3.23}$$

where $N \to \infty, (H_{w,f} W_f + V_f) \bar{Z}_p^T \to 0$, and $\bar{Z}_p = \frac{1}{N} Z_p$. Equation (3.23) can be proven with following explanatory conditions. It is assumed that $v_k = 0, w_k = 0$ and $T x_k = z_0 = 0$. Therefore, it holds

$$z_k = \begin{bmatrix} z_{1,k} \\ z_{2,k} \\ \vdots \\ z_{s,k} \end{bmatrix} = T x_k = \begin{bmatrix} \alpha_{s,1} & \alpha_{s,2} & \cdots & \alpha_{s,s-1} & \alpha_{s,s} \\ \alpha_{s,2} & \cdots & \cdots & \alpha_{s,s} & 0 \\ \vdots & \cdots & \cdots & \vdots & \vdots \\ \alpha_{s,s} & 0 & \cdots & \cdots & 0 \end{bmatrix} \begin{bmatrix} C \\ CA \\ \vdots \\ CA^{s-1} \end{bmatrix} x_k$$

and furthermore

$$t_1 x_{k+1} = t_1 A x_k + t_1 B u_k \Longleftrightarrow$$
$$z_{1,k+1} = -\alpha_{s,0} C x_k + t_1 B u_k - \alpha_{s,0} D u_k$$
$$t_i x_{k+1} = t_i A x_k + t_i B u_k, i = 2, \cdots s \Longleftrightarrow$$
$$z_{i,k+1} = z_{i-1,k} - \alpha_{s,i-1} C x_k + t_i B u_k - \alpha_{s,i-1} D u_k =$$
$$\sum_{j=1}^{i} \left(t_{i-j+1} B u_{k-j+1} - \alpha_{s,i-j} D u_{k-j+1} - \alpha_{s,i-j} C x_{k-j+1} \right). \tag{3.24}$$

Comparing Eq.(3.23) with Eq. (3.24), we can write for $j = 0, \cdots, s-1$

$$\left(\begin{array}{c} B_{z,1} U_{i+s-j} - \alpha_{s,0} C X_{i+s-j} + \\ \cdots + B_{z,j} U_{i+s} - \alpha_{s,j} C X_{i+s} \end{array} \right) Z_p^T = Q_{i+s-j,i+s} = Z_{j+1,i+s} Z_p^T \tag{3.25}$$

where

$$Z_{j+1,i+s} = \left[\begin{array}{cccc} z_{j+1,i+s} & z_{j+1,i+s+1} & \cdots & z_{j+1,i+s+N-1} \end{array} \right] \in \mathbf{R}^N.$$

Thus the state sequence Z_{i+s} can be recovered from Eq.(3.25) as the projection onto $\bar{Z}_p^T$, i.e.

$$\hat{Z}_{i+s} = \left[\begin{array}{c} \hat{Z}_{1,i+s} \\ \vdots \\ \hat{Z}_{s,i+s} \end{array} \right] = \left[\begin{array}{c} Q_{i+s,i+s} \\ \vdots \\ Q_{i+1,i+s} \end{array} \right] \left(\bar{Z}_p \bar{Z}_p^T \right)^{-1} \bar{Z}_p. \tag{3.26}$$

Similarly another state sequence, $\hat{Z}_{i+s-1}$ can also be identified. Both these results can be combined to yield

$$z_{k+1} - A_z z_k - L_z y_k - B_z u_k = T w_k - L_z v_k = \bar{w}_k \tag{3.27}$$
$$g_z y_k - c_z z_k - d_z u_k = \alpha_{s,s} y_k - z_{s,k} - \alpha_{s,s} H_{s,s} = g_z v_k = \bar{v}_k. \tag{3.28}$$

From Eq.(3.27) and Eq. (3.28), the noise variance can be calculated as

$$\left[\begin{array}{cc} V_{\bar{w}\bar{w}} & V_{\bar{w}\bar{v}} \\ V_{\bar{w}\bar{v}}^T & V_{\bar{v}\bar{v}} \end{array} \right] = \frac{1}{N} \left[\begin{array}{c} \bar{W} \\ \bar{V} \end{array} \right] \left[\begin{array}{cc} \bar{W}^T & \bar{V}^T \end{array} \right] \tag{3.29}$$

with

$$\bar{W} = \hat{Z}_{i+s} - A_z \hat{Z}_{i+s-1} - L_z Y_{i+s-1} - B_z U_{i+s-1} \tag{3.30}$$
$$\bar{V} = \alpha_{s,s} Y_{i+s-1} - \hat{Z}_{s,i+s-1} - \alpha_s H_{s,s} U_{i+s-1}. \tag{3.31}$$

From the knowledge of $\bar{W}$, $\bar{V}$, and their variance, Kalman gain can be computed by solving a straightforward Riccati equation, i.e.

$$L_{kf} = -\Phi c_z^T \left(c_z \Phi c_z^T + V_{\bar{v}\bar{v}} \right)^{-1} \tag{3.32}$$

with Φ solving

$$\Phi = A_z \left(\Phi - \Phi c_z^T \left(c_z \Phi c_z^T + V_{\bar{v}\bar{v}} \right)^{-1} c_z \Phi \right) A_z^T + V_{\bar{w}\bar{w}}. \tag{3.33}$$

As a result, the residual generator in Eq.(3.19)-(3.20) delivers an innovation sequence whose variance is:

$$\mathbf{E}\left(r_i r_j \right) = \left(c_z \Phi c_z^T + V_{\bar{v}\bar{v}} \right) \delta_{ij} \tag{3.34}$$

The design procedure is summarized in the following algorithm:

Algorithm DOKF: Design of data-driven Kalman filter

- Estimate state sequence $\hat{Z}_{i+s}$ and $\hat{Z}_{i+s-1}$

- Estimate $\bar{W}$ and $\bar{V}$ from the results in Eq.(3.30) and (3.31)

- Determine the variance and covariance $\bar{W}$ and $\bar{V}$ and solve discrete time Riccati equation in (3.33)

- Compute Kalman filter gain L_{kf} as shown in Eq.(3.33)

3.1.4 Residual evaluation

An efficient residual generator with a suitable post-processing mechanism will enhance the performance of overall FDI system by making it robust against stochastic disturbances and sensitive to faults. This entails selecting a residual evaluation method and a threshold depending upon allowable false alarm rate and missed detections. To this end, the generalized likelihood ratio (GLR) based method can be adopted here. The fault is assumed as an additive change in the residual signal:

$$r_k = \varepsilon_k + f_k, f = \begin{cases} 0 : \text{fault-free} \\ \neq 0 : \text{faulty} \end{cases},$$

where $\varepsilon_k \in N(0, \sigma_r^2)$. The GLR based technique involves squaring the normal (Gaussian) distributed residual signal and therefore the threshold is selected

from χ^2 distribution table. The confidence interval α is generally selected by the user which determines the false alarm and missed detection rate [47]. The steps to determine the threshold for fault detection are summarized as:

Algorithm JTH: Residual evaluation and threshold selection

- Determine χ_α from χ^2 distribution table with 1-degree of freedom and confidence interval α

- Set threshold $J_{th} = \chi_\alpha$

- Define testing statistic

$$J = \frac{1}{2\sigma_r^2 N} \left(\sum_{i=1}^{N} r_i \right)^2$$

- Define detection logic

$$J = \begin{cases} < J_{th}, \text{no fault} \\ > J_{th}, \text{a fault is detected} \end{cases}$$

Based on the theory presented so far, other diagnostic features such as fault isolation and sensor reconstruction can be introduced now. The proceeding section deals with the data-driven procedure to isolate sensor faults.

3.2   Sensor fault isolation

It is important in an industrial application with several components to quickly locate where the fault has originated. Therefore, a data-driven method based on PSi is presented in this section. It is assumed that the sensor fault can be modeled with the help of following output equation:

$$y_k = Cx_k + Du_k + v_k + f_{sen,k} \tag{3.35}$$

$$y_k = \begin{bmatrix} y_{1,k} \\ \vdots \\ y_{m,k} \end{bmatrix}, f_{sen,k} = \begin{bmatrix} f_{1,sen} \\ \vdots \\ f_{m,sen} \end{bmatrix}, C = \begin{bmatrix} c_1 \\ \vdots \\ c_m \end{bmatrix}, D = \begin{bmatrix} d_1 \\ \vdots \\ d_m \end{bmatrix}.$$

Based on this, a parity space based residual generator can be defined as:

$$r_{i,k} = \upsilon_{i,s} y_{k,s} - \rho_{i,s} u_{k,s} = \upsilon_{i,s} f_{sen,k}. \tag{3.36}$$

with $i = 1, \cdots, sm - n$. Similarly, the error dynamics of the diagnostic observer can be described as

$$
\begin{align}
e_{i,k+1} &= \bar{A}_{z,i} e_{i,k} + T_i w_k - L v_k - L f_{sen,k} \tag{3.37}\\
r_{i,k} &= c_{z,i} e_{i,k} + g_i v_k + g_i f_{sen,k}. \tag{3.38}
\end{align}
$$

For the design of fault isolation scheme, the parity space is divided in s_f blocks,

$$
v_s = \begin{bmatrix} v_{s,0} & v_{s,1} & \cdots & v_{s,s_f} \end{bmatrix} \in \mathbf{R}^{\eta \times s_f m}
$$

where $v_{s,i} \in \mathbf{R}^{\eta \times m}, i = 1, \cdots, s_f$. It is required now to obtain a diagonal structure by multiplying v_s from left. To this end, following linear equations must be solved:

$$
\begin{align}
\bar{P} v_{s,j} &= 0, j = \xi + 1, \cdots, s_f\\
\bar{P} v_{s,j} &= diag \begin{pmatrix} \bar{v}_{1,j} & \bar{v}_{2,j} & \cdots & \bar{v}_{m,j} \end{pmatrix}, j = 0, \cdots, \xi
\end{align}
$$

where $\bar{P} \in \mathbf{R}^{m \times \eta}, \xi \leq n$ and $\bar{v}_{i,j}$ are arbitrary constants. This simple construction allows following residual generator in vector form:

$$
r_k = \bar{P} v_s (y_{k,s} - H_{u,f} u_{k,s}) \tag{3.39}
$$

and in scalar form:

$$
r_{k,j} = v_j (y_{k,j} - H_{u,j} u_{k,j}), j = 1, \cdots, m. \tag{3.40}
$$

The secondary form of residual generator is constructed according to the steps mentioned in algorithm PS2DO. It has following form:

$$
\begin{align}
z_{i,k+1} &= A_{z,i} z_{i,k} + B_{z,i} u_k + L_i y_{i,k} - L_{o,i} r_{i,k} \tag{3.41}\\
r_{i,k} &= g_i y_{i,k} - c_{z,i} z_{i,k} - d_{z,i} u_k, i = 1, \cdots, m \tag{3.42}
\end{align}
$$

$$
B_{z,i} = \begin{bmatrix} \rho_{i,0} \\ \vdots \\ \rho_{i,\xi-1} \end{bmatrix}, L_i = - \begin{bmatrix} v_{i,0} \\ \vdots \\ v_{i,\xi-1} \end{bmatrix}
$$

$$
g_i = v_{i,\xi}, d_{z,i} = \rho_{i,\xi}, i = 1, \cdots, m
$$

Note here that this type of bank of residual generator is inspired by earlier work in [43], [113]. As mentioned earlier, for enhanced performance, it is necessary to design a proper residual evaluation scheme and a suitable threshold. Then it is sufficient to conclude that fault has occurred in the ith sensor, if i^{th} residual signal is larger than its threshold value.

3.3   Construction of soft-sensor

A soft-sensor is an analytical redundancy based solution to monitor health of the sensor itself. Principally, measurements from all the sensors, excluding the one under consideration are utilized to reconstruct its measurement. If the process model is available, a soft-sensor can be realized by a single output observer. But the motivation behind the method presented here is to design it directly from the test data obtained from the plant.

The problem is formulated as: *Given the identified* $\Gamma_s^\perp, \Gamma_s^\perp H_{u,f}$, *process input data* u_k *and sensor signals* $y_{1,k}, \cdots, y_{i-1,k}, y_{i+1,k}, \cdots, y_{m,k}$, *find an estimate for* $y_{i,k}$. The solution is summarized in the following theorem.
Theorem: Given the process model in (3.1)-(3.2) and assuming that the pair $(\bar{C}_i, A)$ *is observable, where*

$$\bar{C}_i = \left[\begin{array}{ccccccc} c_1^T & \cdots & c_{i-1}^T & c_{i+1}^T & \cdots & c_m^T \end{array} \right]^T \in \mathbf{R}^{(m-1)\times n}$$

then there exists a (row) vector $p \in \mathbf{R}^{s_f m}$ *satisfying*

$$p\Gamma_{s_f-1}^\perp := \alpha_{s_f-1} = \left[\begin{array}{cccc} \alpha_{n-1} & 0 & \cdots & 0 \end{array} \right], \alpha_{n-1} \in \mathbf{R}^{nm} \qquad (3.43)$$

$$\alpha_{n-1} = \left[\begin{array}{cccc} \alpha_{n-1,0} & \cdots & \alpha_{n-1,n-2} & \alpha_{n-1,n-1} \end{array} \right]$$

$$\alpha_{n-1,j} = \left[\begin{array}{cccccc} \alpha_{j,1}^{n-1} & \cdots & \alpha_{j,i-1}^{n-1} & 0 & \alpha_{j,i+1}^{n-1} & \cdots & \alpha_{j,m}^{n-1} \end{array} \right] \in \mathbf{R}^m, j = 0, \cdots, n-2$$

$$\alpha_{n-1,n-1} = \left[\begin{array}{cccccc} \alpha_{n-1,1}^{n-1} & \cdots & \alpha_{n-1,i-1}^{n-1} & -1 & \alpha_{n-1,i+1}^{n-1} & \cdots & \alpha_{n-1,n-1}^{n-1} \end{array} \right] \in \mathbf{R}^m$$

Proof [20]: Note that α_{s_f-1} defined in Eq.(3.43) gives

$$\alpha_{s_f-1}\Gamma_{s_f-1} = \bar{\alpha}_{n-1} \left[\begin{array}{c} \bar{C}_i \\ \bar{C}_i A \\ \vdots \\ \bar{C}_i A^{n-1} \end{array} \right] - c_i A^{n-1}.$$

Since $(\bar{C}_i, A)$ is observable, for $c_i A^{n-1}$, an $\bar{\alpha}_{n-1}$ defined by (3.45) can be found so that

$$\bar{\alpha}_{n-1} \left[\begin{array}{c} \bar{C}_i \\ \bar{C}_i A \\ \vdots \\ \bar{C}_i A^{n-1} \end{array} \right] = c_i A^{n-1} \Longrightarrow \bar{\alpha}_{n-1} \left[\begin{array}{c} \bar{C}_i \\ \bar{C}_i A \\ \vdots \\ \bar{C}_i A^{n-1} \end{array} \right] - c_i A^{n-1} = \alpha_{s_f}\Gamma_{s_f-1} = 0.$$

This proves that α_{s_f-1} is a parity vector. Remember that p satisfies

$$p\Gamma_{s_f-1}^\perp H_{s_f-1,u} = \left[\begin{array}{cccc} \alpha_{n-1}H_{n-1,u} & 0 & \cdots & 0 \end{array} \right].$$

A parity space based residual generator with α_{n-1} and $\alpha_{n-1}H_{n-1,u}$ can be constructed as:

$$r_k = \alpha_{n-1}y_{n-1,k} - \alpha_{n-1}H_{n-1,u}u_{n-1,k} \qquad (3.44)$$

which leads to

$$r_k = \bar{\alpha}_{n-1}\bar{y}_{i,n-1,k} - \alpha_{n-1}H_{n-1,u}u_{n-1,k} - y_{i,k} = 0$$

$$\bar{y}_{i,n-1,k} = \begin{bmatrix} \bar{y}_{i,k-n+1} \\ \vdots \\ \bar{y}_{i,k} \end{bmatrix}, \bar{y}_{i,k-j} = \begin{bmatrix} y_{1,k-j} \\ \vdots \\ y_{i-1,k-j} \\ y_{i+1,k-j} \\ \vdots \\ y_{m,k-j} \end{bmatrix}$$

$$\bar{\alpha}_{n-1} = \begin{bmatrix} \bar{\alpha}_{n-1,0} & \cdots & \bar{\alpha}_{n-1,n-1} \end{bmatrix} \in \mathbf{R}^{n(m-1)} \qquad (3.45)$$

$$\bar{\alpha}_{n-1,j} = \begin{bmatrix} \alpha_{j,1}^{n-1} & \cdots & \alpha_{j,i-1}^{n-1} & \alpha_{j,i+1}^{n-1} & \cdots & \alpha_{j,m}^{n-1} \end{bmatrix} \in \mathbf{R}^{(m-1)},$$

where $j = 0, \cdots, n-1$ and in the observer form

$$z_{k+1} = A_z z_k + B_z u_k + \bar{L}_i \bar{y}_{i,k}, \qquad (3.46)$$
$$r_k = \bar{g}_i \bar{y}_{i,k} - c_z z_k - d_z u_k - y_{i,k} \qquad (3.47)$$

with $\bar{L}_i = -\begin{bmatrix} \bar{\alpha}_{n-1,0} \\ \vdots \\ \bar{\alpha}_{n-1,n-2} \end{bmatrix}, \bar{g}_i = \bar{\alpha}_{n-1,n-1}.$

As a result, $y_{i,k}$ can be estimated by the primary residual generator:

$$\hat{y}_{i,k} = \bar{\alpha}_{n-1}\bar{y}_{n-1,k} - \alpha_{n-1}H_{n-1,u}u_{n-1,k} \qquad (3.48)$$

or by the secondary residual generator:

$$z_{k+1} = A_z z_k + B_z u_k + \bar{L}_i \bar{y}_{i,k}, \qquad (3.49)$$
$$\hat{y}_{i,k} = \bar{g}_i \bar{y}_{i,k} - c_z z_k - d_z u_k. \qquad (3.50)$$

Thus, the diagnostic observer based secondary residual generator delivers the output of ith sensor based on the rest of the measurements.

3.4 Isolation of actuator faults

Similar to the problem mentioned in section 3.2 for sensors, actuator faults can also be isolated. Assume that the process model is given by Eqs.(3.1)-

(3.2), where the actuator fault is denoted by f_{act}, i.e.

$$x_{k+1} = Ax_k + Bu_k + Bf_{act,k} + w_k \qquad (3.51)$$

$$y_k = Cx_k + Du_k + Df_{act,k} + v_k, f_{act,k} = \begin{bmatrix} f_{1,act,k} \\ \vdots \\ f_{l,act,k} \end{bmatrix}$$

In the presence of a fault, the dynamics of the primary form of residual generator can be described as

$$r_k = \alpha_s \begin{bmatrix} D & 0 & \cdots & 0 \\ CB & D & \cdots & 0 \\ \vdots & \ddots & \ddots & \vdots \\ CA^{s-1}B & \cdots & CB & D \end{bmatrix} f_{s,act,k}, f_{s,act,k} = \begin{bmatrix} f_{act,k-s} \\ \vdots \\ f_{act,k} \end{bmatrix} \qquad (3.52)$$

and that of the secondary form as

$$\begin{aligned} e_{k+1} &= \bar{A}_z e_k + Tw_k - \bar{L}v_k - \left(TB - \bar{L}D\right) f_{act,k} & (3.53) \\ r_k &= c_z e_k + gv_k + gDf_{act,k}. & (3.54) \end{aligned}$$

For the sake of convenience, a new notation form is introduced as follows:

$$\begin{aligned} \bar{B}_i &= \begin{bmatrix} b_1 & \cdots & b_{i-1} & b_{i+1} & \cdots & b_l \end{bmatrix}, \\ H_{s,\bar{u}_i} &= \begin{bmatrix} \bar{D}_i & 0 & \cdots & 0 \\ C\bar{B}_i & \bar{D}_i & \cdots & 0 \\ \vdots & \ddots & \ddots & \vdots \\ CA^{s-1}\bar{B}_i & \cdots & C\bar{B}_i & \bar{D}_i \end{bmatrix}, H_{s,u_i} = \begin{bmatrix} d_i & 0 & \cdots & 0 \\ Cb_i & d_i & \cdots & 0 \\ \vdots & \ddots & \ddots & \vdots \\ CA^{s-1}b_i & \cdots & Cb_i & d_i \end{bmatrix}. \end{aligned}$$

Let $s = n$. Then, a matrix $P \in \mathbf{R}^{(\beta-n) \times \beta}, \beta = (n+1)m$, can be found so that

$$P\Gamma_{s_f-1}^{\perp} = \begin{bmatrix} \Phi & 0 & \cdots & 0 \end{bmatrix}, \Phi \in \mathbf{R}^{(\beta-n) \times \beta}, rank\left(\Phi\right) = \beta - n$$

which also leads to

$$P\Gamma_{s_f-1}^{\perp} H_{s_f-1,u} = \begin{bmatrix} \Phi H_{n,u} & 0 & \cdots & 0 \end{bmatrix}. \qquad (3.55)$$

Under the assumption that

$$(n+1)l - n \leq rank\left(\Phi H_{n,u}\right) \leq (n+1)m - n \implies (s+1)l \leq (s+1)m \quad (3.56)$$

which is interpreted as the isolability of the l actuator faults, it leads to

$$\bar{H}^{\perp}_{n,\bar{u}_i} P\Gamma^{\perp}_{s_f-1} H_{s_f-1,u} = \bar{H}^{\perp}_{n,\bar{u}_i} \Phi H_{n,u_i} \neq 0$$

$$\bar{H}^{\perp}_{n,\bar{u}_i} = I - \Phi H_{n,\bar{u}_i} \left(H^T_{n,\bar{u}_i} \Phi^T \Phi H_{n,\bar{u}_i} \right)^{-1} H^T_{n,\bar{u}_i} \Phi^T, i = 1, \cdots, l \qquad (3.57)$$

since $\bar{H}^{\perp}_{n,\bar{u}_i} \Phi H_{n,\bar{u}_i} = 0$,

$$rank\left(\Phi H_{n,\bar{u}_i}\right) \leq (n+1)(l-1) < (n+1)l - n.$$

Therefore, an $\alpha_i \in \mathbf{R}^{(\beta-n)}, i = 1, \cdots, l$, can be found so that

$$\alpha_i \bar{H}^{\perp}_{n,\bar{u}_i} \Phi H_{n,u_i} \neq 0 \qquad (3.58)$$

which allows construction of l residual generators

$$r_{i,k} = \alpha_i \bar{H}^{\perp}_{n,\bar{u}_i} \Phi y_{n,k} - \alpha_i \bar{H}^{\perp}_{n,\bar{u}_i} \Phi H_{n,u} u_{s,k} = \alpha_i \bar{H}^{\perp}_{n,\bar{u}_i} \Phi H_{n,u_i} f_{s,i,act,k} \qquad (3.59)$$

$$f_{s,i,act,k} = \begin{bmatrix} f_{i,act,k-s} \\ \vdots \\ f_{i,act,k} \end{bmatrix}, i = 1, \cdots, l.$$

It is evident that these l residual generators yield an isolation of the actuator faults. Let

$$\bar{\alpha}_i = \alpha_i \bar{H}^{\perp}_{n,\bar{u}_i} \Phi, \bar{\alpha}_i H_{n,u} = \alpha_i \bar{H}^{\perp}_{n,\bar{u}_i} \Phi H_{n,u}, i = 1, \cdots, l$$

then following (3.53)-(3.54), corresponding to (3.59), l observer based residual generators can also be constructed

$$z_{i,k+1} = A_{z,i} z_{i,k} + B_{z,i} u_k + L_{i,k} y_k - L_{o,i} r_{i,k} \qquad (3.60)$$

$$r_{i,k} = g_i y_{i,k} - c_{z,i} z_{i,k} - d_{z,i} u_k. \qquad (3.61)$$

As the last step, an appropriate residual evaluation and threshold must also be selected. Then, if i^{th} residual signal crosses its threshold, it can be concluded that a fault in i^{th} actuator has occurred.

3.5   Concluding remarks

In this chapter, the novel approach to design data-driven fault detection and isolation systems is presented. This work is based on author's publications, for instance [19], [20]. The core of this method is the identification of a primary form of residual generator in terms of the parity space. To do so, it is

not necessary to identify the complete state space model. A secondary residual generator is also designed for the sake of efficient on-line implementation and enhanced performance. A detailed procedure to identify a Kalman filter gain directly from the data is also provided.

As one of its several important features, the novel method does not rely on exact knowledge of the model order. The order of the parity space is determined simply from the singular value decomposition. For the design of secondary observer, the relationship between the parity space and the solution of Luenberger equation is exploited. The design is extended to the sensor and actuator fault isolation schemes. A diagnostic system for sensor itself is also developed by designing a data-driven soft-sensor.

Extending this concept in the forthcoming chapters, two important problems are discussed with the help of this novel data-driven approach. The first problem deals with the uncertain parameter variation within the plant and its effect on fault detection performance. It is solved by recursively estimating the design vectors of the primary residual generator. The second problem considers the problem of optimal identification of parity vectors and it is solved by closed-loop identification framework.

Chapter 4

Adaptive designs of FD systems

The novel approach to design data-driven FD systems is suitable for plants with little or no *a priori* knowledge about their mathematical model. This idea can be extended to broader class of dynamic systems. In this chapter, a class of nonlinear systems, i.e. parameter-varying linear systems, is considered. It is because large-scale processes often exhibit such behavior if one or more of their parameters vary with time. For instance, a chemical reactor may have multiple operating regions depending on its input feed.

Linear parameter-varying systems (LPV) are also dealt within the model identification based on subspace techniques. See [77], [81], [82]. Felici et al., Verhaegen and Yu have designed identification methods for periodically varying systems [33], [106], whereas Kameyama and Ohsumi, Liu have proposed SIM for arbitrary time-varying systems [61], [74]. But in complex systems with several hundred measured variables, it is difficult to apply such techniques because of the CPU memory and processing constraints.

Therefore, the identification-oriented design for FD systems is treated here as that of adaptive subspace tracking problem. It is solved by recursive estimation technique which is more interesting because of its consistency and on-line computation cost. There are several such algorithms popularly used in signal processing application. See e.g. [9], [10], [16], [45], [114]. Each technique has its own advantage and disadvantage which eventually depends upon the application.

In the present work, two efficient FD systems based on perturbation theory of eigenvalues and orthogonal iteration are proposed for LPV system. The algorithms are numerically robust as they do not involve any computation of matrix inverse and produce consistent estimates of the parameters. The next section formulates the design problem of adaptive FD system and the later sections provide mathematical background and the detailed algorithms.

4.1   Problem formulation

The novel data-driven design of FD system in chapter 3 requires only the identification of $\Gamma_s^\perp$ and $\Gamma_s^\perp H_{u,f}$. The residual signal of either primary or secondary residual generator is close to zero if the process operates under normal conditions and no fault occurs. Since residual generation implicitly depend on the model parameters, which are held constant, any deviation from this assumption will result in significant residual variance and false alarms. Therefore, for the plants with frequent deviations in the nominal values of their parameters, it is important to recursively adapt the residual generators.

A parameter varying linear system is described with following state space equations modified from Eq.(2.1)-(2.2):

$$x_{k+1} \;=\; A\left(\theta_k\right) x_k + B\left(\theta_k\right) u_k + w_k \tag{4.1}$$

$$y_k \;=\; C\left(\theta_k\right) x_k + D\left(\theta_k\right) u_k + v_k \tag{4.2}$$

where θ_k is the time varying parameter. For instance, it can represent a shift in the operating point or change in one of the coefficients of A, B, C or D. For Eq.(4.1)-(4.2), the extended state space equation (similar to Eq.(3.5)) can be written as:

$$Y_{f,s} = \Gamma_s\left(\theta_k\right) X_{k-s+1} + H_{u,f}\left(\theta_k\right) U_{f,s}^k + H_{w,f}\left(\theta_k\right) W_{f,s}^k + V_{f,s}^k \tag{4.3}$$

where $Y_{f,s}^k$ and $U_{f,s}^k$ are constructed in the same way as in algorithm PSi. The remaining unknown matrices are defined as

$$\Gamma_s\left(\theta_k\right) = \begin{bmatrix} C\left(\theta_k\right) \\ C\left(\theta_k\right) A\left(\theta_k\right) \\ \vdots \\ C\left(\theta_k\right) A^{s-1}\left(\theta_k\right) \end{bmatrix}$$

and

$$H_{u,f}\left(\theta_k\right) = \begin{bmatrix} D\left(\theta_k\right) & O & \cdots & O \\ C\left(\theta_k\right) B\left(\theta_k\right) & D\left(\theta_k\right) & \ddots & \vdots \\ \vdots & & \ddots & O \\ C\left(\theta_k\right) A^{s-2}\left(\theta_k\right) B\left(\theta_k\right) & C\left(\theta_k\right) A^{s-1}\left(\theta_k\right) B\left(\theta_k\right) & \cdots & D\left(\theta_k\right) \end{bmatrix}.$$

The matrix, $H_{w,f}\left(\theta_k\right)$ can be defined similar to $H_{u,f}\left(\theta_k\right)$. Thus, to design an adaptive primary residual generator, a time-dependent orthogonal complement of $\Gamma_s\left(\theta_k\right)$ is required, i.e.

$$P_s\left(\theta_k\right) = \{v_s\left(\theta_k\right) \Gamma_s\left(\theta_k\right) = 0, \forall v_s\left(\theta\right) \in P_s\left(\theta_k.\right)\} \tag{4.4}$$

Then the residual generator will have following form:

$$r_k = v_s\left(\theta_k\right)Y_s - \rho_s\left(\theta_k\right)U_s, \tag{4.5}$$

where $v_s\left(\theta_k\right) \in \Gamma_s^\perp\left(\theta_k\right)$ and $\rho_s\left(\theta_k\right) \in \Gamma_s^\perp\left(\theta_k\right)H_{u,f}\left(\theta_k\right)$. The secondary residual generator is constructed by transforming the primary form with following matrices:

$$A_z = \begin{bmatrix} 0 & 0 & \cdots & -l_0 \\ 1 & 0 & \cdots & -l_1 \\ \vdots & \vdots & \vdots & \vdots \\ 0 & 0 & 1 & -l_{s-2} \end{bmatrix}, B_z = \begin{bmatrix} \rho_0\left(\theta_k\right) \\ \rho_1\left(\theta_k\right) \\ \vdots \\ \rho_{s-2}\left(\theta_k\right) \end{bmatrix} + \begin{bmatrix} l_0 \\ l_1 \\ \vdots \\ l_{s-2} \end{bmatrix} \rho_{s-1}\left(\theta_k\right)$$

$$L = \begin{bmatrix} v_0\left(\theta_k\right) \\ v_1\left(\theta_k\right) \\ \vdots \\ v_{s-2}\left(\theta_k\right) \end{bmatrix} + \begin{bmatrix} l_0 \\ l_1 \\ \vdots \\ l_{s-2} \end{bmatrix} v_{s-1}\left(\theta_k\right), d_z = \rho_{s-1}\left(\theta_k\right), g_z = v_{s-1}\left(\theta_k\right).$$

where $L_o = \begin{bmatrix} l_1 & l_2 & \cdots & l_{s-2} \end{bmatrix}^T$ is feedback gain such that $A_z - L_o c_z$ is stable and is constant. Based on these equations, an adaptive diagnostic observer can be designed as:

$$z_{k+1} = A_z z_k + B_{z,\theta} u_k + L_{z,\theta} y_k - L_o r_k \tag{4.6}$$

$$y_k = c_z z_k + d_{z,\theta} u_k + g_{z,\theta} y_k \tag{4.7}$$

Thus the computation cost of adaptation is only in the recursive identification of the primary residual generator. It has been shown in Eq. (3.14), that the primary form is constructed from the singular vectors belonging to the smallest singular values of the product term $Z_f Z_p^T$. Therefore, the adaptive design of FD system transforms into that of recursive updating of the singular values and singular vectors.

4.2 Recursive subspace tracking

One solution to above mentioned problem is the approximate eigendecomposition technique. The first method proposed here is based on the perturbation theory of eigenvalues (and eigenvectors) of positive definite matrices [29], [84], [85]. It is well established and requires no complex mathematics. The second technique has even more attractive feature, in that, it does not need updating the entire eigendecomposition if only a single eigenvector is to be tracked [29], [85], [116]. Hence, the on-line computation cost of adaptation is significantly reduced. In the next subsection, the perturbation theory based method is presented.

4.2.1   First order perturbation theory

For the application under consideration, only the first order perturbation theory is discussed because the second and higher order perturbations are generally negligible [96]. To begin with, consider a vector of sampled measurement $z_k \in \mathbf{R}^q$. Its covariance matrix can be defined as

$$\Phi_z = \frac{1}{N} \sum_{j=1}^{N} z_j z_j^T \in \mathbf{R}^{q \times q} \tag{4.8}$$

where N is the sample length. Assume that Φ_z is a positive definite matrix at time k, then its eigenvalue equation can be written as:

$$\Phi_{z,k} v_{i,k} = \lambda_{i,k} v_{i,k} \tag{4.9}$$
$$v_i^T v_j = \delta_{ij}. \tag{4.10}$$

where δ_{ij} is Kronecker delta. The covariance could also be computed recursively as:

$$\Phi_{z,k} = \alpha \Phi_{z,k-1} + (1 - \alpha) z_k z_k^T \tag{4.11}$$

where α is a forgetting factor such that $0 \leq \alpha \leq 1$. This equation is transformed in a more useful form as:

$$\Phi_{z,k} = \Phi_{z,k-1} + \varepsilon \left(z_k z_k^T - \Phi_{z,k-1} \right) \tag{4.12}$$

where $\varepsilon = 1 - \alpha$. It follows from the fundamental theory of perturbation of positive definite matrices that the eigenvalues and eigenvectors can be expanded in the power series form as:

$$v_{i,k} = v_{i0,k} + \varepsilon v_{i1,k} + \varepsilon^2 v_{i2,k} + \cdots, v_{i0,k} = v_{i,k-1} \tag{4.13}$$
$$\lambda_{i,k} = \lambda_{i0,k} + \varepsilon \lambda_{i1,k} + \varepsilon^2 \lambda_{i2,k} + \cdots, \lambda_{i0,k} = \lambda_{i,k-1}. \tag{4.14}$$

Since first order perturbation analysis is generally sufficient for slow varying processes, the terms of order higher than one are omitted [10]. If the two terms in Eq.(4.11) are defined separately,

$$\Phi_0 = \Phi_{z,k-1} \tag{4.15}$$
$$\Phi_1 = z_k z_k^T - \Phi_{z,k-1}. \tag{4.16}$$

Substituting Eq.(4.15)-(4.16) in Eq.(4.14) and collecting the terms with equal power of ε,

$$\Phi_0 v_{i0} + \varepsilon \left(\Phi_0 v_{i1} + \Phi_1 v_{i0} \right) = \lambda_{i0} v_{i0} + \varepsilon \left(\lambda_{i0} v_{i1} + \lambda_{i1} v_{i0} \right). \tag{4.17}$$

Eq.(4.17) is valid within a small neighborhood ε. Equating the terms with the same power,

$$\Phi_0 v_{i0} = \lambda_{i0} v_{i0} \tag{4.18}$$

$$\Phi_0 v_{i1} + \Phi_1 v_{i0} = \lambda_{i0} v_{i1} + \lambda_{i1} v_{i0}. \tag{4.19}$$

With these two equation and from Eq.(4.12), the task is to find out the unknown parameters λ_{i1}, and v_{i1}. Multiplying Eq.(4.19) with v_{i0}^T gives

$$\lambda_{i1} = v_{i0}^T \Phi_1 v_{i0}. \tag{4.20}$$

Similarly, multiplying Eq.(4.19) with $v_{j0}^T, j \neq i$ gives

$$(\lambda_{j0} - \lambda_{i0}) v_{j0}^T v_{i1} = -v_{j0}^T \Phi_1 v_{i0}. \tag{4.21}$$

From Eq.(4.12) and using orthonormality of eigenvectors, another useful relation can be written as:

$$v_{i1}^T v_{j0} + v_{i0}^T v_{j1} = 0. \tag{4.22}$$

Equations (4.20)-(4.22) provide the basic set of equations to find the unknowns λ_{i1} and v_{i1} for $i = 1, \cdots, q$. The eigenvalues are updated as:

$$\lambda_{k,i} = \alpha \lambda_{k-1,i} + (1 - \alpha) v_{k-1,i}^T z_k z_k^T v_{k-1,i} \tag{4.23}$$

for each $i = 1, \cdots, q$. Similarly, for the eigenvectors

$$v_{k,i} = v_{k-1,i} + \sum_{j=1}^{q} b_{ji} v_{k-1,j} \tag{4.24}$$

where $b_{ii} = 0$ and

$$b_{ji} = \frac{v_{k-1,i}^T z_k z_k^T v_{k-1,j}}{(\lambda_{k-1,i} - \lambda_{k-1,j})}, b_{ij} = -b_{ji}$$

Since algorithm PSi uses singular value decomposition (SVD) which is nothing but eigenvalue decomposition of square of the matrix, the main results are summarized for SVD as well. To this end, a multi-dimensional signal $z_k \in \mathbf{R}^q$ with a total of N samples of it is considered.

$$Z_k = \begin{bmatrix} z_{k,1} & z_{k+1,1} & \cdots & z_{k+N-1,1} \\ z_{k,2} & z_{k+1,2} & \cdots & z_{k+N-1,2} \\ \vdots & \vdots & \ddots & \vdots \\ z_{k,q} & z_{k+1,q} & \cdots & z_{k+N-1,q} \end{bmatrix} \in \mathbf{R}^{q \times N} \tag{4.25}$$

Similarly, $Z_\tau \in \mathbf{R}^{q \times N}$ consisting of instrument variables is also defined. As instrument variable, set of past measurements Z_τ is considered. It is defined as

$$Z_\tau = \begin{bmatrix} z_{k-\tau,1} & z_{k-\tau+1,1} & \cdots & z_{k-\tau+N,1} \\ z_{k-\tau,2} & z_{k-\tau+1,2} & \cdots & z_{k-\tau+N,2} \\ \vdots & \vdots & \ddots & \vdots \\ z_{k-\tau,q} & z_{k-\tau+1,q} & \cdots & z_{k-\tau+N,2} \end{bmatrix} \in \mathbf{R}^{q \times N}. \tag{4.26}$$

The product of Z_k and Z_τ for N samples is denoted by $\Phi_z \in \mathbf{R}^{q \times q}$ and it is computed as

$$\Phi_z = \frac{1}{N} Z_k Z_\tau^T. \tag{4.27}$$

In a non-stationary environment, it is also calculated recursively as

$$\Phi_{z,k} = \alpha \Phi_{z,k-1} + (1-\alpha) z_k z_\tau^T \tag{4.28}$$

where α is a suitably chosen forgetting factor in the range $[0, 1]$. It should be noted that by definition, Φ_z is a positive definite matrix and represents the product in *Step 2* of PSi. The SVD of $\Phi_{z,k}$ then gives,

$$\Phi_{z,k} = U_k \Sigma_k V_k^T, \tag{4.29}$$

$$U_k U_k^T = I, V_k^T V_k = I, \tag{4.30}$$

where $U_k \in \mathbf{R}^{q \times q}$ and $V_k \in \mathbf{R}^{q \times q}$ are matrices containing left and right singular vectors and $\Sigma = diag(\sigma_1, \sigma_2, \cdots, \sigma_q)$. Equation (4.29) can be also rewritten in a recursive manner as

$$\Phi_{z,k} = \Phi_{z,k-1} + E = U_{k-1}(\Sigma_{k-1} + F) V_{k-1}^T, \tag{4.31}$$

where $E \in \mathbf{R}^{q \times q}$ is the first order perturbation matrix. The matrix $F \in \mathbf{R}^{q \times q}$ is straight-forward to compute,

$$F = U_{k-1}^T E V_{k-1}.$$

Lemma 1 [99]: If all the singular values of Φ_{k-1} are simple and the perturbation matrix $E \to 0$, then the singular vectors and singular values of the updated matrix Φ_k can be described as

$$\bar{U}_k = U_{k-1}(I + P) \quad \text{and} \quad \bar{V}_k = V_{k-1}(I + Q)$$
$$\sigma_{k,i} = \sigma_{k-1,i} + f_{ii} + O(\|E\|^2)$$

where f_{ii} is an element of F. The elements of matrices P and Q are given as for $i = j$, $p_{ij} = q_{ij} = 0$,

for $i < j$,

$$p_{ji} = \frac{\sigma_{k-1,i} f_{ji} + \sigma_{k-1,j} f_{ij}^*}{\sigma_{k-1,i}^2 - \sigma_{k-1,j}^2} + O\left(\|E\|^2\right) \tag{4.32}$$

$$q_{ji} = \frac{\sigma_{k-1,i} f_{ij}^* + \sigma_{k-1,j} f_{ji}}{\sigma_{k-1,i}^2 - \sigma_{k-1,j}^2} + O\left(\|E\|^2\right), \tag{4.33}$$

for $i > j$, $p_{ji} = -p_{ij}^T$, $q_{ji} = -q_{ij}^T$.

Willink [112] has suggested that the overall complexity of the algorithm could be much lowered, if we assume additionally that $\sigma_i \gg \sigma_i + 1$. The new update equations of matrix P, Q are then given simply as

$$p_{ji} = \frac{f_{ji}}{\sigma_{k-1,i}}, q_{ji} = \frac{f_{ij}}{\sigma_{k-1,j}} \qquad \text{for } i < j.$$

This lemma provides a basis for the recursive algorithm to identify the parity space vectors.

4.2.2 FDPM based recursive subspace tracking

The second technique for adaptive design of FD system is based on data projection method (DPM) [23], [115]. It is adaptive version of the so-called orthogonal iteration procedure (OIP), which is relatively old numerical method to compute singular vectors corresponding to the most dominant singular values of a nonnegative definite, symmetric matrix [44]. The complexity of DPM is naturally lower than performing SVD at each step. Its performance can be further improved by the so-called fast DPM proposed in [23], [24].

The fast DPM (FDPM) takes the advantage of the fact that in many applications instead of true singular vectors, projection onto their range space is more important. The application of such low complexity subspace tracking algorithms is to track singular vectors of the most dominant singular values, also called signal subspace. But it has also been successfully used in noise subspace tracking, i.e. orthogonal complement of the signal subspace. It is robust against the round-off errors and its convergence rate is exponential. The method is explained next with the help of following lemma.

Lemma 2 [24]: Let $\Phi_z \in \mathbf{R}^{q \times q}$ be a symmetric, nonnegative matrix with the singular values σ_i and the corresponding singular vectors u_i, where $i = 1, \cdots, q$ and

$$\sigma_1 \geq \cdots \sigma_p > \sigma_{p+1} \geq \cdots \geq \sigma_q \geq 0.$$

Also, let $U_j \in \mathbf{R}^{q \times p}$ be the sequence of matrices defined by the iteration

$$U_j = orthnorm\left\{\Phi_z U_{j-1}\right\}, j = 1, 2, \cdots, \tag{4.34}$$

then

$$\lim_{j \to \infty} U_j = \begin{bmatrix} u_1 & \cdots & u_p \end{bmatrix},$$

where *orthnorm* denotes the orthonormalization procedure using QR decomposition or Gram-Schmidt procedure.

The covariance matrix Φ_z is defined as shown in Eq.(4.27) and its recursive estimate $\Phi_{z,k}$ as in Eq.(4.28). According to above lemma, the sequence of matrices U_j composed of eigenvectors corresponding to either the most dominant or the smallest eigenvalues can be represented as:

$$U_j = orthnorm \left\{ (I_q \pm \mu \Phi_{z,k}) U_{j-1} \right\} \tag{4.35}$$

where $+$ and $-$ gives estimates of *signal* and *noise* space, respectively. This alternate algorithm has complexity equal to $O(q^2 p)$, where p is the number of dominant singular values [24].

In the majority of subspace tracking applications, the focus is on the projection onto the range space of the true singular vectors than the true singular vectors themselves. Thus U_j can be treated as the projection operator and the convergence of $U_j U_j^T$ can be estimated recursively. This has enabled the development of the alternative of OIP, called data projection method (DPM) [115].

4.2.3   Fast DPM

The identification techniques generally require that U_j is orthonormal. In FDPM, this property is slightly compromised in achieving additional cost saving in going from $O(q^2 p)$ to $O(qp)$. At the same time, the algorithm is made stable and extremely robust against round-off errors. It is known from Eq.(4.35),

$$U_j = \left(I_q \pm \mu z_j z_j^T \right) U_{j-1} H_j \tag{4.36}$$

where H_j performs additional steps to orthonormalize U_j. Now, forming the product,

$$U_j^T U_j = H_j^T \left(U_{j-1}^T U_{j-1} + \delta r_j r_j^T \right) H_j \tag{4.37}$$

with $\delta = \left(\pm 2 + \mu^2 \|z_j\|^2 \right)$ and $r_j = U_{j-1}^T z_j$. If H_n is only orthonormal matrix, Eq.(4.37) reduces to

$$U_j^T U_j = \left(I_p + \delta \|r_j\|_j^2 \right) e_1 e_1^T \tag{4.38}$$

where $e_1 = \begin{bmatrix} 1 & 0 & \cdots & 0 \end{bmatrix}^T$. Thus the additional reduction in the cost is achieved through formulating the Householder transformation matrix as

$$\begin{aligned} a_j &= r_j - \|r_j\| e_1 \\ H_j &= I_p - \frac{2}{\|a_j\|^2} a_j a_j^T. \end{aligned}$$

The entire algorithm can be implemented with just $6qp + 3p$ multiplications, $6qp$ additions, $p+1$ divisions, $p+1$ square roots. It requires a single parameter μ to be tuned and can track both signal and noise subspaces. The convergence rate of FDPM is the fastest in the low complexity subspace tracking algorithms, but it has minor drawback that it does not necessarily deliver orthonormal basis for the subspace of the true singular vectors [24].

4.3 Adaptive design of primary residual generator

In this section, the two recursive updating techniques are applied to solve the problem of adaptive fault detection system. In that, the perturbation theory based algorithm updates the entire eigen/singular value decomposition, whereas the orthogonal iteration based procedure is customized to obtain just a single parity vector. The two algorithms are later also compared with other popular recursive techniques.

4.3.1 FOP based approach: RPSi-1

The initial set of singular values and singular vectors are assumed to be available from off-line identification with a small training dataset. The primary and secondary residual generators are designed by PSi and PS2DO respectively. The on-line procedure to update the parity space begins with the current measurements obtained from the plant. It is denoted by $z_k \in \mathbf{R}^q, q = s(l + m)$,

$$z_k = \begin{bmatrix} y_{k-s+1:k}^T & u_{k-s+1:k}^T \end{bmatrix}^T, \tag{4.39}$$

where $y_{k-s+1:k} = \begin{bmatrix} y_{k-s+1} & \cdots & y_k \end{bmatrix}$ and $u_{k-s+1:k} = \begin{bmatrix} u_{k-s+1} & \cdots & u_k \end{bmatrix}$ are column vectors composed of current and past block measurements. Similarly, the instrument variable vector, $z_\tau \in \mathbf{R}^q$, can be constructed with the previous measurements,

$$z_\tau = \begin{bmatrix} y_{k-\tau-s+1:k-\tau}^T & u_{k-\tau-s+1:k-\tau}^T \end{bmatrix}^T. \tag{4.40}$$

Next, the forgetting factor is chosen as a function $\alpha = 0.99 \left(k - 1/k \right)$, and a set of transitory variables is defined as:

$$\bar{z}_k = \sqrt{1 - \alpha} U_{k-1}^T z_k \in \mathbf{R}^q, \bar{z}_\tau = \sqrt{1 - \alpha} V_{k-1}^T z_\tau \in \mathbf{R}^q,$$

and

$$p_{u,0} = \sqrt{1 - \alpha} z_k \in \mathbf{R}^q, q_{u,0} = \begin{bmatrix} 0 & \cdots & 0 \end{bmatrix}^T \in \mathbf{R}^q.$$

Then to update left singular vectors following operations are performed:

$$
\begin{align}
p_{u,i} &= p_{u,i-1} - \bar{z}_{k,i} U_{i,k-1} \tag{4.41} \\
q_{u,i} &= q_{u,i-1} + \sigma_i^{-1} \bar{z}_{\tau,i} U_{i,k-1} \tag{4.42} \\
\bar{U}_{i,k-1} &= U_{i,k-1} + \sigma_i^{-1} \bar{z}_{\tau,i} p_{u,i} - \bar{z}_{k,i} q_{u,i} \tag{4.43}
\end{align}
$$

Here, the subscript $1 \leq i \leq q$ stands for the ith element for vectors, and column for matrices. Broadly speaking, if suppose $p = sl + n$ is the dominant subspace, then the matrix $\begin{bmatrix} U_{11,k} & U_{12,k} \end{bmatrix}^T$ characterizes the $sl + n$ dimensional subspace of time-indexed input-output equation in (3.9), i.e.

$$\begin{bmatrix} U_{11,k} \\ U_{12,k} \end{bmatrix} = \begin{bmatrix} \Gamma_{s,k} & H_{u,s,k} \\ O & I \end{bmatrix}, \tag{4.44}$$

where the subscript k shows the time instant. Now, to update right singular vectors following transitory variables are defined,

$$p_{v,0} = \sqrt{1 - \alpha} z_\tau \in \mathbf{R}^q, q_{v,0} = \begin{bmatrix} 0 & \cdots & 0 \end{bmatrix}^T \in \mathbf{R}^q.$$

The right singular vectors are computed as follows:

$$
\begin{align}
p_{v,i} &= p_{v,i-1} - \bar{z}_{\tau,i} V_{i,k-1} \tag{4.45} \\
q_{v,i} &= q_{v,i-1} + \sigma_i^{-1} \bar{z}_{k,i} V_{i,k-1} \tag{4.46} \\
\bar{V}_{i,k-1} &= V_{i,k-1} + \sigma_i^{-1} \bar{z}_{k,i} p_{v,i} - \bar{z}_{\tau,i} q_{v,i} \tag{4.47}
\end{align}
$$

The singular values are updated as

$$\bar{\Sigma}_{i,k} = \alpha \Sigma_{i,k-1} + (1 - \alpha) U_{i,k-1}^T z_k z_\tau^T V_{i,k-1}. \tag{4.48}$$

Equation (4.48) provides valuable information about the dimension of the dominant subspace and in turn about the parity space. Equations (4.43), (4.47), and (4.48) are only the scaled singular vectors and singular values, the final set of normalized quantities can be obtained as

$$U_{i,k} = \frac{\bar{\Sigma}_{i,k} \bar{U}_{i,k}}{\left\| \bar{\Sigma}_{i,k} \bar{U}_{i,k} \right\|}, \Sigma_{i,k} = abs \left(\bar{\Sigma}_{i,k} \right), V_{i,k} = \frac{\bar{V}_{i,k}}{\left\| \bar{V}_{i,k} \right\|}. \tag{4.49}$$

The left singular vectors corresponding to the smallest $sm-n$ singular values can now be defined as parity vectors. Following equations give the relation between singular vectors and updated parity vectors:

$$v_{s,k} = U_{21,k}^T, \rho_{s,k} = U_{22,k}^T. \tag{4.50}$$

4.3.2 FOP based updating of single parity vector

The computation cost of RPSi-1 can be further reduced, if as a special case, a single vector orthogonal to the $(sl+n)$-dimensional subspace is to be updated. It is achieved by following steps and after updating the $(sl+n)$ dominant singular values and singular vectors as shown above. The left singular vector can be updated as

$$\bar{U}_{\perp,k} = \bar{U}_{k,sl+n} - \bar{z}_{k,sl+n} q_{u,sl+n}. \tag{4.51}$$

Similarly, the right singular vector can be updated as

$$\bar{V}_{\perp,k} = \bar{V}_{z,sl+n} - \bar{z}_{\tau,sl+n} q_{v,sl+n}. \tag{4.52}$$

At last, the smallest singular value can be updated as

$$\bar{\Sigma}_{\perp,k} = \alpha \bar{\Sigma}_{sl+n+1,k} - (1-\alpha) \bar{U}_{sl+n+1,k}^T z_k z_\tau^T \bar{V}_{sl+n+1,k}. \tag{4.53}$$

The parity vector can be constructed from $\bar{U}_{\perp,k}$ as shown in Eq.(4.50).

4.3.3 FDPM based approach: RPSi-2

The on-line computation begins with the estimate of the matrix, $\Phi_{z,0} \in \mathbf{R}^{q \times q}$ available from off-line identification and is defined as

$$\Phi_{z,0} = \frac{1}{N} Z Z^T, \tag{4.54}$$

where Z is constructed as shown in Eq.(4.25). The current measurement vector, $z_k \in \mathbf{R}^q$ is same as defined earlier. Note that due to the symmetric nature of Φ_z, the instrument variable vector is not considered here and the disturbance is assumed independent, identically distributed (iid). The matrix $\Phi_{z,k}$ is updated recursively as

$$\Phi_{z,k} = \alpha \Phi_{z,k-1} + (1-\alpha) z_k z_k^T. \tag{4.55}$$

The subspace to be tracked is defined as $\Omega_z \in \mathbf{R}^{q \times sm-n}$ and its initial estimate is obtained from off-line identification,

$$\Omega_{z,0} = \begin{bmatrix} U_{21} \\ U_{22} \end{bmatrix}. \tag{4.56}$$

Next, $\xi \in \mathbf{R}$ is defined and it is updated at every time step:

$$\xi_{z,k} = \alpha \xi_{z,k-1} + (1 - \alpha)\, z_k^T z_k. \tag{4.57}$$

Its initial value is assumed to be 1. Then, μ is updated as:

$$\mu_k = \xi_{z,k}^{-1}. \tag{4.58}$$

Note here that for the algorithm to converge μ is selected such that $0 < \mu \ll (1/\sigma_1)$ where σ_1 is the largest singular value Φ_z [22], [24]. Following μ, an intermediate matrix $M_{z,k} \in \mathbf{R}^{q \times q}$ is updated:

$$M_{z,k} = I_{q \times q} - \mu_k \Phi_{z,k}, \tag{4.59}$$

where I indicates identity matrix. Finally, $\bar{\Omega}_{z,k}$, the updated parity space can be computed as:

$$\bar{\Omega}_{z,k} = M_{z,k}\Omega_{z,k-1}. \tag{4.60}$$

Note here that $(\bar{\cdot})$ indicates scaling and $\bar{\Omega}_{z,k}$ must then be normalized.

$$\Omega_{z,k} = \frac{\bar{\Omega}_{z,k}}{\left\|\bar{\Omega}_{z,k}\right\|} \tag{4.61}$$

The notation, $\|.\|$ is slightly abused with a purpose to indicate that each column has the 2-norm equal to unity. As can be seen that the computation cost of RPSi-2 is directly proportional to the dimension of the subspace $(sm - n)$ to be updated. Thus, in case if just a single vector needs to be updated, the cost reduction is substantial. The parity vectors are constructed the same way as in the earlier section.

   The structure of the adaptive design of FD system based on both RPSi-1 and RPSi-2 is presented on the previous page. It is assumed that the initial set of parity vectors are available. The forgetting factor, α is also chosen aforehand, the algorithm then begins when a new measurement arrives.

4.3.4   Comparison of computation cost

In this subsection, algorithms RPSi-1 and RPSi-2 are compared with other known recursive matrix decomposition methods. The computation cost and complexity is calculated only for complete or partial update of the decomposition of $\Phi_z \in \mathbf{R}^{q \times q}$. In case of partial updating, the subspace is assumed l-dimensional. The results of the comparison are summarized in Table (4.1), where the symbol K, denotes the average number of eigenvalue iterations per update, see [16].

Algorithm RPSi-1 and RPSi-2: Adaptive design of FD system

- *Step 1:* Collect the new measurements $y_k \in \mathbf{R}^m$ and $u_k \in \mathbf{R}^l$ and stack it in the block measurement vector

$$z_k = \begin{bmatrix} y_{k-s+1:k}^T & u_{k-s+1:k}^T \end{bmatrix}^T.$$

- *Step 2 (Only for RPSi-1): Update the instrument variable from the past measurement*

$$z_\tau = \begin{bmatrix} y_{k-\tau-s+1:k-\tau}^T & u_{k-\tau-s+1:k-\tau}^T \end{bmatrix}^T.$$

- *Step 3:* Update $\Phi_{z,k}$, for RPSi-1:

$$\Phi_{z,k} = \alpha\Phi_{z,k-1} + (1-\alpha)\, z_k z_\tau^T, \qquad (4.62)$$

  and for RPSi-2:

$$\Phi_{z,k} = \alpha\Phi_{z,k-1} + (1-\alpha)\, z_k z_k^T. \qquad (4.63)$$

- *Step 4:* For RPSi-1, update SVD and then the parity vectors

$$v_i = U_{21,k}, \rho_i = U_{22,k}. \qquad (4.64)$$

  For RPSi-2, update $\Omega_{z,k}$ and the parity vectors

$$v_i = \Omega_{z,k}^i\,(1:sm)\,, \rho_i = \Omega_{z,k}^i\,(sm+1:s(l+m)) \qquad (4.65)$$

  where $i = 1, \cdots, sm - n$ and the numbers inside the brackets indicate corresponding elements of the ith column.

- *Step 5:* Transform v_i and ρ_i into an observer by following steps in PS2DO.

- *Step 6:* Check if there is any fault, if no, then continue from Step 1. If there is a fault, terminate the recursive algorithm.

Method	Flops	Complexity
SVD	$22q^3 + 4q^2$	$O\left(q^3\right)$
Inverse iteration	$2/3q^3p + 2q^2p + 5qp + p$	$O\left(q^3p\right)$
Rank-1 update	$2q^3 + 9q^2 + 4q + 1$	$O\left(q^3\right)$
STAN	$22p^3 + 74p^2 + 92p + 42$	$O\left(p^3\right)$
PAST	$7/2q^2 + 6qp + 4p^2$	$O\left(q^2\right)$
ROSE	$qp^2 + 3Kp^2 + 2qp + 2p^2$	$O\left(qp^2\right)$
RPSi-1	$14q^2 + 7q$	$O\left(q^2\right)$
RPSi-2	$13qp + 2q + 7p + 7$	$O\left(qp\right)$

Table 4.1: Comparison of computation cost

To begin with, the singular value decomposition involves the highest cost of the order $O\left(q^3\right)$. The inverse iteration procedure proposed in [44] reduces the computation cost of online SVD by introducing matrix inversion. A Rank-1 update proposed in [73] involves solving an eigenvalue problem whose size depends on q. The complexity of these algorithms predominantly depends on q instead of the reduced dimension p and thus the application entails lengthier computations compared to RPSi-1 and RPSi-2.

The so-called subspace tracking based on noise-subspace (STAN) formulates the recursive update of Φ_z as a $p + 1$ dimensional SVD problem, where the most dominant subspace has rank p, see [45]. The extra dimension represents the noise averaged subspace. Hence the computation cost and complexity are also equivalent to reduced dimensional SVD.

The projection based algorithms such as PAST (projection approximation for subspace tracking) solve the problem in a manner similar to recursive least square. The Frobenius norm of approximation error of the low rank subspace is minimized at each step [114]. The computation cost is significantly less compared to the methods that update complete matrix decomposition, but the identification of left orthogonal complement (e.g. parity space) requires few additional steps as compared to RPSi-1 and RPSi-2.

The Rank-1 signal eigenstructure (ROSE) is also popularly used in tracking low rank subspaces [16]. From Table (4.1), ROSE is the only other efficient algorithm whose computation cost is slightly higher than RPSi-1 and RPSi-2, but it procures the orthogonal complement of the signal space as a single vector of averaged noise. Between the two least expensive techniques,

RPSi-1 allows update of both signal and its orthogonal complement to be updated recursively, without any averaging. If only a single subspace needs to be tracked, RPSi-2 significantly reduces the computation load.

To summarize, RPSi-1 provides better approximation accuracy than RPSi-2 but it comes at slightly higher flops per update, and therefore the choice of RPSi-1 over RPSi-2 depends upon the trade-off between consistency and on-line computation.

4.4   Simulation examples

From the comparative analysis, it can be concluded that the two algorithms are efficient but produce different basis for the subspace estimation. In this section, such distinctive features are demonstrated by building a simulation example. To this end, a mathematical model to generate simulated data is used and its state space equation are given as follows:

$$x_{k+1} = \begin{bmatrix} 0.7 + \delta & 0 \\ 0 & 0.2 + \delta \end{bmatrix} x_k + \begin{bmatrix} 2 \\ 1 \end{bmatrix} u_k + \Phi_{ww} w_k \qquad (4.66)$$

$$y_k = \begin{bmatrix} 1 & 2 \end{bmatrix} x_k + 0.05 u_k + \Phi_{vv} v_k \qquad (4.67)$$

Equations (4.66)-(4.67) are simulated in Matlab-based simulation environment. In the experiments, the parameter variation (denoted by δ) affecting the dynamics is dealt with. The simplest case is the shift in the eigenvalues of the A matrix, which considerably varies the covariance properties of input and output. The parameter variation is either abrupt or incipient (slowly developing) and the latter is considered for the results shown here.
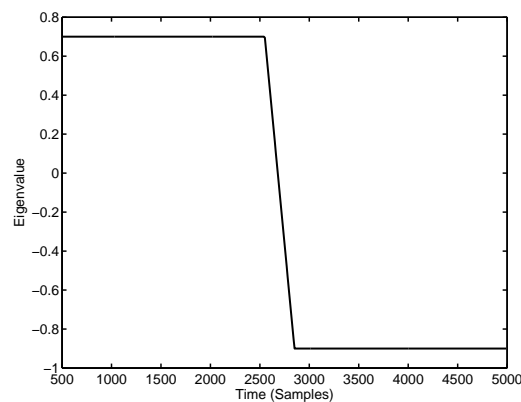

Figure 4.1: Eigen mode variations during the simulation

In the design phase, the observability parameter, s is set equal to 5. The model order is assumed unchanged and stochastic disturbances have standard deviation (Φ_{ww} and Φ_{vv}) equal 0.1. In the testing and validation phase, the system is simulated to gather 5000 sampled measurements. The input selected for the experiments is a mixture of three sinusoidal signals of different frequencies:

$$u_k = \sum_{i=1}^{3} a_i \sin\left(2\pi\omega_i t_s\right)$$

where $a_1 = 0.2, a_2 = 0.4, a_3 = 0.2$ and $\omega_1 = 100, \omega_2 = 250, \omega_3 = 500$. The plots of inputs and outputs from single simulation run consisting 5000 samples are shown in Fig.(4.2), where the change in the output plot clearly shows the effect of change in the eigenmodes.
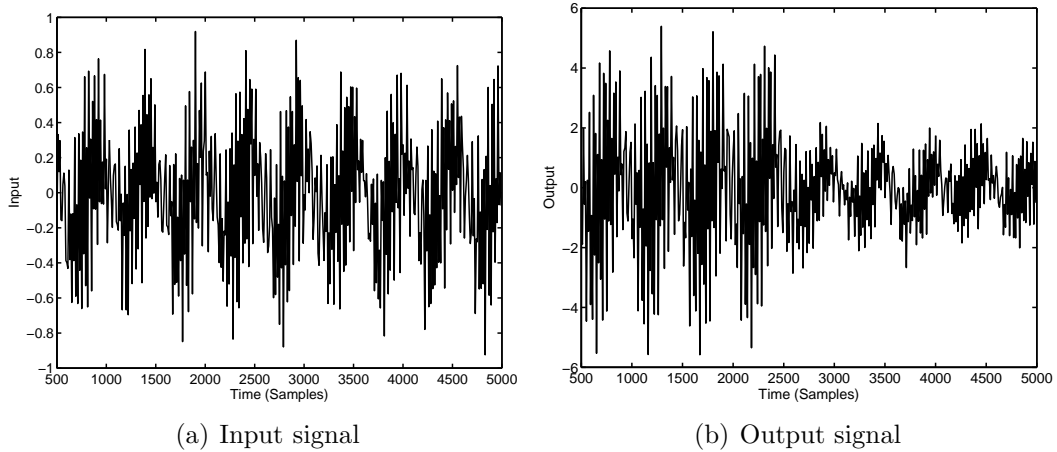

| (a) Input signal | (b) Output signal |

Figure 4.2: Input and output collected from the system

4.4.1   Approximation of dominant subspace

In the first set of simulation results, the approximation performance of RPSi-1 and RPSi-2 is compared. The comparison is within the identification framework and deals exclusively with the symmetric, positive semi-definite covariance matrices. It is already known that SVD of such a matrix can be expressed as:

$$\frac{1}{N}Z_f Z_p^T = U\Sigma V^T \tag{4.68}$$

where $Z_f \in \mathbf{R}^{s(l+m)\times N}$ and $Z_p \in \mathbf{R}^{s(l+m)\times N}$ are stacked input and output Hankel matrices of length s. We know that SVD and EVD are mutually

related operations such that

$$\Phi_Z^1 = \frac{1}{N} Z_f Z_p^T Z_p Z_f^T = V \Lambda V^T = U \Sigma^2 U^T. \tag{4.69}$$

The equation allows RPSi-1 to update the eigendecomposition of the left hand side. To this end, Eq.(4.69) can also be written in a recursive manner as

$$\Phi_{z,k}^1 = \alpha \Phi_{z,k-1}^1 + (1-\alpha) \sum_{j=k-N+1}^{k} z_k z_{k-\tau+1}^T = V_k \Lambda_k V_k^T. \tag{4.70}$$

The orthogonal iteration based recursive approach, RPSi-2 works with eigendecomposition of covariance matrix:

$$\Phi_Z^2 = \frac{1}{N} Z_f Z_f^T. \tag{4.71}$$

The recursive update of Φ_Z can be expressed as:

$$\Phi_{z,k}^2 = \alpha \Phi_{z,k-1}^2 + (1-\alpha) \sum_{j=k-N+1}^{k} z_k z_k^T. \tag{4.72}$$

The approximation error can now be measured as the normalized mean squared error (NMSE) as suggested in [112].

$$NMSE_1 = \frac{\left\| \Phi_{z,k}^1 - V_{i,k} \Lambda_{i,k} V_{i,k}^T \right\|_F^2}{\left\| \Phi_{z,k} \right\|_F^2} \tag{4.73}$$

where $i = 1, 2, \cdots, s(l+m)$ and F stands for Frobenius norm.

Algorithm RPSi-2 does not update the eigenvector explicitly but tracks vector belonging to either the signal or the noise subspace with the help of positive definite matrices. Therefore, the approximation performance must be computed differently. Doukopoulos and Moustakides in [24] have recommended following projection approximation with the help of updated vectors:

$$NMSE_2 = \frac{\left\| \Omega_k \Omega_k^T - V_i V_i^T \right\|_F^2}{\left\| V_i V_i^T \right\|_F^2} \tag{4.74}$$

where Ω_k belongs to the dominant subspace. The true dominant subspace is computed with the help eigendecomposition performed at each time step. In Eq.(4.74), V_i is the true left eigenvectors.

Next, the two recursive algorithms, RPSi-1 and RPSi-2 are compared with non-adaptive SVD based approximation. In the experiment, the eigenvalues of matrix A shift from 0.7 to 0.9 and 0.2 to -0.2 after 2550 samples.
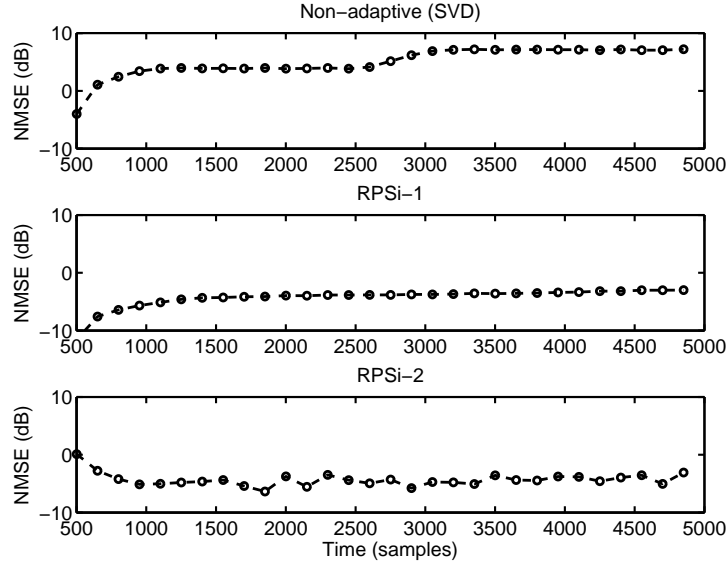
Figure 4.3: NMSE comparison

The variation is shown in Fig.(4.1). The forgetting factor is chosen as 0.99. From the Fig.(4.3), it can be seen that NMSE based performance index is extremely low for the recursive methods. For RPSi-1, it is roughly around -2 dB, whereas for RPSi-2 it stays consistently at -5 dB. For non-adaptive approach, the approximation error is much larger, hovering at $+10$ dB.

Generally, in the identification based designs, an orthonormal set of eigenvectors that span the signal (or noise) subspace is desired. For RPSi-1, following positive, scalar index is developed for orthonormality:

$$orth_1 = \left\| V_k^T v_1 \right\|_2^2 \tag{4.75}$$

where v_1 is the major eigenvector (corresponding to Λ_1) of $\Phi_{z,k}^1$. Similarly, for the second algorithm, assuming that Ω_k tracks the component corresponding to the major eigenvector, the index can be computed as

$$orth_2 = \left\| \Omega_1 v_1 \right\|_2^2 \tag{4.76}$$

where v_1 corresponds to major eigenvector of $\Phi_{z,k}^2$. These scalar indices are mapped in Fig.(4.4) after taking their logarithm to the base 10, i.e. $\log_{10}(orth_1)$ and $\log_{10}(orth_2)$. From the plot it can be seen that both, RPSi-1 and RPSi-2, only slightly exhibit divergence from the orthonormality after the eigenmodes of the plant change.

The orthonormality can also be understood as the projection error seen from the difference from unit value. This way, the performance of the recursive algorithms can be compared under different stochastic disturbances.
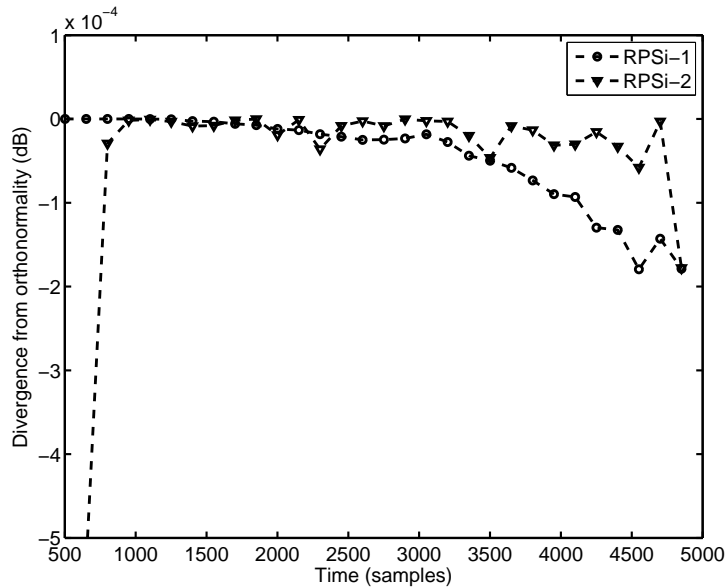
Figure 4.4: Orthonormality of eigenvectors

To this end, a test vector is projected each time and its value is tracked for increasing level of variance of disturbance. Figure (4.5) shows the plot of mean-free values of projection error obtained from RPSi-1 and RPSi-2 in an experiment with no change in the plant's eigenmodes.

It can be seen that RPSi-2 is more stable against the stochastic noise since only a single vector is updated. Therefore, minimum influence of noise terms is incurred in the computation of updated eigenvectors. But in case of RPSi-1, the increased amount of computation cost can not cope with the noise. This is reflected by the increasing value of projection error for increasing value of variance of disturbance.

4.4.2 Adaptive algorithms for fault detection

So far the adaptive techniques are compared in terms of their approximation properties, convergence to orthonormal set of vectors, and robustness against stochastic noise. For the design of primary residual generator, it is important to obtain consistent estimate of the parity space. Also, the residual signal generated from on-line computation must have non-arbitrary distribution so that a threshold for fault detection can be determined. Therefore, in this subsection the FD related properties of RPSi-1 and RPSi-2 algorithms are analyzed.

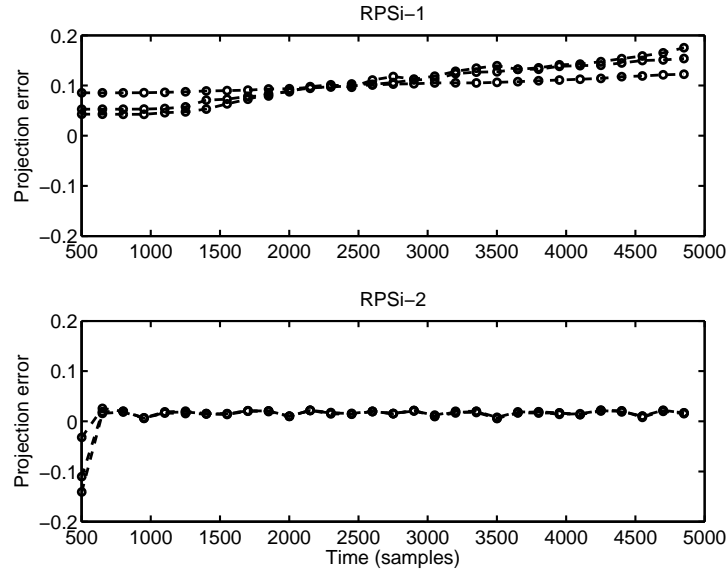In the ideal case, if the stochastic disturbances are assumed Gaussian

Figure 4.5: Robustness against stochastic disturbance

normal, then the residual signal will follow Gaussian normal distribution. Figure (4.6) shows this situation where the probability distribution in the ideal case is shown in the left hand plot. The rest of the two plots show probability distribution of residual signals obtained from RPSi-1 and RPSi-2, respectively. From these plots, it can be assumed that RPSi-1 and RPSi-2 produced nearly normal-distributed residuals. Therefore, for the threshold selection GLR-based technique as mentioned in algorithm JTH can be applied.

In the next experiment, the two adaptive design algorithms are applied to the simulation benchmark in Eq.(4.69)-(4.70). In Fig.(4.7), the residual signals obtained from non-adaptive design (algorithm PSi) and that from RPSi-1 and RPSi-2 are plotted. The threshold is selected from χ^2 distribution according to the steps mentioned in algorithm JTH and it is indicated by the dotted line. The mode change occurs after 1550 samples and lasts for 2100 samples. It is clear from plots that residual signal from non-adaptive design will yield more false alarms. RPSi-1 and RPSi-2 produce residual signals that are below the threshold value during the mode change. Therefore, it is recommended to use them further for fault detection purpose.

Although, adaptive approaches are recommended to design FD systems for applications such as above, care must be taken in not adapting during the faulty process operation. Unfortunately, this issue has not received much attention. In this work, an additional assumption on the parameter change is
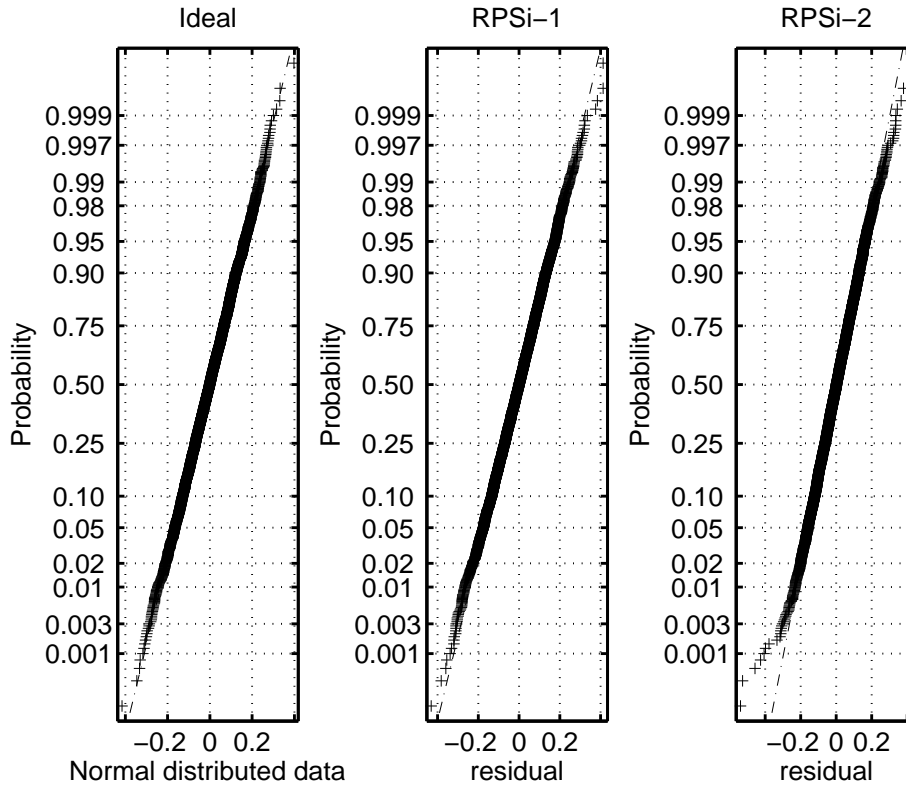
Figure 4.6: Probability distribution: comparison

is required to solve the problem. In the adaptive computation, the parameter changes that are normal are assumed slower compared to the changes due to a fault. Since RPSi-1 and RPSi-2 are both approximation-based techniques, it is likely that they will not adopt to the parameter changes due to the faults and in such case, the adaptation mechanism can be terminated as soon as the fault is detected.

4.5   Concluding remarks

In this chapter, two algorithms to design adaptive FD systems are proposed. These algorithms update primary residual generator with the help of efficient, recursive identification techniques. The first algorithm is based on the perturbation theory of the eigenvalues. It updates each eigenvalue-eigenvector pair recursively with a simple set of additions and multiplications. Despite of being an approximate method, it yields stable and consistent estimates of eigenvectors which are later used to extract parity space. The second
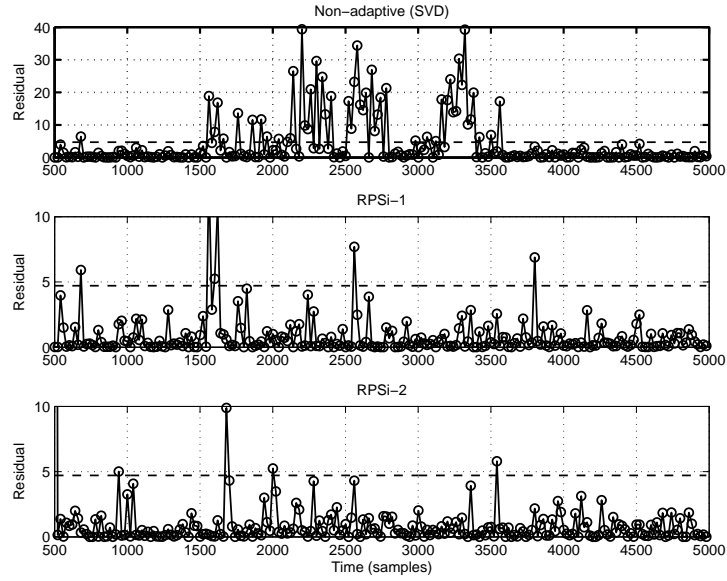
Figure 4.7: Residual signal in on-line application

algorithm differs from the first, in that, it directly updates the projection onto the eigenvectors and not the actual eigenvectors. The computation cost of these algorithms is the lowest in their class and thus they are extremely suitable for the design of FD systems in large-scale processes.

Chapter 5

Optimal design of FD systems

The data-driven algorithm PSi offers an alternative to design fault detection systems without requiring explicit knowledge about plant's model. This simple and effective technique requires minimal set of parameters to be determined by identification. To improve the performance of the FD systems, a diagnostic observer is designed as the secondary form of residual generator. For on-line application in noisy environments, a Kalman filter gain can also be identified.

From the theoretical perspective, the primary form of residual generator has crucial importance in the design phase. Its identification from plant's measurement eventually affects the application of the FD systems based on it. Therefore, it is important to study issues related to consistency and optimal identification of its parameters [4], [107]. This is considered in the subspace based identification of state space matrices and is a separate field of research. See e.g. [67], [92], [108].

Thus, this chapter shifts the focus of the work on the optimality issues of design of the primary residual generators. More specifically, it deals with optimal identification of the parity space from the training dataset. The problem is formulated in the closed-loop identification (CLID) framework which is sometimes also called Kalman filter identification [21], [50], [88]. The main contribution of this chapter is an optimized PSi algorithm (OPSi). Its theoretical derivation is presented in next sections.

5.1 Problem formulation

In this section, the state space representation of dynamic system introduced in Eq.(2.1)-(2.2) is used. For the sake of continuity, the model is rewritten

here:

$$x_{k+1} = Ax_k + Bu_k + E_d w_k \tag{5.1}$$
$$y_k = Cx_k + Du_k + F_d v_k \tag{5.2}$$

where $x \in \mathbf{R}^n$, $u \in \mathbf{R}^l$, and $y \in \mathbf{R}^m$ are states, inputs and outputs of the system. The vectors $w \in \mathbf{R}^n$ and $v \in \mathbf{R}^m$ are process and measurement disturbances, which are assumed Gaussian white noise sequences. Moreover, the state vector and disturbance variables are uncorrelated.

For the problem of identifying the optimal parameters, the above equations are written in closed-loop, Kalman filter form:

$$\hat{x}_{k+1} = (A - L_{kf}C)\,\hat{x}_k + (B - L_{kf}D)\,u_k + L_{kf}y_k \tag{5.3}$$
$$\hat{y}_k = C\hat{x}_k + Du_k + e_k \tag{5.4}$$

where $e_k \in \mathbf{R}^m$ is the so-called innovation and L_{kf} is Kalman gain. The model is also referred to as an innovation form wherein the residual signal obtained by subtracting the estimated output from the actual has minimal variance [21].

The extended state equation can be written for Eq.(5.3) based on technique explained in 2.2.1, starting from the initial condition, k_0:

$$\hat{X}_i = \bar{A}^i \hat{X}_0 + H_{u,i} U_p + H_{y,i} Y_p \tag{5.5}$$

where $\bar{A} = A - L_{kf}C$ and $\bar{B} = B - L_{kf}D$. The state sequence, $\hat{X}_i$ can be defined as:

$$\hat{X}_i = \begin{bmatrix} \hat{x}_i & \hat{x}_{i+1} & \cdots & \hat{x}_{i+j-1} \end{bmatrix} \in \mathbf{R}^{n \times j}.$$

Similar to the arrangement in algorithm PSi, the input and output distribution matrices are defined as:

$$H_{u,i} = \begin{bmatrix} \bar{A}^i \bar{B} & \bar{A}^{i-1} \bar{B} & \cdots & \bar{B} \end{bmatrix} \in \mathbf{R}^{n \times il}$$
$$H_{y,i} = \begin{bmatrix} \bar{A}^i L_{kf} & \bar{A}^{i-1} L_{kf} & \cdots & L_{kf} \end{bmatrix} \in \mathbf{R}^{n \times im}.$$

The input and output block Hankel matrices are arranged as:

$$U_p = \begin{bmatrix} u_0 & u_1 & \cdots & u_N \\ u_1 & u_2 & \cdots & u_{N-1} \\ \vdots & \vdots & \ddots & \vdots \\ u_{i-1} & u_i & \cdots & u_{N-i+1} \end{bmatrix} \in \mathbf{R}^{li \times N},$$

$$Y_p = \begin{bmatrix} y_0 & y_1 & \cdots & y_N \\ y_1 & y_2 & \cdots & y_{N-1} \\ \vdots & \vdots & \ddots & \vdots \\ y_{i-1} & y_i & \cdots & y_{N-i+1} \end{bmatrix} \in \mathbf{R}^{mi \times N}.$$

Then the extended output equation based on Eq.(5.4) can be written as:

$$Y_f = \Gamma_s \hat{X}_i + H_{u,f} U_f + E_f. \tag{5.6}$$

The matrices Γ_s and $H_{u,f}$ follow usual definition except for the usage of $\bar{A}$ and $\bar{B}$ instead of A and B,

$$\Gamma_s = \begin{bmatrix} C \\ C\bar{A} \\ \vdots \\ C\bar{A}^{s-1} \end{bmatrix} \in \mathbf{R}^{sm \times n}, H_{u,f} = \begin{bmatrix} D & O & \cdots & O \\ C\bar{B} & D & \cdots & O \\ \vdots & \vdots & \ddots & \vdots \\ C\bar{A}^{s-2}\bar{B} & C\bar{A}^{s-3}\bar{B} & \cdots & D \end{bmatrix} \in \mathbf{R}^{sm \times sl}.$$

Substituting Eq.(5.5) in (5.6),

$$Y_f = \Gamma_s \left(\bar{A}^i \hat{X}_0 + H_{u,i} U_p + H_{y,i} Y_p \right) + H_{u,f} U_f + E_f. \tag{5.7}$$

Since the observer in Eq.(5.3)-(5.4) is stable, $\bar{A}^i = (A - L_{kf}C)^i \to 0$. Hence, substituting Eq.(5.7) becomes:

$$Y_f = \Gamma_s H_{u,i} U_p + \Gamma_s H_{y,i} Y_p + H_{u,f} U_f + E_f \tag{5.8}$$

It is known from the previous chapters that the primary form of residual generator requires the orthogonal complement of the extended observability matrix, Γ_s. The residual signal from it is obtained as:

$$r_k = \Gamma_s^\perp y_{k,s} - \Gamma_s^\perp H_{u,f} u_{k,s} = \Gamma_s^\perp e_{k,s} \tag{5.9}$$

where $y_{k,s} = \begin{bmatrix} y_{k-s+1} & y_{k-s+2} & \cdots & y_k \end{bmatrix}^T \in \mathbf{R}^{sm}$ and similarly $u_{k,s} = \begin{bmatrix} u_{k-s+1} & u_{k-s+2} & \cdots & u_k \end{bmatrix}^T \in \mathbf{R}^{sl}$. The variance of this residual signal can be computed as:

$$\Phi_{rr} = \frac{1}{N} r_k r_k^T = \frac{1}{N} \Gamma_s^\perp e_{k,s} e_{k,s}^T \Gamma_s^{\perp T} = \Phi_{ee} \tag{5.10}$$

where Φ_{ee} is the variance of the innovation signal and is minimum for the system in Eq.(5.3)-(5.4). Therefore, the primary form of the residual generator is termed as the optimal. In the next section, the procedure to identify the residual generator in a closed-loop framework is explained.

5.2 Least squares based solution

The data-driven approach via algorithm PSi constructs the primary form of residual generation by identifying two subspaces, namely $\Gamma_s^\perp \in \mathbf{R}^{\eta \times sm}$

and $\Gamma_s^\perp H_{u,f} \in \mathbf{R}^{\eta \times sl}$, where η is the dimension of the so-called parity space. The least squares based solution to extract one of these two components is relatively straightforward. To this end, $H_{u,f}$ can be estimated by projecting the column space of the future outputs on the column space of future inputs,

$$\hat{H}_{u,f} = Y_f U_f^T \left(U_f U_f^T \right)^{-1}.$$

(5.11)

In the second step, this estimate is substituted back in Eq.(5.6) and SVD is performed,

$$Y_f - \hat{H}_{u,f} U_f = \Gamma_s H_{u,i} U_p + \Gamma_s H_{y,i} Y_p + E_f.$$

(5.12)

Assuming that the input signal is persistently exciting of the order n, i.e.

$$rank\left(\Phi_{uu}\right) = rank\left(\frac{1}{N} U_f U_f^T\right) = n,$$

(5.13)

then,

$$Y_f - \hat{H}_{u,f} U_f = \begin{bmatrix} U_1 & U_2 \end{bmatrix} \begin{bmatrix} \Sigma_1 & O \\ O & \Sigma_2 \end{bmatrix} \begin{bmatrix} V_1^T \\ V_2^T \end{bmatrix}$$

(5.14)

where $\Sigma_1 \in \mathbf{R}^{n \times n}$ has exactly n non-zero singular values which implies,

$$rank\left(Y_f - \hat{H}_{u,f} U_f\right) = rank\left(\Gamma_s\right) = n,$$

(5.15)

and accordingly

$$U_1 \in \mathbf{R}^{sm \times n}, U_2 \in \mathbf{R}^{sm \times sm-n}.$$

(5.16)

So, the left orthogonal complement of Γ_s can be identified as:

$$\Gamma_s^\perp \in U_2^T.$$

(5.17)

and the primary form of the residual generator is constructed by selecting two vectors, $\upsilon_s \in \Gamma_s^\perp$ and $\rho_s \in \Gamma_s^\perp \hat{H}_{u,f}$. The residual is obtained as

$$r_k = \upsilon_s y_{k,s} - \rho_s u_{k,s}.$$

(5.18)

The secondary form of residual generator is designed according to the algorithm PS2DO and DOKF.

Remarks: The left orthogonal complement identified in Eq.(5.17) can also be interpreted as the least squares projection, i.e. the singular vector corresponding to the smallest singular value obtains the best possible estimate $\Gamma_s^\perp$ in terms of residual variance.

5.3 CLID based design of FD systems

In section 5.1 and in 5.2, the concept of identifying optimal parameters related to the primary form of residual generator is stated in a rather crude form. For robust design, the solution must be stated in a more concise and systematic form. To this end, the oblique projection technique is introduced briefly and the algorithm OPSi is derived based on it.

5.3.1 Oblique projection operator

From the operator theory, it is known that the orthogonal projection operator, Π has the following basic property

$$\Pi = \Pi^2,$$

i.e., it is idempotent in addition to being symmetric. The non-orthogonal projection also shows the above property, but it is not a symmetric operator. Nevertheless, it has many features, but unfortunately, very few studies are dedicated to this topic, see for instance [6] and references therein.

The orthogonal projection operator, Π_B defines the projection of row space of matrix $A \in \mathbf{R}^{p \times j}$ onto the row space of $B \in \mathbf{R}^{q \times j}$.

$$A/B = A\Pi_B = AB^T \left(BB^T\right)^\dagger B. \tag{5.19}$$

Its null space is given by,

$$\Pi_{B^\perp} = I_j - \Pi_B. \tag{5.20}$$

It decomposes A into two matrices with orthogonal row spaces as:

$$A = A\Pi_B + A\Pi_{B^\perp}. \tag{5.21}$$

An oblique projection decomposes the row space of A into a linear combination of two non-orthogonal matrices B and C and their orthogonal complements $B^\perp, C^\perp$. Mathematically, projection of A onto C along B can be obtained by first projecting the row space of A onto the combined row space of B and C and decomposing the result along the row space of C, i.e.

$$A \bigg/ \left(\begin{array}{c} C \\ B \end{array} \right) = A \left[\begin{array}{cc} C^T & B^T \end{array} \right] \left[\begin{array}{cc} CC^T & CB^T \\ BC^T & BB^T \end{array} \right]^\dagger \left[\begin{array}{c} C \\ B \end{array} \right]. \tag{5.22}$$

This projection can be divided in two parts as:

$$A \bigg/ \left(\begin{array}{c} C \\ B \end{array} \right) = A/_B C + A/_C B. \tag{5.23}$$

Equation (5.23) leads to the definition of oblique projection of the row space of A along the row space of B onto the row space of C, i.e.

$$A/_B C = A \begin{bmatrix} C^T & B^T \end{bmatrix} \begin{bmatrix} CC^T & CB^T \\ BC^T & BB^T \end{bmatrix}^\dagger \begin{bmatrix} C \\ O \end{bmatrix}. \tag{5.24}$$

Therefore, it can be seen that the oblique projection is a degenerative case of orthogonal projection. The oblique projection is also idempotent. To this end, if it is assumed that $A = \begin{bmatrix} B & O \end{bmatrix}^T$, then

$$\begin{aligned} A \bigg/ \begin{pmatrix} C \\ B \end{pmatrix} &= A/_B C + A/_C B = B \\ &\Rightarrow A/_B C = B, A/_C B = O. \end{aligned} \tag{5.25}$$

Similarly, for $A = \begin{bmatrix} O & C \end{bmatrix}^T$, the projection onto the row space of B,

$$\begin{aligned} A \bigg/ \begin{pmatrix} C \\ B \end{pmatrix} &= A/_B C + A/_C B = C \\ &\Rightarrow A/_B C = O, A/_C B = C. \end{aligned} \tag{5.26}$$

For oblique projection operator to be idempotent, it is required to prove following equation:

$$\Pi_C^B = \Pi_C^{B^2}. \tag{5.27}$$

Applying the results in Eq.(5.23) and Eq.(5.25)-(5.26),

$$\Pi_{BC}^2 = \left(\Pi_C^B + \Pi_B^C \right) \left(\Pi_C^B + \Pi_B^C \right) = \Pi_{BC}^2 + \Pi_{CB}^2 = \Pi_{BC}.$$

The cross-terms of the product in the brackets vanish because the row space of Π_C^B is in the null space of Π_B^C and vice versa. Thus, from the definition and the fact that both Π_B^C and Π_C^B are disjoint sets,

$$\Pi_B^{C^2} = \Pi_B^C, \Pi_C^{B^2} = \Pi_C^B.$$

From these results, it can be concluded that the non-orthogonal projection operator such as oblique projection has an intimate relationship with orthogonal projection.

5.3.2   Oblique projection based algorithm

For the identification of optimal primary residual generator with the help of oblique projection, the extended state space model in Eq.(5.7) is rewritten:

$$Y_f = \Gamma_s \left(\bar{A}^i \hat{X}_0 + H_{u,i} U_p + H_{y,i} Y_p \right) + H_{u,f} U_f + E_f. \tag{5.28}$$
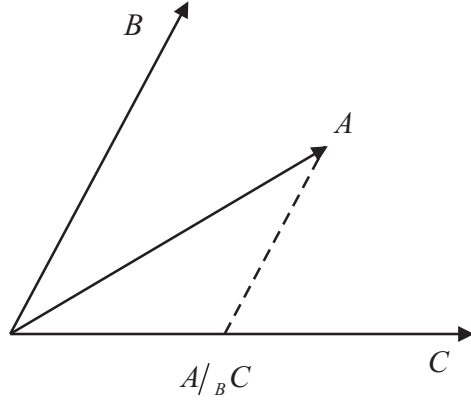
Figure 5.1: Oblique projection

Since the observer is asymptotically stable, the term associated with $\hat{X}_0$ can be omitted,

$$Y_f = \Gamma_s H_{w,p} W_p + H_{u,f} U_f + E_f \tag{5.29}$$

where

$$H_{w,p} = \begin{bmatrix} H_{u,i} & H_{y,i} \end{bmatrix}, W_p = \begin{bmatrix} U_p \\ Y_p \end{bmatrix}.$$

Now, to estimate $H_{u,f}$, the effect of past inputs and outputs must be removed. This can be achieved by an orthogonal projection onto the null space of W_p such as:

$$Y_f \Pi_{W_p^\perp} = \Gamma_s H_{w,p} W_p \Pi_{W_p^\perp} + H_{u,f} U_f \Pi_{W_p^\perp} + E_f \Pi_{W_p^\perp}. \tag{5.30}$$

Since the innovation signal is uncorrelated with past inputs and outputs, its product in Eq.(5.32) can be equated to zero. The remaining terms can be rearranged as

$$\left(Y_f \Pi_{W_p^\perp} \right) \left(U_f \Pi_{W_p^\perp} \right)^\dagger U_f = H_{u,f} U_f \Pi_{W_p^\perp} \left(U_f \Pi_{W_p^\perp} \right)^\dagger U_f. \tag{5.31}$$

The left hand side of Eq.(5.31) is nothing but oblique projection of future outputs along the row space spanned by past inputs and outputs, onto the row space of future inputs, i.e.

$$Y_f \big/_{W_p} U_f = H_{u,f} U_f. \tag{5.32}$$

Equation (5.32) is the crux of the solution to the closed-loop identification problem stated in section 5.1. The next step is to identify Γ_s which follows from the same procedure explained in section 5.2. The consistency and optimality of this oblique projection based identification method is explained in the following theorem.

Theorem: If the innovation sequence is a white noise sequence with relatively small variance, then the minimum variance estimate of $H_{u,f}$ can be obtained as

$$\hat{H}_{mv} = Y_f \big/ W_p U_f \left(U_f^\dagger \right), \tag{5.33}$$

if both the input and the innovation signal are Gaussian white noise sequences, then

$$\lim_{\xi \to \infty} \hat{H}_{u,f} = \hat{H}_{mv} \tag{5.34}$$

where $\xi = \frac{\sigma_{W_p}^2}{\sigma_E^2}$ and $\hat{H}_{mv}$ is the minimum variance estimate.

Proof: The above two important conclusions can be explained based on the analysis presented in [6].

It has been stated in section 5.2 that the optimal identification of primary residual generator is in fact a problem of obtaining the minimum variance estimates of $\Gamma_s^\perp$ and $H_{m,u}$. Thus, the least squares method solves it as:

$$\hat{\Gamma}_{mv}, \hat{H}_{mv} = \arg\min \left\| y_{k,s} - \hat{\Gamma} x_{k-s+1} - \hat{H}_{u,f} u_{k,s} \right\|_2^2. \tag{5.35}$$

There are two special cases considered for the proof part wherein the input signal is either persistently exciting or a random noise sequence. In the first case, it is assumed that the innovation signal is a white noise sequence. Then the least square estimates of Γ_s and $H_{m,s}$ are also the maximum likelihood estimates minimizing the residual error,

$$e_{k,s} = y_{k,s} - \hat{\Gamma}_{mv} x_{k-s+2} - \hat{H}_{mv} u_{k,s}. \tag{5.36}$$

Since the state sequence x_{k-s+1} is not known *a priori*, it is replaced by past input and output as shown in Eq.(5.29). Thus, the ordinary least squares equation solves the problem as:

$$
\begin{aligned}
\begin{bmatrix} \hat{\Gamma}_s \hat{H}_{w,p} & \hat{H}_{m,u} \end{bmatrix} &= Y_f \begin{bmatrix} W_p \\ U_f \end{bmatrix}^\dagger \\
&= Y_f \begin{bmatrix} W_p \\ U_f \end{bmatrix}^T \begin{bmatrix} W_p W_p^T & W_p U_f^T \\ U_f W_p^T & U_f U_f^T \end{bmatrix}^{-1}.
\end{aligned} \tag{5.37}
$$

Now, if the inversion formula for 2×2 matrix is applied and above equation is solved for unknown parameters, then

$$\hat{H}_{u,f} = Y_f \left[I - U_f^T \left(U_f \Pi_{W_p^\perp} U_f^T \right)^{-1} U_f \Pi_{W_p^\perp} \right] U_f^\dagger. \tag{5.38}$$

With the help of the definition of oblique projection, Eq.(5.38) can be written in a concise form as

$$Y_f\big/_{W_p}U_f = H_{u,f}U_f. \tag{5.39}$$

Equation (5.39) shows that the least squares estimate of $\hat{H}_{u,f}$ is a result of the oblique projection onto U_f along W_p. Therefore, the solution will be degenerative case of an *ordinary least squares* based one, if the external disturbance signal, $e_{k,s}$ is independent of the input signal. Moreover, if the disturbance is also Gaussian white, then it is also the maximum likelihood estimate.

In the second case, both X_{k-s+1} and e_k are assumed to be additive disturbances following normal distribution with known variance. Moreover, X_{k-s+1} is a structured disturbance entering through $H_{x,f} = \Gamma_s H_{w,p}$ and is independent of the distribution of $e_{k,s}$.

The variance of these two sources of disturbance can be described by their variance:

$$\Phi_{xx} = \frac{1}{N}X_iX_i^T, \Phi_{ee} = \frac{1}{N}E_fE_f^T.$$

With slight abuse of notation, let Δ define combined additive disturbance as,

$$\Delta_{k,N}^s = \Gamma_s X_i + E_f \tag{5.40}$$

which is also Gaussian distributed with $\Phi_{\Delta\Delta} = \Gamma_s\Phi_{xx}\Gamma_s^T + \Phi_{ee}$. Now, the minimum variance estimate of $H_{u,f}$ can be achieved by following projection:

$$\hat{H}_{u,f} = Y_fU_f^T\Phi_{\Delta\Delta}^{-1}\left(U_fU_f^T\Phi_{\Delta\Delta}^{-1}\right)^{-1}U_fU_f^\dagger. \tag{5.41}$$

If Eq.(5.41) is rearranged such that

$$\hat{H}_{u,f} = Y_fU_f^T\left(I + \xi\Gamma_s\Gamma_s^T\right)^{-1}\left(U_fU_f^T\left(I + \xi\Gamma_s\Gamma_s^T\right)^{-1}\right)^{-1}U_fU_f^\dagger \tag{5.42}$$

where $\xi = \frac{\Phi_{xx}}{\Phi_{ee}}$. The newly introduced term in the bracket is an alternative way to define projection onto the null space [6].

$$\Pi_{X_i^\perp} = \lim_{\Phi\to\infty}\left(I + \xi\Gamma_s\Gamma_s^T\right)^{-1}. \tag{5.43}$$

If now the states are replaced by past inputs and outputs, then following expression can be obtained:

$$\Pi_{W_p^\perp} = \lim_{\Phi\to\infty}\left(I + \Phi H_{x,f}H_{x,f}^T\right)^{-1}. \tag{5.44}$$

Based on Eq.(5.44), the main conclusion can be stated in two extreme situations:

- If $\xi = 0$, i.e. there is no structured disturbance term, W_p, then the estimate of $H_{u,f}$ in Eq.(5.42) simply converges to that obtained by orthogonal projection.

$$\hat{H}_{u,f} = Y_f U_f^T \left(U_f U_f^T \right)^{-1} \tag{5.45}$$

- On the other hand if $\xi \to \infty$, then there is no other disturbance acting excluding W_p. Thus, the estimate in Eq.(5.42) is exactly the same as in Eq.(5.39).

$$\hat{H}_{u,f} = Y_f /_{W_p} U_f \left(U_f^\dagger \right) \tag{5.46}$$

End

Remark: Based on this theorem, it can also be said that if the disturbances acting on the systems are not strong, then the oblique projection yields minimum variance estimates. In fact, the projection operator converges to the orthogonal projection. Despite of this wonderful feature, the oblique projection operator has a tendency to amplify the noise in certain subspaces. So, if the disturbance signal is full rank, then the oblique projection will amplify it in the subspace parallel to the one it is projecting onto.

5.3.3   Numerical optimization with QR decomposition

The projection operators have many attractive features in the estimation and identification problems. From the point of view of numerical implementation and computation cost, oblique projection based method to identify parity space can be further enhanced if it is implemented with QR decomposition. The advantages of QR based identification are as follows:

- the geometric operations such as orthogonal projection on the null spaces, oblique projection can be easily expressed in terms of QR decomposition,

- all the calculations require only R factor

- the computation cost of R factor is $i^2 j$ where i is the number of block rows and j is the number of columns. Since $j \gg i$, QR decomposition is extremely efficient.

To implement it, the input and output block Hankel structures, defined in section 5.1, are arranged in a different way. They are stacked as shown

below:

$$
\begin{bmatrix} U_p \\ U_i \\ U_f \\ Y_p \\ Y_i \\ Y_f \end{bmatrix} = \begin{bmatrix} R_{11} & 0 & 0 & 0 & 0 & 0 \\ R_{21} & R_{22} & 0 & 0 & 0 & 0 \\ R_{31} & R_{32} & R_{33} & 0 & 0 & 0 \\ R_{41} & R_{42} & R_{43} & R_{44} & 0 & 0 \\ R_{51} & R_{52} & R_{53} & R_{54} & R_{55} & 0 \\ R_{61} & R_{62} & R_{63} & R_{64} & R_{65} & R_{66} \end{bmatrix} \begin{bmatrix} Q_1^T \\ Q_2^T \\ Q_3^T \\ Q_4^T \\ Q_5^T \\ Q_6^T \end{bmatrix}. \tag{5.47}
$$

where R is the lower triangular matrix and Q is the orthonormal basis. From the definition of oblique projection,

$$
Y_f / _{W_p} U_f = Y_f / W_p^{\perp} \left(U_f / W_p^{\perp} \right)^{\dagger} U_f \tag{5.48}
$$

where

$$
Y_f / W_p^{\perp} = R_{[5:6,1:6]} \left(I - R_{[1,4,1:6]} \left(R_{[1,4,1:6]} R_{[1,4,1:6]}^T \right)^{-1} R_{[1,4,1:6]} \right)
$$

$$
U_f / W_p^{\perp} = R_{[2:3,1:6]} \left(I - R_{[1,4,1:6]} \left(R_{[1,4,1:6]} R_{[1,4,1:6]}^T \right)^{-1} R_{[1,4,1:6]} \right).
$$

Now, $\hat{H}_{u,f}$ can be identified as

$$
\hat{H}_{u,f} = Y_f / _{W_p} U_f \left(R_{[2:3,1:6]} \right)^{\dagger}. \tag{5.49}
$$

To identify the primary residual generator, SVD is performed:

$$
R_{[5:6,1:6]} - \hat{H}_{u,f} R_{[2:3,1:6]} = U \begin{bmatrix} \Sigma_1 & O \\ O & \Sigma_2 \end{bmatrix} V^T. \tag{5.50}
$$

and U is divided such that

$$
U_1 \in \mathbf{R}^{sm \times n}, U_2 \in \mathbf{R}^{sm \times sm - n}. \tag{5.51}
$$

Then, the left orthogonal complement of the extended observability matrix can be identified as:

$$
\hat{\Gamma}_s^{\perp} \in U_2^T. \tag{5.52}
$$

From the estimates in Eq.(5.49) and (5.52), the primary form of residual generator can be constructed by selecting two vectors $v_s \in \hat{\Gamma}_s^{\perp}, \rho_s \in \hat{\Gamma}_s^{\perp} \hat{H}_{u,f}$. The secondary residual generator is designed according to algorithms PS2DO and DOKF.

Algorithm OPSi: Optimal parity space identification

- Construct the datasets, $U_p, Y_p, Y_p, Y_f, U_i, Y_i$ and perform QR decomposition as shown in Eq.(5.47)

- Identify $\hat{H}_{u,f}$, determine the model order from the SVD step in Eq.(5.49) and identify $\hat{\Gamma}_s^{\perp}$ from Eq.(5.52)

- Select $\upsilon_s \in \hat{\Gamma}_s^{\perp}$ and $\rho_s \in \hat{\Gamma}_s^{\perp} \hat{H}_{u,f}$ and construct the primary residual generator

- Construct secondary form of residual generator based on PS2DO or DOKF

5.4 Simulation example

In this section, the optimal identification based design of FD systems is applied to a demonstrative example. In the experiment, both deterministic and stochastic cases are considered. Since the simulation model is already known, the results are compared with model-based designs of FD systems as well. The classic subspace identification based approach and the recently developed, FICSI (Fault detection and Identification approach Connected to Subspace Identification) based residual generators are also implemented.

The process under consideration is a single input, single output discrete LTI system. It can be described by following state space model:

$$x_{k+1} = \begin{bmatrix} 0.7 & 0 \\ 0 & 0.2 \end{bmatrix} x_k + \begin{bmatrix} 2 \\ 1 \end{bmatrix} u_k + \Phi_{ww}w_k \qquad (5.53)$$

$$y_k = \begin{bmatrix} 1 & 2 \end{bmatrix} x_k + 0.05u_k + \Phi_{vv}v_k. \qquad (5.54)$$

Equations (5.53) and (5.54) can be easily simulated in Matlab-based Simulink environment. The parameters Φ_{ww} and Φ_{vv} determine the degree of stochastic interference. Note here that for the data-driven design, only the sampled measurements obtained from the simulation are required and for the theoretical analysis, the additional knowledge of the state space matrices is utilized.

5.4.1 Application of OPSi

To ensure persistent excitation as seen in Eq.(5.13), a pulse-shaped input signal is chosen and the width of each pulse is modulated with a pseudorandom number generator. This type of signal is a recommended source in identification experiments [88], and Fig.(5.2) shows one example of it.
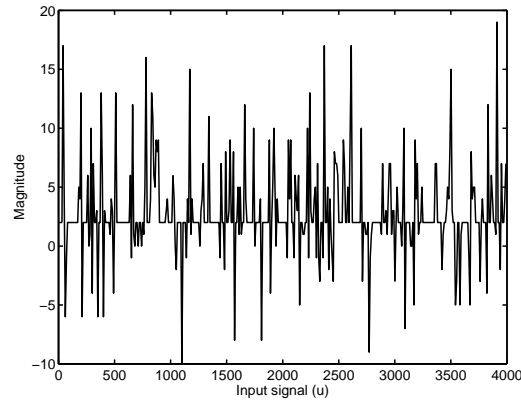
Figure 5.2: Persistently exciting input signal

For the design of FD system based on OPSi technique, matrices U_p, U_f and Y_p, Y_f are constructed with 500 sampled measurements. The parameter s is chosen as 5. These measurements are collected from a single simulation run. The matrices $H_{u,f} \in \mathbf{R}^{5 \times 5}$ and $\Gamma_s^{\perp}$ are identified according to Eq.(5.47) and (5.52). To design the primary form of residual generator, the orthogonal complement of Γ_s is required. To this end, the correct model order must be determined first. This is achieved by the singular value plot as shown in Fig.(5.3).

It can be seen that the singular values after the second one are nearly equal to zero. But for automatic selection, a ratio-based check can be also be implemented to determine the correct cut-off. The next step is to design the diagnostic observer according to algorithms PS2DO and DOKF.
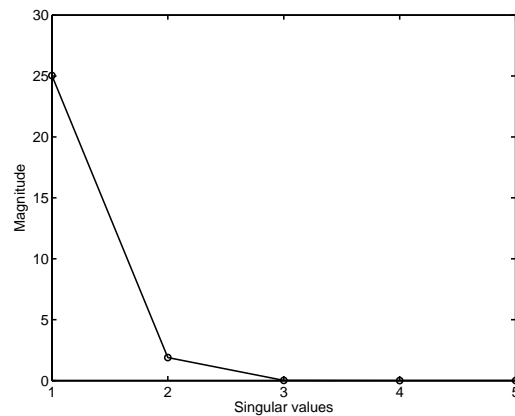

Figure 5.3: Determination of model order

In the experiments, the process and sensor measurement noises are as-

sumed normally distributed and their standard deviations, Φ_{ww} and Φ_{vv}, are set to 0.2 and 0.01, respectively. For system in Eq.(5.53)-(5.54), the variance of the innovation signal can be pre-calculated as follows:

$$\Phi_{ee} = \frac{1}{N} \left(C\Phi_{ww}C^T + \Phi_{vv} \right) = 1.01 \tag{5.55}$$

To compare the results with OPSi, SIM-based observer and FICSI-based residual generator are also designed. SIM-based observer requires the state space matrices to be identified first. To this end, Matlab-based toolbox designed by Overschee and Moor [88] is used. The optimal feedback gain for this observer is computed by following standard technique in Kalman filter theory [18]. For reference, FICSI-based design of FD systems is presented in the appendix.
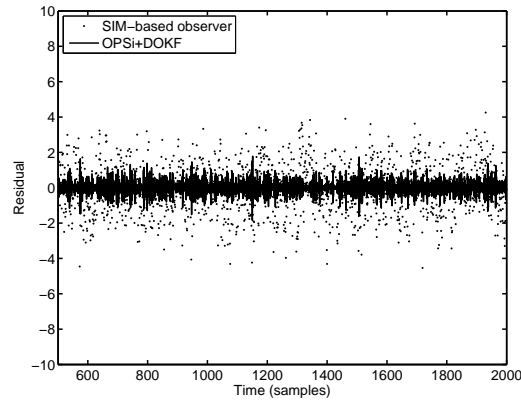

Figure 5.4: Residuals generated by SIM and OPSi-based observer

Figure (5.4) shows a comparative picture of the residuals generated by the diagnostic observer with OPSi and a SIM-driven observer. Next, different residual generators are compared in the stochastic environment. The results with these residual generators is provided in Tables (5.1) and (5.2). The residuals are derived from an independent validation dataset gathered from normal operation of the process in Eq.(5.53)-(5.54).

$\Phi_{vv} = 0.01$	SIM-based	PSi+DOKF	FICSI	OPSi+DOKF
$\Phi_{ww} = 0.00$	0.01	**0.00**	0.01	**0.00**
$\Phi_{ww} = 0.02$	0.23	0.02	0.23	**0.01**
$\Phi_{ww} = 0.20$	2.13	**0.18**	2.15	0.23

Table 5.1: Variance of residuals with fixed measurement noise

$\Phi_{ww} = 0.02$	SIM-based	PSi+DOKF	FICSI	OPSi+DOKF
$\Phi_{vv} = 0.00$	0.20	**0.01**	0.20	0.02
$\Phi_{vv} = 0.02$	0.24	**0.02**	0.25	**0.02**
$\Phi_{vv} = 0.20$	0.42	**0.05**	0.43	0.06

Table 5.2: Variance of residuals with fixed process noise

In Fig.(5.5), the residual signals obtained from SIM-based observer, PSi, FICSI, and OPSi based observers are plotted. It can be concluded that both PSi and OPSi based diagnostic observers show similar performance, but they fare better than SIM-based observer and FICSI-based residual generator which have significantly large variance.
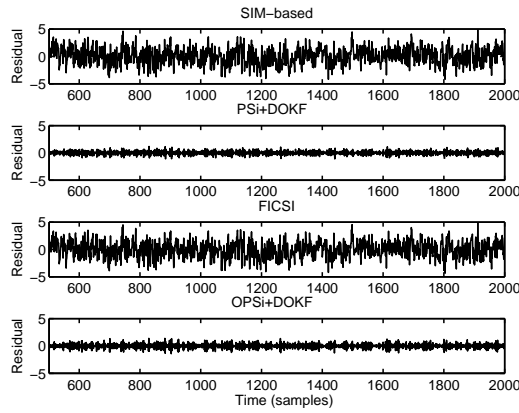

Figure 5.5: Comparison of SIM, PSi, FICSI, and OPSi based FD systems

5.4.2 Residual evaluation and fault detection

Before proceeding with the fault detection, a residual evaluation stage must be designed and an appropriate threshold must also be selected. To this end, the GLR-based approach mentioned in algorithm JTH is applied as follows:

$$r_{ev,k} = \frac{1}{2\Phi_{rr}^2 N} \sum_{j=k-N+1}^{k} r_j^T r_j \qquad (5.56)$$

where N is the length of the moving window. Depending upon the distribution of process and measurement disturbances, the residual in Eq.(5.56) can be assumed to be χ^2 distributed. Therefore the threshold can be chosen as

$$J_{th} = \chi_{\alpha}, \qquad (5.57)$$

where α is the confidence interval selected depending upon allowable false alarms and missed detections. For the experiment here, it is chosen as 99%. The fault considered here is the malfunctions in sensor. The sensor fault is the simplest of the faults and thus the FD system which fails to detect this fault, will have difficulty to detect other faults as well. The fault is simulated by adding $25 \sim 27\%$ bias to the measured values of the output. The residuals generated by PSi and OPSi based observers are shown in Fig.(5.6), where the dotted line indicates the threshold value.
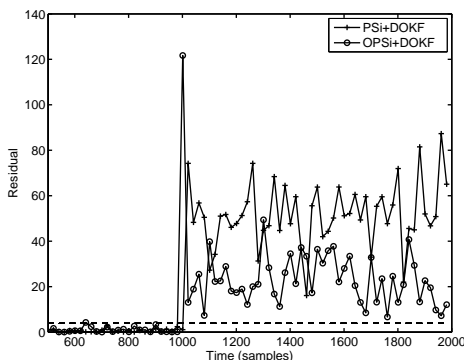

Figure 5.6: Sensor fault detection

5.5 Concluding remarks

In this chapter, an extension to the work on PSi-based designs is presented. In that an oblique projection based optimal identification procedure for the primary form of residual generator, OPSi is designed. This is achieved by studying the parity space identification problem in the closed-loop framework. More precisely, the unknown dynamic system is formulated as Kalman filter and optimal orthogonal complement of its observability matrix is obtained.

The algorithm is efficiently implemented with the help of QR decomposition. The advantages are also provided which make OPSi suitable for large-scale applications. The secondary form of residual generators are designed based on algorithms already presented in chapter 3. The FD system is compared with other popularly used techniques. In the next chapter, the algorithms developed in this chapter and previous are tested on industrial benchmarks.

Chapter 6

Tests with benchmarks

This chapter focuses on data-driven designs for FD systems from the perspective of industrial applications. The algorithms presented here are implemented on Tennessee Eastman chemical process (TE) [25] and continuous stirred tank heater (CSTH) [100]. The PSi-based design of FD systems is applied on TE process, since it is part of earlier work published in [20]. For the main contribution, in terms of RPSi-1, RPSi-2, and OPSi, a recent benchmark model of CSTH is used.

The simulation of TE process is realistic representation of a chemical plant with 50 internal states, 11 manipulated and 40 measured variables. Since the mathematical equations of the process are extremely complex to derive, it is a preferred benchmark to test data-driven algorithms for control, process monitoring and fault diagnosis. The model plant of CSTH is developed by [100] which is a hybrid one, derived from real data and rigorous modeling.

The organization of this chapter is done as follows. In the next section, a brief introduction of the two plants and their process monitoring-relevant information is provided. Then section 6.2, PSi-based design of diagnostic observer is applied to the TE process and the representative results are presented for brevity. In section 6.3, the adaptive designs based on RPSi-1 and RPSi-2 are applied to CSTH and then in 6.4, OPSi-based design of observer is applied to the same plant.

6.1   Benchmark models

The Tennessee Eastman (TE) plant model is a realistic benchmark which has found wide acceptance in the research community. See e.g. [60], [62], [66], [97]. It is an excellent platform to test data-driven approaches, since the mathematical model of the process is deliberately confiscated. It is highly

instrumented process with more than 50 measured variables, which makes this process challenging for application relevant study. The plant has 5 major units, 8 components, and 6 operating points as introduced in [25]. The simulation code is originally developed in Fortran computing language. But for the tests that are carried out here, it is transformed into Matlab based Simulink environment.

The schematic diagram of the plant is shown in Fig.(6.1). Since the plant is open-loop unstable, the distributed controller proposed in [78] is implemented. It consists of 9 proportional integral (PI) controllers and 21 set-points all together. The plant allows 53 variables to be directly measured, out of which 41 are process variables and 12 are manipulable control signals. The sampling time is chosen as 3 minutes which is sufficient since the majority of the time constants in the closed-loop are about 2 hours. The process does not employ any higher level quality control.
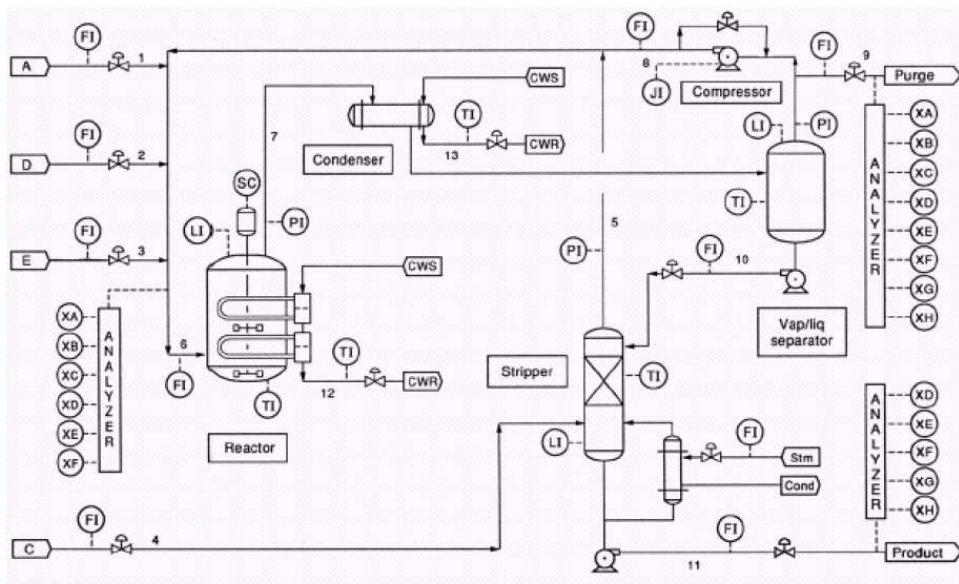

Figure 6.1: Tennessee Eastman process

Juricek et al. [60] have implemented subspace identification based algorithm for controller design. The statistical methods such as PCA, PLS are already tested on TE process [97]. In this study, PSi and PS2DOS designs of diagnostic observer are applied for the detection of 20 pre-defined faults in the process. The details of these faults are provided in [25]. For the sake of brevity, only those discussed in this chapter are given in Table (6.2). These faults mainly affect process variables, reaction kinetics, feed concentrations

and actuators such as pumps, valves.

Variable name	Number	Base value(%)	Units
D feed flow	XMV(1)	63.053	$\text{kg}h^{-1}$
E feed flow	XMV(2)	53.980	$\text{kg}h^{-1}$
A feed flow	XMV(3)	24.644	kscmh
A and C feed flow	XMV(4)	61.302	kscmh
Compressor recycle valve	XMV(5)	22.210	%
Purge valve	XMV(6)	40.064	%
Separator pot liquid flow	XMV(7)	38.100	m^3h^{-1}
Stripper liquid product flow	XMV(8)	46.534	m^3h^{-1}
Stripper steam valve	XMV(9)	47.446	%
Reactor cooling water flow	XMV(10)	41.106	m^3h^{-1}
Condenser cooling water flow	XMV(11)	18.114	m^3h^{-1}
Agitator speed	XMV(12)	50.000	rpm

Table 6.1: Process manipulated variables

The first fault that will be discussed here is relatively easy to detect. It involves step change in the ratio of two input feeds. The second fault affects the temperature of one of the important component of the process, the reactor, and thereby affects the process dynamics. The third fault is of unknown nature, but has influence on many measured variables. The results with other faults are summarized in Table (B.2) in the appendix.

Fault	Process variable	Type
IDV(0)	Normal operation	-
IDV(1)	A/C feed ratio, B composition constant	Step
IDV(4)	Reactor cooling water inlet temperature	Step
IDV(17)	Unknown	Unknown

Table 6.2: Process faults

The simulation model of continuous stirred tank heater (CSTH) is developed by Thornhill et al. [100]. It is *hybrid* simulation, combining Matlab-based mathematical model with experimental data obtained from actual plant. The stochastic disturbance models are realistic and are derived from the real measurements. The nonlinear behavior and hard constraints are also precisely captured in the look-up tables. Therefore, CSTH plant offers challenging task especially for the data-driven process monitoring approaches.

A simple sketch of the plant is shown in Fig.(6.2). It consists of a rig in which hot and cold water are mixed and then heated using the stream

Variable name	Op. 1	Op. 2	Units
Level	12.00	12.00	mA
Level	20.48	20.48	cm
Cold water flow	11.89	7.330	mA
Cold water flow	9.038×10^{-5}	3.823×10^{-5}	$m^3 s^{-1}$
Cold water valve	12.96	7.704	mA
Temperature	10.50	10.50	mA
Temperature	42.52	42.52	°C
Steam valve	12.57	6.053	mA
Hot water valve	0	5.500	mA
Hot water valve	0	5.215×10^{-5}	$m^3 s^{-1}$

Table 6.3: CSTH operating mode parameters

through the heating coil. The water is then drained from the tank through a long pipe. The mixture is well stirred inside the tank, so that the temperature inside the tank can be assumed to be the same as that of the outflow. The plant has three proportional integral controllers namely for cold water level, temperature and flow. The plant inputs are hot water, cold water, and steam valve position. The level of the cold water and temperature are regulated. The cold water flow, level and temperature of the tank are measured output signals. All the signals are in the same range, i.e. 4-20 mA.
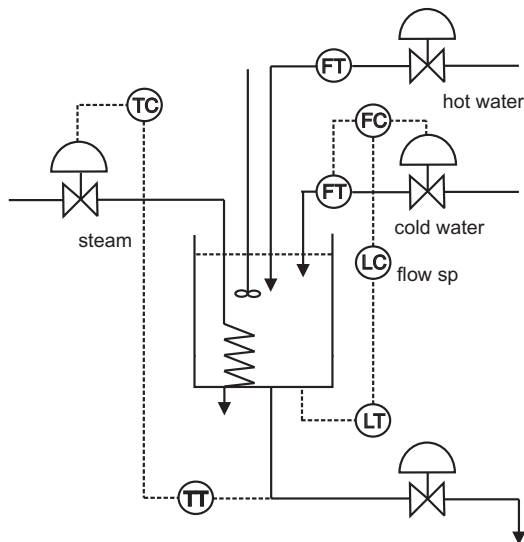

Figure 6.2: CSTH plant

The stirred tank heater is interesting for both model-based as well as

adaptive fault detection approaches. On one hand, CSTH has fewer measured variables compared to TE process and is thus appropriate for model identification based algorithms, but on the other hand, plant's dynamics is time varying, requiring frequent adjusting of the parameters of the FD system. Therefore, CSTH is used as a benchmark for RPSi-1, RPSi-2 and OPSi based algorithms.

6.2 PSi based FD system

The training dataset of TE process is collected from 24 hours of operation. This translates into 480 samples of 52 measurements. Clearly, this would cause tremendous computation overhead and memory overruns in the identification experiment, raising serious questions about the reliability. To avoid this difficulty, the measurements are divided into 8 blocks. This approach is suggested in [65] and is commonly referred to as multi-block design in statistical process monitoring. In TE process, each block is associated with a physical unit, e.g. reactor, separator, stripper, etc., only except the fifth block which is a collection of all the measurements that are not included in any other block. See Tab.(B.1) for the classification.

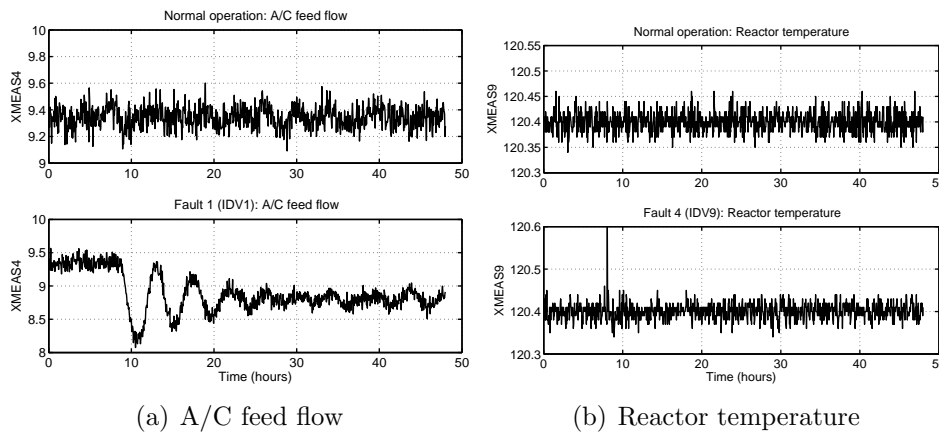(a) A/C feed flow (b) Reactor temperature

Figure 6.3: Comparison for IDV1 and IDV4

The next step is to identify the parity vectors and construct an observer for each separate block. The input and output measurements of each block are scaled with respect to their mean values and standard deviations. The design steps of FD system can be illustrated with an example of the input feed block. This block has 11 manipulated variables as its inputs and feed flow rates of components A, B, D, and E as outputs. Setting the value

of s to 5 and N to 100, the input and output block Hankel matrices are constructed as $U_p, U_f \in \mathbf{R}^{55 \times 100}$ and $Y_p, Y_f \in \mathbf{R}^{20 \times 100}$. The parity vectors $v_s \in \mathbf{R}^{1 \times 20}, \rho_s \in \mathbf{R}^{1 \times 55}$ are identified as shown in PSi.

(a) Input feed   (b) Reactor

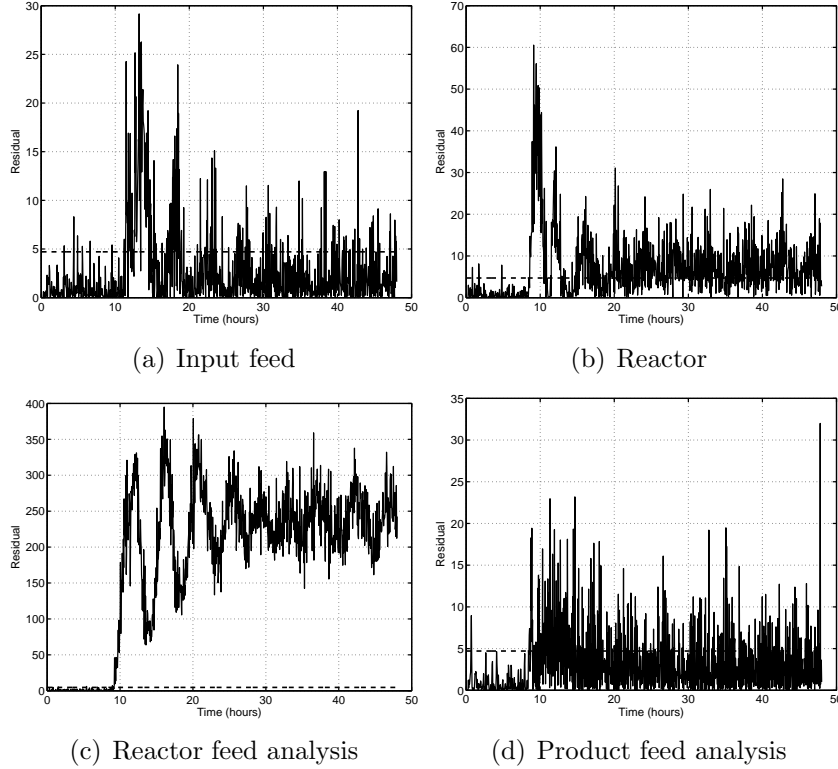(c) Reactor feed analysis   (d) Product feed analysis

Figure 6.4: Residuals in case of IDV1

The final form of residual generator can either be in the form of parity space or diagnostic observer. Here, diagnostic observer is chosen for its considerable ease in on-line implementation and additional design in obtaining the closed-loop gain. By applying the PS2DO, the observer is constructed from the parity vectors by computing the matrices $A_z \in \mathbf{R}^{4 \times 4}$, $B_z \in \mathbf{R}^{4 \times 11}$, $c_z \in \mathbf{R}^{1 \times 4}$, $d_z \in \mathbf{R}^{1 \times 8}$, $g \in \mathbf{R}^{1 \times 4}$ and $L \in \mathbf{R}^{4 \times 4}$. For the closed-loop implementation, the observer gain matrix L_o is chosen such that all the eigenvalues of the matrix $(A_z - L_o c_z)$ are at -0.1 in the unit circle.

It is also recommended in order to improve the detection of smaller faults, the residual is filtered. Therefore, GLR-based residual evaluation method as mentioned in algorithm JTH is implemented. The threshold is selected by choosing the false alarm rate based on the confidence interval equal to 95%. It has been shown in the figures by a dotted line. Note that this type of residual evaluation strategy is followed for each block separately.

In the next stage, the process is simulated with different faults, and each simulation consists of 48 hours of process operation . As explained in section (6.1), the first type of fault is step type change in the feed ratio of A and C components (IDV1). As seen in the Fig.(6.3), the step change occurs after 8 hours of normal operation. The fault affects material balance equations of the plant, leaving almost half of the monitored variables to change through various control-loops and recycle streams. Figure (6.4) shows that the ob-server based residual generators for input feed, reactor, reactor feed analysis and product analysis blocks detect this fault easily.

(a) Input feed

(b) Reactor

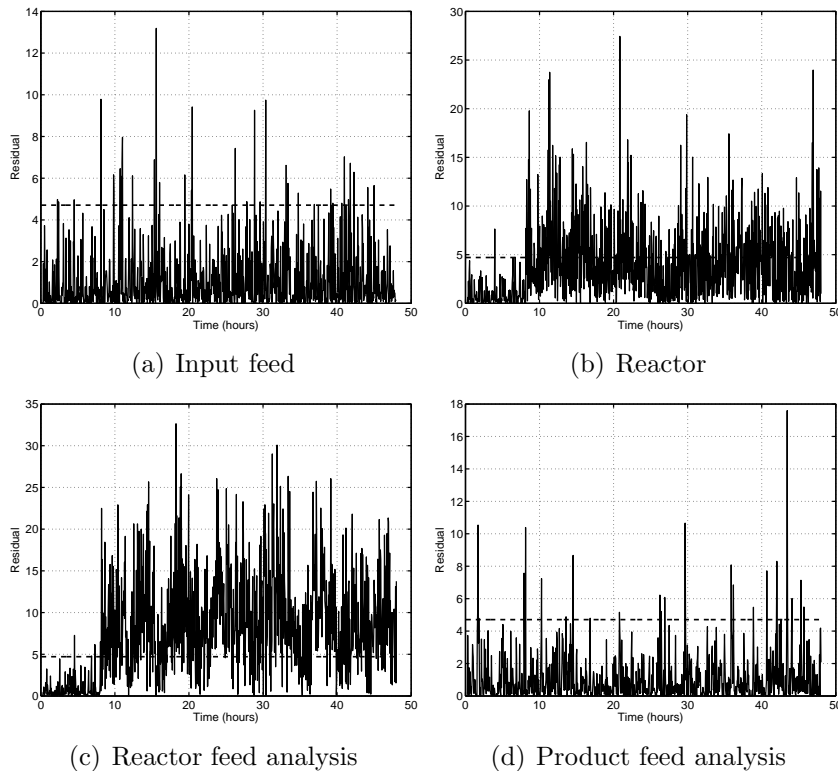(c) Reactor feed analysis

(d) Product feed analysis

Figure 6.5: Residuals in case of IDV4

The second type of fault is also a step type change in the reactor cooling water inlet temperature (IDV4). This fault significantly affects the reactor variables such as temperature, cooling water flow rate. Some of the plant variables are left unaltered, letting this fault become more difficult to trace than the previous one. Figure (6.5) shows that the residual generators de-signed for reactor, reactor feed analysis and product feed analysis perform better over input feed block, which shows significant missed detections. For the plant operator, it is necessary to consider the results from all the residual

generators running parallel, to avoid any wrong decision.

In the last experiment, the process parameters are altered in an unknown way (IDV17). The exact nature and magnitude of this fault is not provided, but it is periodic in nature as seen from the inflicted measurements. This could be attributed to stiction in the actuators, typically pumps. It is seen from Fig.(6.6), the residuals of the input feed, reactor, reactor feed analysis and product analysis clearly cross their thresholds during the fault. To summarize, PSi-based FD system can detect 17 of the total 20 faults given in [25]. Also see appendix B. The higher percentage of the missed detections in case of faults 3, 9 and 15 can be attributed to the insignificant change caused by the faults in the measurement space in [97].

(a) Input feed

(b) Reactor

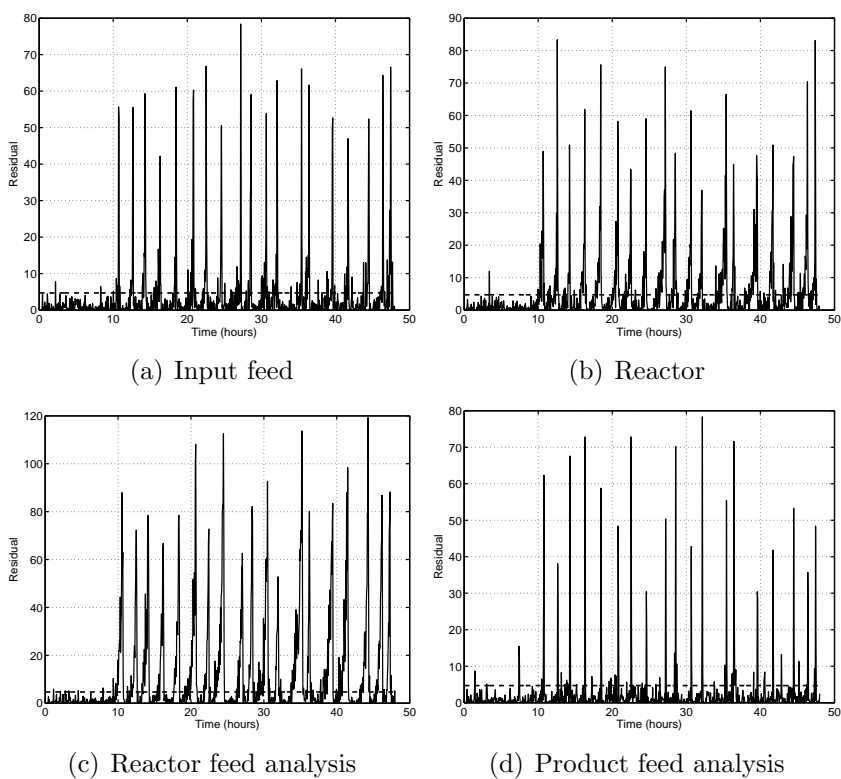(c) Reactor feed analysis

(d) Product feed analysis

Figure 6.6: Residuals in case of IDV17

Construction of a soft-sensor

In TE process, analyzer measurements are slow compared to other measurements such as temperature, pressure, and mass flow. For instance, product analysis of D occurs every 15 minutes and it takes 15 minutes to complete.

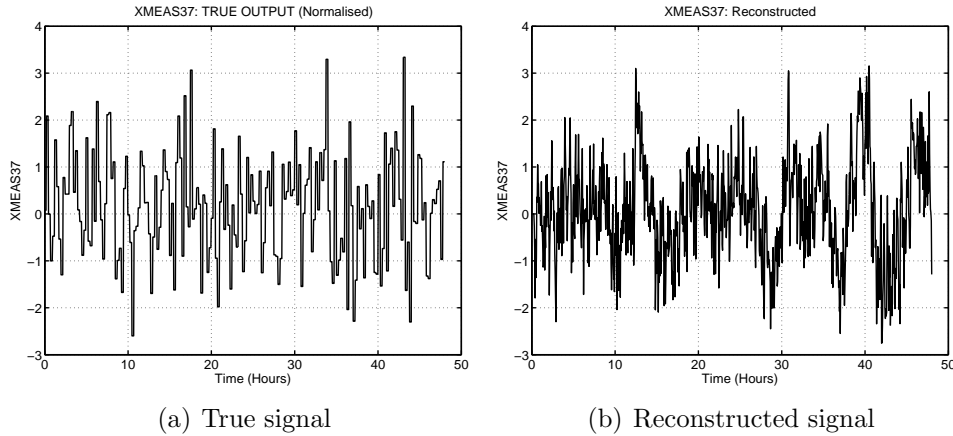(a) True signal   (b) Reconstructed signal

Figure 6.7: Soft-sensor for XMEAS(37)

This may present difficulty in controller design and monitoring, since the plant measurements are sampled with different frequencies. To deal with such issues, a soft-sensor can be designed which generates approximate yet fast and regularly sampled measurements for further applications.

To design a soft-sensor, a primary residual generator is identified according to PSi and modified as suggested in section 3.3. In this demonstrative example, sensor XMEAS37 for product feed analyzer is reconstructed. It performs quality analysis of product D. The primary residual generator based soft-sensor requires two vectors, $\bar{v}_s \in \mathbf{R}^{1 \times 15}$ and $\bar{\rho}_s \in \mathbf{R}^{1 \times 55}$ and the soft-sensor has following on-line implementation form:

$$\hat{y}_{xmeas4}(k) = \bar{v}_s \bar{y}_{s-1}(k) - \bar{\rho}_s u_s(k) \tag{6.1}$$

For comparison, the actual measurement of XMEAS37 is scaled to zero mean
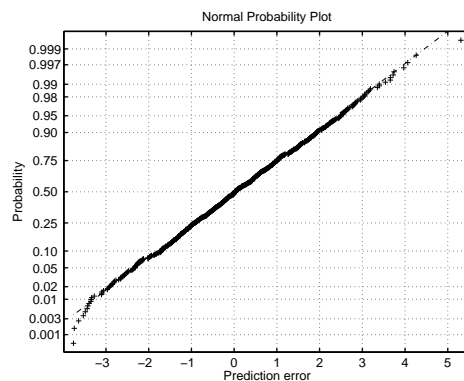

Figure 6.8: Probability density function of prediction error

and unit variance. It is plotted in Fig.(6.7(a)) along with the reconstructed measurement as shown in Fig.(6.7(b)). The prediction error of this soft-sensor, which is a measure of accuracy and effect of stochastic disturbances, is computed as an average difference between the actual and reconstructed output. The probability density function of the error is plotted in Fig. (6.8). The mean value of the prediction error is 0.0627 and the variance is 2.0757.

Remarks

Since Tennessee Eastman process is a typical large-scale process, the secondary form of residual generator is more suitable as compared to the primary form. Since the diagnostic observer-based FD system does not require lagged measurements to be stored on-line, it translates into significant reduction in computation and memory requirements. Also, if the process exhibits transient behaviors, the closed-loop structure will yield better stability and consistency than the primary form of residual generator.

6.3   RPSi-1 and RPSi-2 based FD system

CSTH is basically a nonlinear plant because its states such as volume of the water inside the tank and total enthalpy are functions of input water flow. The thermodynamic properties of the tank and output flow also exhibit nonlinear characteristics. Moreover, a non-steady reference signal causes plant's dynamics to change with manipulated variables. It is also frequently subjected to deterministic oscillatory disturbances as mentioned in [100].
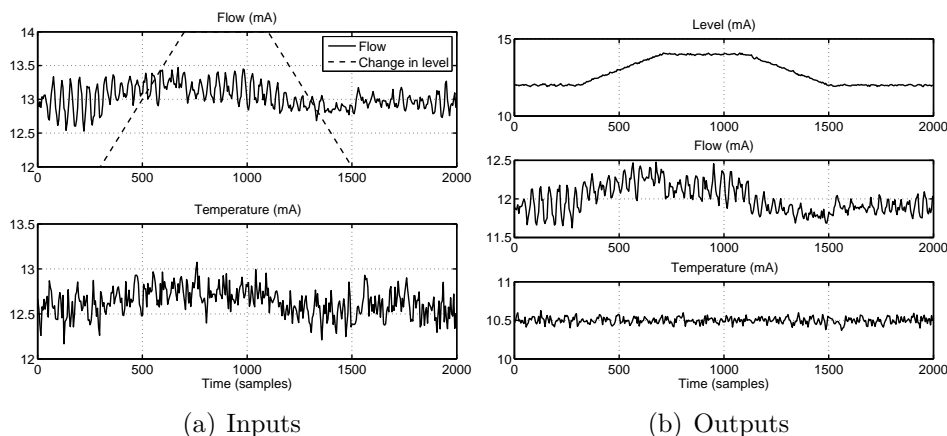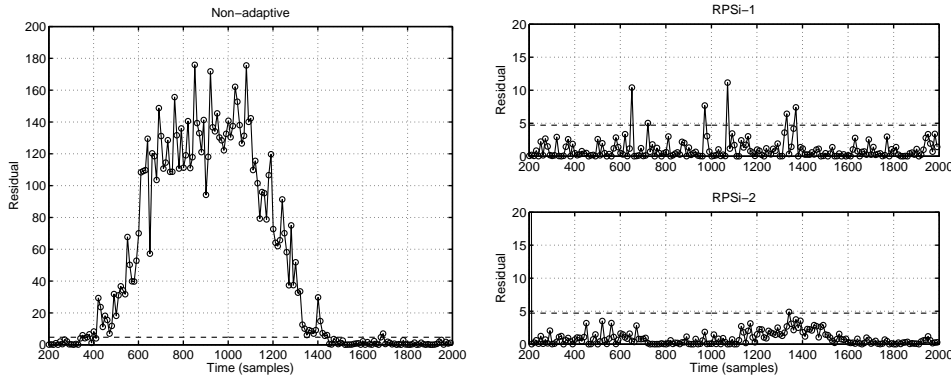

(a) Inputs   (b) Outputs

Figure 6.9: Plant measurements

(a) Residual obtained by non-recursive (b) Comparison of approximation error
SVD

Figure 6.10: Performance analysis - I

Before designing the adaptive scheme, the initial residual generator must be constructed from the off-line data collected at a single operating point. To this end, PSi-based primary residual generator is identified with 200 samples of measurement data. The order of this residual generator is chosen as 3. To compare the performance, RPSi-1, RPSi-2 and non-adaptive PSi-based FD systems are implemented on the benchmark. The plant is simulated with the desired value of the water level changing twice during the whole run. The measurements are shown in Fig.(6.9) with a dotted line indicating the desired water level.
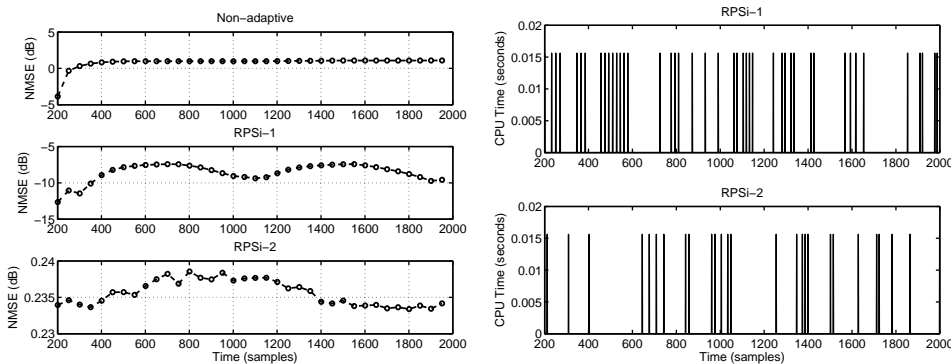
(a) Residuals (b) CPU time

Figure 6.11: Performance analysis - II

The residual signal generated by the non-adaptive design is shown in Fig.(6.10(a)), it crosses the threshold after the water level set-point changes, indicating a false alarm. In comparison, the residuals generated by RPSi-1

and RPSi-2 based residual generator remain below the threshold, except for short time of adaptation. The results are plotted in Fig.(6.10(b)). Note that since the process is in closed-loop, the instrument variable also consists of the reference signals [50]. The adjacent figure (6.11(b)), shows that RPSi-1 involves comparatively more lengthy computations than RPSi-2.

Figure (6.12) shows the residual distributions obtained by the three different implementations, where the + sign indicates residual and the dotted line shows the locus of samples of zero-mean, Gaussian distributed data. As can be seen that the residual obtained by non-adaptive approach does not conform to normal distribution, whereas RPSi-1 and RPSi-2 generated residuals give better approximation of Gaussian normal distribution.

$$NMSE_1 = \frac{\left\|U_k \Sigma_k V_k^T - \Phi_{z,k}\right\|_F^2}{\left\|\Phi_{z,k}\right\|_F^2} \qquad \text{for RPSi-1} \qquad (6.2)$$

$$NMSE_2 = \frac{\left\|\Omega_{z,k} \Phi_{z,k} \Omega_{z,k}^T - \Phi_{z,k}\right\|_F^2}{\left\|\Phi_{z,k}\right\|_F^2} \qquad \text{for RPSi-2} \qquad (6.3)$$

where $\Phi_{z,k} = \alpha\Phi_{z,k} + (1-\alpha)\, z_{k,f} z_{\tau,p}^T$ for RPSi-1 and for RPSi-2, $\Phi_{z,k} = \alpha\Phi_{z,k} + (1-\alpha)\, z_{k,f} z_{k,f}^T$.
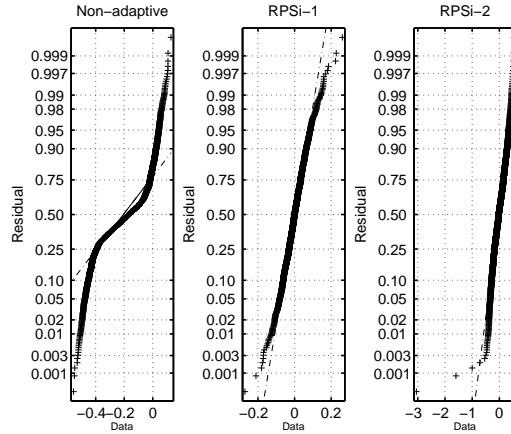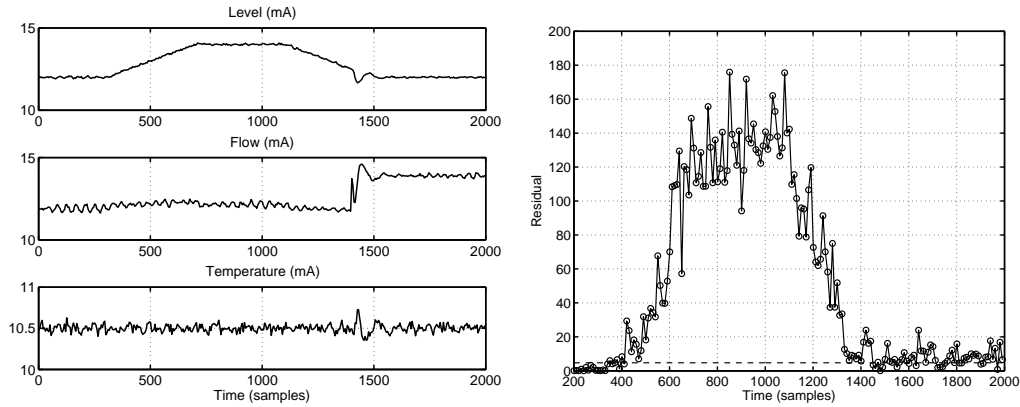

Figure 6.12: Performance analysis - III

The results of RPSi-1, RPSi-2 and non-adaptive approach with NMSE index are plotted in Fig.(6.11(a)). It can be seen that RPSi-1 produces approximate of the dominant subspace with least error as compared to RPSi-2. The approximation error grows slowly for the non-adaptive approaches

(a) Output measurements in faulty opera- (b) Residual obtained by non-recursive SVD
tion

Figure 6.13: Sensor fault detection: non-adaptive approach

which could render it unusable for process monitoring application. Therefore, the selection of adaptive approaches amongst RPSi-1 and RPSi-2 depends on the trade-off between approximation consistency and computation cost.
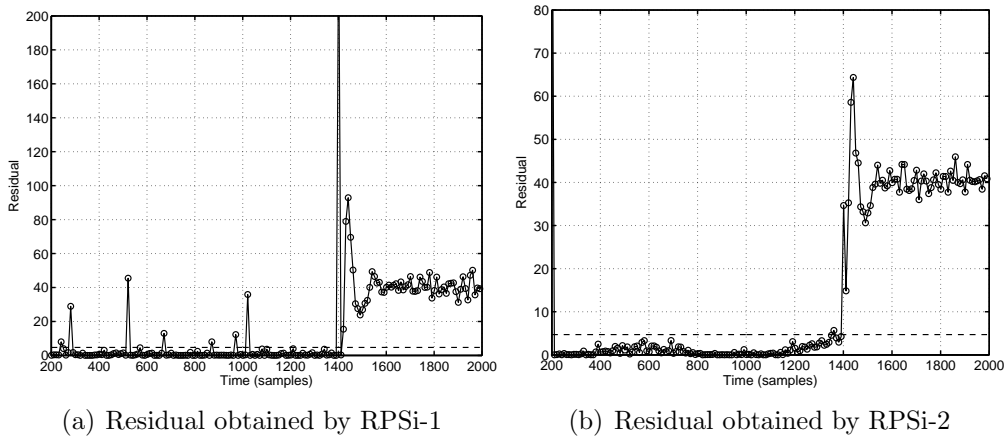
(a) Residual obtained by RPSi-1   (b) Residual obtained by RPSi-2

Figure 6.14: Sensor fault detection: adaptive approach

In the last experiment, a small sensor fault is simulated inside the CSTH plant, with all other operating conditions remaining unchanged. The fault occurs after 1400th sample and it adds approximately 10% bias to the actual flow measurement. The output measurements are shown in Fig.(6.13(a)). The residual signals obtained by non-adaptive approach such as PSi-based is shown in Fig.(6.13(b)) and that obtained from RPSi-1 and RPSi-2 are shown in Fig.(6.14). Note that the residual signal is evaluated and the threshold is

selected (shown by the dotted line in the figures) based on algorithm JTH.

It can be seen that non-adaptive approach fails to detect the sensor fault as it has already crossed the threshold after the change in the water level set-point. On the contrary, the adaptive designs based on RPSi-1 and RPSi-2 comfortably detect the fault after 1400th sample. Therefore, for effective process monitoring and fault detection in CSTH, adaptive approaches are more suitable.

Remarks

From the results, it can be concluded that non-adaptive FD systems perform poorly on a plant with time-varying behavior. The RPSi-1 and RPSi-2 based adaptive design of primary residual generators or diagnostic observers not only reduces the on-line computation cost, but also effectively deal with such nonlinear behavior. Although, the adaptive algorithms are able to detect faults, there is a need to implement a stopping mechanism so that the faulty measurements are not used in adaptive calculations. This can either be achieved by reconstructing a fault-free measurement by estimating the magnitude of the fault [73], or by monitoring relative change in parameters of residual generators. For the latter, relative change larger than a pre-specified threshold will indicate fault and stop adaptive computations.

6.4   OPSi based FD systems

In this section, the OPSi-based design of FD system is implemented on the stirred tank heater. The plant is simulated in the second operating region, where it has both hot and cold water feeds. The details of this operating condition are provided in Tab.(6.3). For comparative analysis, subspace identification based observer and FICSI based residual generation schemes are also implemented.

In the off-line model identification stage, 200 sample measurements of inputs and outputs are collected. For subspace based identification, the inputs are perturbed by random binary signal as specified in [100] and a third order model is identified using Matlab-based toolbox. Then a closed-loop observer-based FD system is designed which has following form:
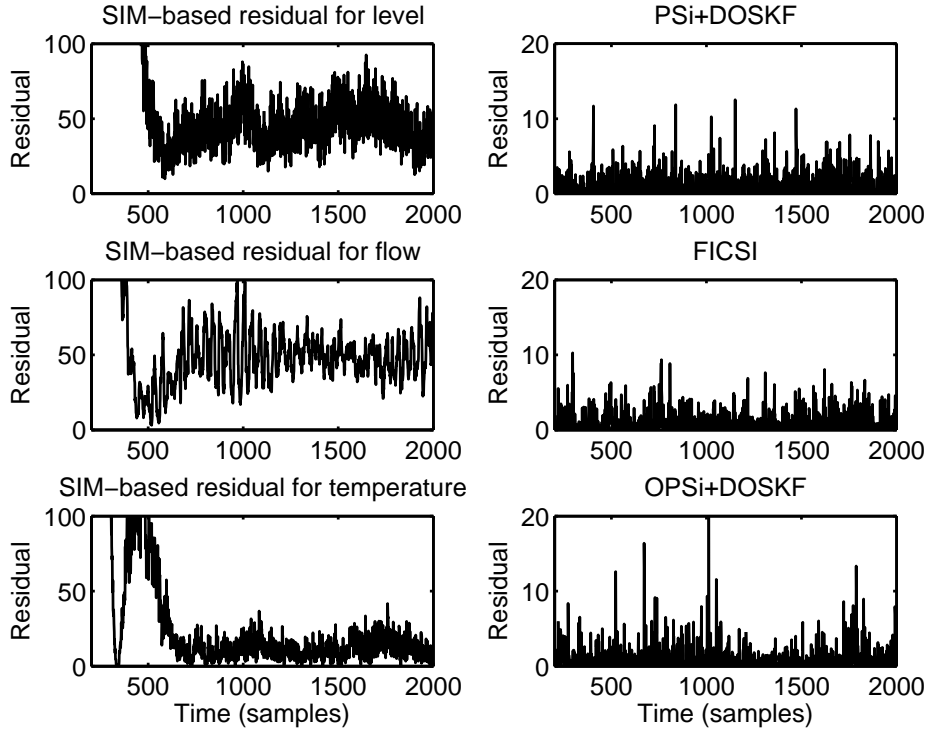
Figure 6.15: Comparison of different residuals

$$
x_{k+1} = \begin{bmatrix} 0.99 & 0.01 & 0.11 \\ 0.02 & 1.01 & 0.03 \\ 0.03 & -0.11 & 0.83 \end{bmatrix} x_k + \begin{bmatrix} -0.03 & -0.00 \\ 0.00 & -0.01 \\ 0.39 & 0.01 \end{bmatrix} u_k
$$

$$
+ \begin{bmatrix} -0.27 & -0.07 & -0.30 \\ 0.45 & 0.08 & -1.23 \\ 0.40 & 1.57 & -0.36 \end{bmatrix} r_k \tag{6.4}
$$

$$
\hat{y}_k = \begin{bmatrix} -0.72 & 0.21 & -0.05 \\ -0.20 & 0.06 & 0.35 \\ -0.66 & -0.22 & -0.01 \end{bmatrix} x_k + \begin{bmatrix} -0.04 & -0.00 \\ -0.15 & -0.01 \\ -0.05 & -0.02 \end{bmatrix} u_k \tag{6.5}
$$

$$
r_k = y_k - \hat{y}_k \tag{6.6}
$$

The PSi and OPSi based primary residual generators are designed according to the algorithms provided in chapter 3 and chapter 5 respectively. To this end, the sample size N is the 200 and the observability parameter s is chosen as 5. For on-line implementation, the diagnostic observer is designed according to PS2DO and the Kalman filter gain is identified according to

Method	Residual variance
SIM-based	0.0014
PSi+DOKF	0.0013
FICSI	3.0134×10^6
OPSi+DOKF	9.6602×10^4

Table 6.4: Comparison of FD systems

DOKF. The FICSI-based design of residual generator is also implemented according to algorithm provided in the appendix A.

Figure (6.15) shows the residuals generated by SIM-based observer, PSi and OPSi based diagnostic observer and FICSI based residual generator. The variance of these residual signals is provided in the Tab.(6.4) below. Note here that for the SIM-base method, the residual signal is vector-valued and hence the variance is computed as an average of all the three individual values.

It is clear that SIM-based observer has large transient after the initial condition and it converges very slowly. The FD system produces residual with large variance, which may pose difficulty in detecting small faults. The PSi-based design also has comparatively larger variance compared to both FICSI and OPSi-based designs. Therefore, in the applications requiring smallest deviations to be detected, FICSI or OPSi-based designs are recommendable.

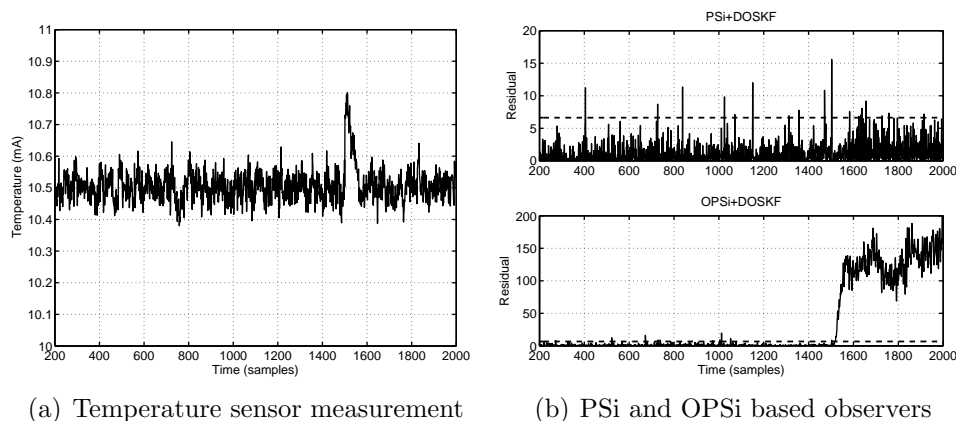(a) Temperature sensor measurement   (b) PSi and OPSi based observers

Figure 6.16: Fault in temperature sensor

In the next set of experiments, PSi and OPSi based diagnostic observers are compared under several faulty conditions which can frequently affect the plant. These faults are described in Tab.(C.1) [46] and are simulated for process run consisting of 2000 samples, of which first 200 samples are used to

design the FD system. For the sake of brevity of this section, only two cases are discussed. The pictorial summary for the rest of the cases is provided in appendix C.

The first case is of small bias on the temperature measuring sensor. The faulty measurement is shown in Fig.(6.16(a)) and the residuals produced by both PSi and OPSi-based observer are plotted in Fig.(6.16(b)) where the threshold (see algorithm JTH) is indicated by dotted line. Note that the sensor fault is compensated by regulative action by the control system and therefore even if the fault appears to have disappeared, the residual is still above its threshold.

In the next experiment, stiction inside a valve that feeds cold water to the tank is simulated. Stiction is very common in actuator malfunction and it may cause damage to the plant, since actuators are essential control components. In CSTH, the stiction inside the cold water valve affects the mass balance equation and disturbing almost all measured variables such as level, flow and temperature. Therefore, this fault is relatively easy to detect for both PSi and OPSi based observer, as seen from Fig. (6.17).

(a) CW valve stiction (b) PSi and OPSi based observers
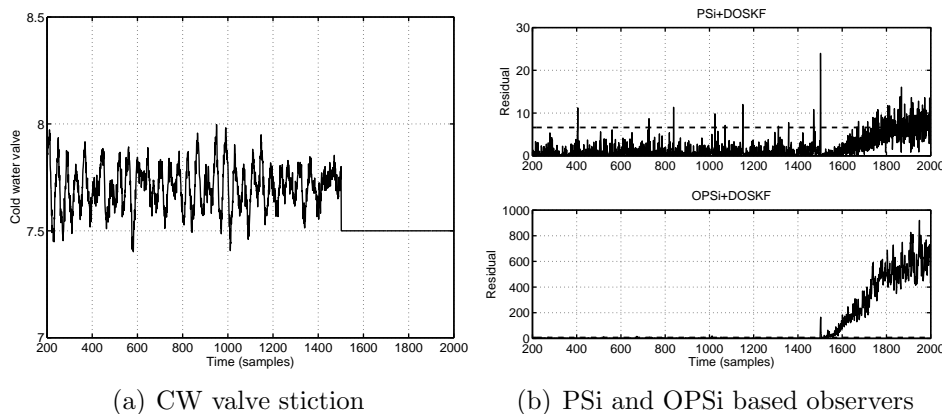
Figure 6.17: Fault in cold water valve

On the contrary side, stiction inside the steam valve poses relatively more difficult challenge to the FD systems. The faulty actuator is shown in Fig. (6.18(a)), it affects only the temperature of the out-flowing water without disturbing the level and flow variables. But as seen from residuals in Fig.(6.18(b)), OPSi-based observer successfully detects this fault, whereas PSi-based residual fails to detect it. The results with remaining cases of faults are provided in appendix C.

(a) Steam valve stiction   (b) PSi and OPSi based observers

Figure 6.18: Fault in steam valve

Remarks

In this section, the OPSi-based design of optimal residual generator is implemented on the continuously stirred tank heater. The design scheme is compared with SIM-based observer design, FICSI based residual generator and PSi-based diagnostic observer. In terms of residual variance, OPSi-based residual generators improves the original PSi-base design. The OPSi-based diagnostic observer also outperforms PSi-based one in detecting several commonly occurring faults in CSTH.

6.5   Concluding remarks

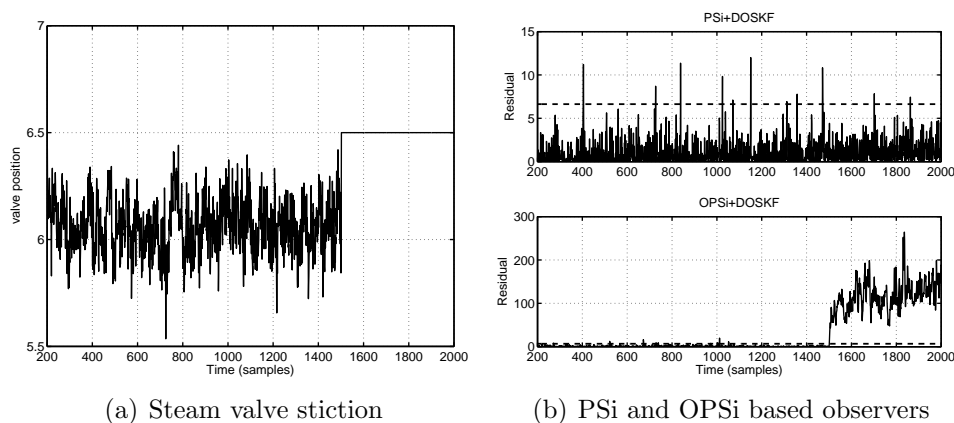In the first part of this chapter, the novel data-driven method to design primary (PSi) and secondary (PS2DO, DOKF) residual generators are implemented on Tennessee Eastman process. The process is realistic representation of a large-scale industrial plant. Therefore, the efficacy of the new method implemented on it shows promise for its industrial application. In the remaining part of the chapter, the adaptive (RPSi-1, RPSi-2) and optimal (OPSi) extensions of PSi are implemented on the continuously stirred tank heater. The plant offers wide variety of challenges in terms of changing operating conditions or realistic representation of plant disturbances. In the former case, the adaptive design of monitoring system perform better over non-adaptive scheme, in handling changes in the dynamic behavior of the plant. On the same plant, the OPSi-based design of diagnostic observer also improves the performance of PSi-based design in dealing with stochastic environment.

Chapter 7

Summary

The main goal of this thesis was to study the application of data-driven design of fault detection systems. To begin with, an overview of the popular model-based technique such as linear observer, diagnostic observer, and parity relation is presented. These approaches are well accepted in the industrial field owing to their effectiveness, simplicity, and robustness to plant disturbances. The core of this technique is the analytical model-building, either through meticulous first principles or model identification. The FD systems are enhanced through residual generation, residual evaluation and threshold selection procedures.

As mentioned, the model-based techniques require mathematical knowledge of the plant under consideration. In many cases, such as complex chemical processes, it is clumsy and difficult to obtain a model for entire plant just by deriving its differential equations. A suitable alternative here is to obtain the model from its historical data. Since modern plant designs rely heavily on instrumentation, it is not difficult to obtain chunks of data that captures nominal plant behavior. The work in chapter 3 emphasizes this concept to design an effective fault detection system.

The PSi algorithm presented in chapter 3 identifies only the key components from the process input and output data. It avoids estimating the entire model, thereby saving considerable computation cost. The primary residual generator based on it can be further enhanced by designing a closed-loop diagnostic observer. This observer is extremely efficient for on-line application in large-scale processes and has a further extension as Kalman filter. Based on it, a fault isolation scheme for sensors and actuators, and a soft-sensor are also constructed.

The data-driven FD systems are designed based on the assumption that the data is generated by time invariant plant. In simple words, the plant parameters are held constant. But in reality this may not be true and some

of the variables may undergo temporary changes as a result of variation in operating conditions. The FD system needs to adopt these changes in order not to produce too many false alarms. Therefore, in chapter 4 an adaptive designs of PSi-based FD system are proposed. The techniques (RPSi-1 and RPSi-2) are based on recursive but efficient identification and is suitable for application in large-scale processes.

In chapter 5, the issue of optimal design of data-driven fault detection system is dealt with. In literature for model-based FD technique, the selection of optimal parameters is well addressed topic. But in identification-driven design, this issue has gained less attention. In this work, the optimal design of primary residual generator is achieved by the identification of Kalman filter. To this end, non-orthogonal projection technique is applied and the consistency of the algorithm is also proven. The algorithm is numerically optimized by using QR-based decomposition technique.

Although, this work attempts to build a framework for the data-driven identification based design of FD systems, it is incomplete with respect to couple of important issues. The main focus of this work is on the residual generation stage, as against the strong need to address residual evaluation in more general stochastic framework. This is because often the plant data is corrupted by non-Gaussian noise, non-linearities, and unknown disturbances. Moreover, the plant parameters may exhibit uncertain behavior for which the adaptive design may not be an optimal solution.

Other issues that require attention are the detection of process faults and design of post-filters. Usually, a process fault results in the change in residual variance. Therefore, it is difficult to detect it with classical technique such as GLR test or χ^2 based method. A post-filter can be designed for various purposes such as increasing robustness against plant disturbances or sensitivity to faults. Finally, design of fault-tolerant controller and integrated FDI schemes also require worthy attention in the future.

Appendices

Appendix A

FICSI

The FICSI algorithm (Fault detection and Identification approach Connected to Subspace Identification) is proposed in [21]. The original idea is to include state information to improve fault sensitivity of parity space based residual generator. It is achieved by reconstructing states from past input and output data by applying subspace identification technique. The algorithm is simple and a slightly different version of the one proposed in [21] is provided here for reference. To begin with, an extended state space equation is written as shown Eq.(5.31):

$$Y_f = \Gamma_s H_{w,p} W_p + H_{u,f} U_f + E_f. \tag{A.1}$$

The matrices involved in Eq.(A.1) are defined in chapter 4. The FICSI based residual generator is defined as:

$$r_k = y_{k,s} - \hat{\Gamma}_s \hat{H}_{w,p} \begin{bmatrix} y_{k-s,s} \\ u_{k-s,s} \end{bmatrix} - \hat{H}_{u,s} u_{k,s} \tag{A.2}$$

where

$$y_{k,s} = \begin{bmatrix} y_{k-s+1} \\ y_{k-s+2} \\ \vdots \\ y_k \end{bmatrix}, y_{k-s+2,s} = \begin{bmatrix} y_{k-2s+1} \\ y_{k-2s+2} \\ \vdots \\ y_{k-s} \end{bmatrix},$$

where s is order of the residual generator. Similarly $u_{k,s}$ and $u_{k-s,s}$ are also defined. The estimates of $\Gamma_s H_{w,p}$ and $H_{u,s}$ can be obtained by successive oblique projections. For instance, $\hat{\Gamma}_s \hat{H}_{w,p}$ is estimated by following projection:

$$\hat{\Gamma}_s \hat{H}_{w,p} = Y_f \big/_{U_f} W_p \left(W_p^\dagger \right), \tag{A.3}$$

and similarly $\hat{H}_{u,s}$ is obtained as

$$\hat{H}_{u,s} = Y_f \big/_{W_p} U_f \left(U_f^\dagger \right). \tag{A.4}$$

The residual signal r_k can now be obtained as shown in Eq.(A.2) and after constructing $y_{k,s}, u_{k,s}$ and $y_{k-s,s}, u_{k-s,s}$ from online measurements.

Appendix B

Tests on Tennessee Eastman plant

As explained section 6.2, to design PSi-based FD system for TE process, the plant measurements are divided in 8 blocks and an FDI system is designed for each separate block, G1, G2,..., G8. The arrangement is shown in Tab.(B.1). Table (B.2) shows the missed detection rate (MDR) assuming that the fault begins approximately after 8 hours of normal process operation [25]. The MDR is calculated in the following manner.

Let t_{begin} be the time (in seconds) when the fault first occurs and t_{end} be the time when simulation ends. Then the missed detections are calculated, assuming the fault persistently remains until the simulation ends, as

$$MD = \sum_{k \in N_{sim}} 1 \tag{B.1}$$

where $N_{sim} = \{k : t_{begin} < k \le t_{end} \quad \text{and} \quad r_k < J_{th}\}$, r_k is filtered residual signal and J_{th} is threshold for fault detection. The missed detection rate is then computed as

$$MDR = \frac{MD}{t_{end} - t_{begin}} \times 100 \tag{B.2}$$

Note that since some faults are unknown and random in nature, the missed detection rate unfortunately can not provide correct performance evaluation in all the fault cases.

Block name	Variable name	Variable number
Input feed	A feed (stream 1)	XMEAS(1)
	D feed (stream 2)	XMEAS(2)
	E feed (stream 3)	XMEAS(3)
	A and C feed	XMEAS(4)
Reactor	Reactor feed rate	XMEAS(6)
	Reactor pressure	XMEAS(7)
	Reactor level	XMEAS(8)
	Reactor temperature	XMEAS(9)
Separator	Separator temperature	XMEAS(11)
	Separator level	XMEAS(12)
	Separator pressure	XMEAS(13)
	Separator underflow	XMEAS(14)
Stripper	Stripper level	XMEAS(15)
	Stripper pressure	XMEAS(16)
	Stripper underflow	XMEAS(17)
	Stripper temperature	XMEAS(18)
	Stripper steam flow	XMEAS(19)
Miscellaneous	Recycle flow	XMEAS(5)
	Purge rate	XMEAS(10)
	Compressor work	XMEAS(20)
	Reactor water temperature	XMEAS(21)
	Separator water temperature	XMEAS(22)
Reactor feed analysis	Component A	XMEAS(23)
	Component B	XMEAS(24)
	Component C	XMEAS(25)
	Component D	XMEAS(26)
	Component E	XMEAS(27)
	Component F	XMEAS(28)
Purge gas analysis	Component A	XMEAS(29)
	Component B	XMEAS(30)
	Component C	XMEAS(31)
	Component D	XMEAS(32)
	Component E	XMEAS(33)
	Component F	XMEAS(34)
	Component G	XMEAS(35)
	Component H	XMEAS(36)
Product analysis	Component D	XMEAS(37)
	Component E	XMEAS(38)
	Component F	XMEAS(39)
	Component G	XMEAS(40)
	Component H	XMEAS(41)

Table B.1: Process measurements

Fault	G1	G2	G3	G4	G5	G6	G7	G8
IDV1	78.8	38.2	75.3	87.3	84.5	02.6	**02.1**	97.9
IDV2	16.0	14.2	89.0	53.0	34.6	03.6	**03.3**	34.6
IDV3	96.9	96.6	96.7	96.6	96.0	95.9	96.5	97.1
IDV4	95.9	62.0	95.4	26.4	**22.2**	23.3	95.5	96.7
IDV5	93.5	90.1	93.4	01.9	93.9	**82.8**	93.6	95.4
IDV6	**00.4**	02.5	09.4	08.0	05.5	06.6	01.4	44.4
IDV7	34.2	**30.2**	90.1	90.6	74.2	75.4	92.6	93.9
IDV8	73.6	56.3	73.5	73.0	81.7	**42.6**	43.0	88.6
IDV9	97.0	96.9	97.7	97.9	**96.8**	96.9	97.6	98.3
IDV10	95.6	93.1	95.8	94.3	96.4	**83.6**	95.7	96.3
IDV11	74.9	64.9	92.9	54.3	**47.7**	50.5	92.5	83.7
IDV12	78.8	52.5	71.6	**45.1**	67.2	47.3	79.0	88.9
IDV13	64.2	**31.5**	63.3	47.3	60.3	40.5	42.1	88.7
IDV14	28.2	42.4	**18.0**	41.3	42.9	30.5	20.3	36.1
IDV15	97.5	97.0	96.2	97.1	96.5	**94.9**	97.4	97.1
IDV16	97.4	96.1	96.7	96.0	95.7	**90.0**	96.2	97.6
IDV17	80.2	66.8	87.7	55.8	**50.5**	53.9	89.7	90.2
IDV18	24.3	58.1	17.2	**15.4**	21.3	17.0	23.3	58.3
IDV19	93.5	88.8	84.7	82.1	84.1	90.3	83.5	**78.6**
IDV20	91.7	80.6	91.1	90.3	70.1	**60.6**	95.2	96.6
IDV21	96.7	**75.9**	97.5	87.8	96.6	89.5	91.1	97.9

Table B.2: Missed detection rates

Appendix C

Tests on CSTH

The table below lists the faults that can frequently disturb the continuously stirred tank heater. The figures from (C.2)-(C.5) provides the results obtained by PSi and OPSi-based diagnostic observers with faults 2, 3, 4, 5, and 8.

Fault	Process variable	Type
Fault 1	Temperature sensor	Bias
Fault 2	Hot water temperature	Step
Fault 3	Cold water temperature	Step
Fault 4	Level sensor	Bias
Fault 5	Heat exchanger	Fouling
Fault 6	Cold water valve	Stiction
Fault 7	Steam valve	Stiction
Fault 8	Stirred tank	Leakage

Table C.1: Faults in CSTH

The missed detection rates for both PSi and OPSi-based observer for the faults in Tab. (C.1) are provided in Tab.(C.2).
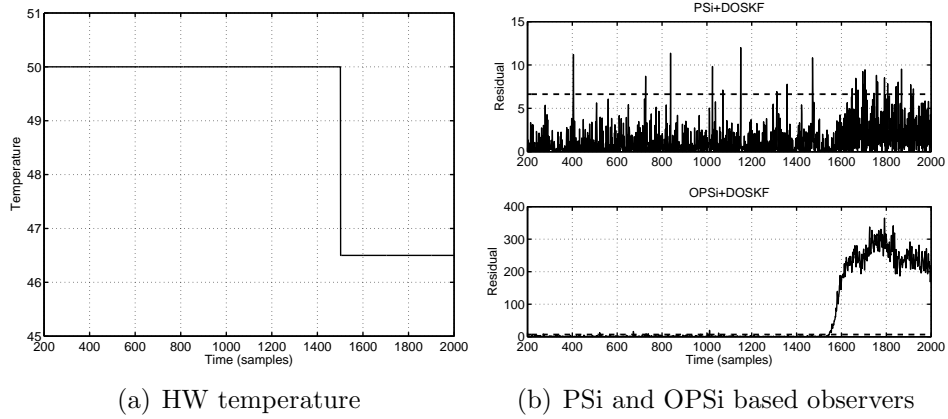
(a) HW temperature   (b) PSi and OPSi based observers

Figure C.1: Fault in hot water temperature

(a) CW temperature   (b) PSi and OPSi based observers
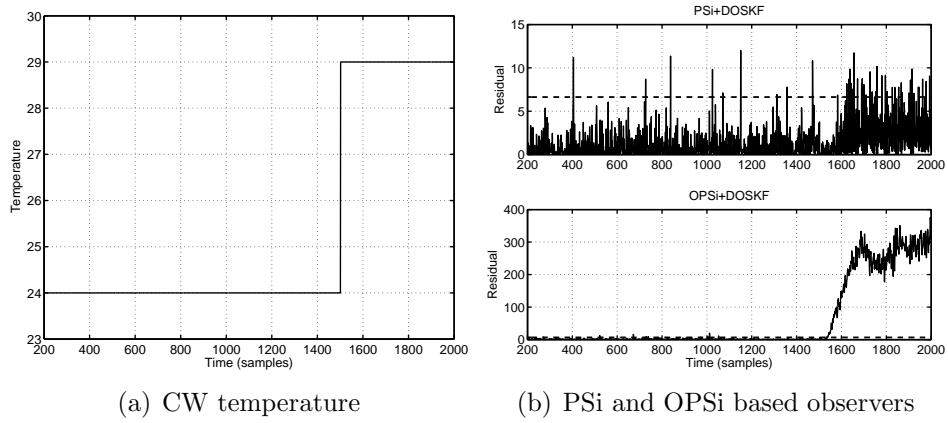
Figure C.2: Fault in cold water temperature

(a) Level sensor measurement   (b) PSi and OPSi based observers
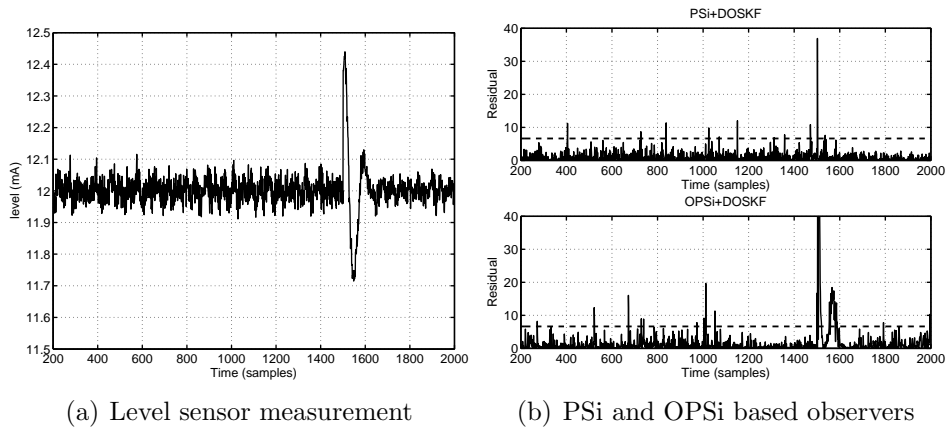
Figure C.3: Fault in level sensor

(a) Input temperature   (b) PSi and OPSi based observers
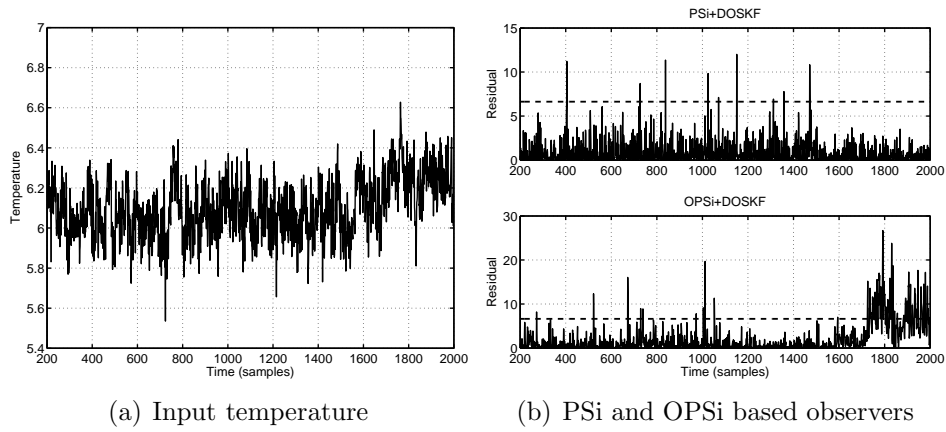
Figure C.4: Fault in heat exchanger

(a) Input temperature   (b) PSi and OPSi based observers
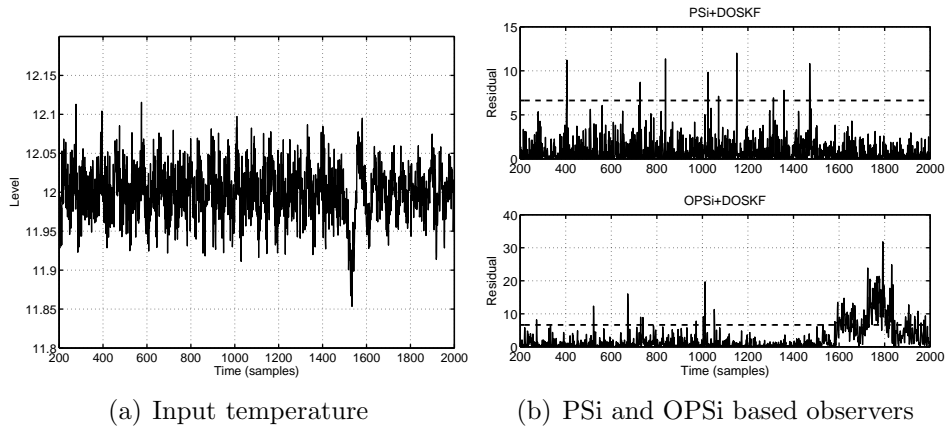
Figure C.5: Fault in tank

Fault	PSi+DOSKF	OPSi+DOSKF
Fault 1	99.2	03.0
Fault 2	96.6	09.0
Fault 3	92.8	07.2
Fault 4	99.4	90.2
Fault 5	99.9	71.4
Fault 6	76.0	04.0
Fault 7	99.6	00.2
Fault 8	99.9	62.4

Table C.2: Missed detection rates

Bibliography

[1] M. Basseville. On-board component fault detection and isolation using the statistical local approach. *Automatica*, 34(11):1391 – 1415, 1998.

[2] M. Basseville and I. Nikiforov. *Detection of Abrupt Changes: Theory and Application.* Prentice Hall, Inc., 1993.

[3] C. Batur, Z. Ling, and Chan Chien-Chung. Support vector machines for fault detection. In *Decision and Control, 2002, Proceedings of the 41st IEEE Conference on*, volume 2, pages 1355 – 1356, 2002.

[4] D. Bauer. Asymptotic properties of subspace estimators. *Automatica*, 41(3):359 – 376, 2005.

[5] R. Beard. *Failure accommodation in linear systems through self-reoragnization.* PhD dissertation, MIT, 1971.

[6] R. Behrens. Signal processing applications of oblique projection operators. *IEEE Transactions on Signal Processing*, 42(6):1413–1424, 1994.

[7] M. Blanke, M. Kinnaert, J. Lunze, M. Staroswiecki, and J. Schröder. *Diagnosis and Fault-Tolerant Control.* Springer-Verlag New York, Inc., 2006.

[8] S. Boyd, L. El Ghaoui, E. Feron, and V. Balakrishnan. *Linear Matrix Inequalities in System and Control Theory*, volume 15 of *Studies in Applied Mathematics.* SIAM, Philadelphia, PA, 1994.

[9] J. Bunch and C. Nielsen. Updating the singular value decomposition. *Numerische Mathematik*, 31:111–129, 1978.

[10] B. Champagne. Adaptive eigendecomposition of data covariance matrices based on first-order perturbations. 42, 1994.

[11] J. Chen and K.-C. Liu. On-line batch process monitoring using dynamic pca and dynamic pls models. *Chemical Engineering Science*, 57(1):63 – 75, 2002.

[12] J. Chen and R. Patton. *Robust model-based fault diagnosis for dynamic systems*. Kluwer Academic Publishers, Norwell, MA, USA, 1999.

[13] J.-H. Cho, J.-M. Lee, S. Choi, D. Lee, and I.-B. Lee. Fault identification for process monitoring using kernel principal component analysis. *Chemical Engineering Science*, 60(1):279 – 288, 2005.

[14] S. Choi and I.-B. Lee. Nonlinear dynamic process monitoring based on dynamic kernel pca. *Chemical Engineering Science*, 59(24):5897 – 5908, 2004.

[15] E. Chow and A. Willsky. Analytical redundancy and the design of robust failure detection systems. *IEEE Transactions on Automatic Control*, 29:603–614, 1984.

[16] R. DeGroat. Noniterative subspace tracking. *IEEE Transactions on Signal Processing*, 40(3):571–577, 1992.

[17] G. Delmaire, J.-P. Cassar., and M. Staroswiecki. Identification and parity space techniques for failure detection in siso systems including modelling errors. In *Decision and Control, 1994., Proceedings of the 33rd IEEE Conference on*, volume 3, pages 2279–2285, 14-16 1994.

[18] S. X. Ding. *Model Based Fault Diagnosis Technique*. Springer Verlag, Berlin, 2007.

[19] S. X. Ding, P. Zhang, B. Huang, and E. L. Ding. Subspace method aided data-driven design of observer based fault detection systems. In *Proc. 16th IFAC World Congress*, Prague, Czech Republic, 2005.

[20] S. X. Ding, P. Zhang, A. S. Naik, E. L. Ding, and B. Huang. Subspace method aided data-driven design of fault detection and isolation systems. *Journal of process control*, 19:1496–1510, 2009.

[21] J. Dong and M. Vehaegen. Subspace based fault detection and identification for lti systems. In *Preprints of the 7th IFAC Symposium on Fault detection, Supervision and Safety of Technical Processes*, 2009.

[22] X. Doukopoulos. *Power techniques for blind channel estimation in wireless communication systems*. PhD dissertation, IRISA-INRIA, University Rennes, Rennes, France, 2004.

[23] X. Doukopoulos and G. Moustakides. Blind adaptive channel estimation in ofdm systems. *Wireless Communications, IEEE Transactions on*, 5(7):1716 –1725, 2006.

[24] X. Doukopoulos and G. Moustakides. Fast and stable subspace tracking. *IEEE Transactions on Signal Processing*, 56:1452–1465, 2008.

[25] J. Downs and E. Fogel. A plant-wide industrial process control problem. *Computers and Chemical Engineering*, 17:245–255, 1993.

[26] R. Dunia. Joint diagnosis of process and sensor faults using principal component analysis. *Control Engineering Practice*, 6(3).

[27] R. Dunia and S. J. Qin. Subspace approach to multidimensional fault identification and reconstruction. *AIChE Journal*, 44(8):1813 – 1831, 1996.

[28] R. Dunia, S. J. Qin, T. Edgar, and T. McAvoy. Identification of faulty sensors using principal component analysis. *AIChE Journal*, 42(10): 2797 – 2812, 1996.

[29] L. Elshenawy, S. Yin, A. S. Naik, and S. X. Ding. Efficient recursive principal component analysis algorithms for process monitoring. *Industrial and Engineering Chemistry Research*, 49(1):252–259, 2010.

[30] A. Emami-Naeini, M.M. Akhter, and S.M. Rock. Effect of model uncertainty on failure detection: the threshold selector. *Automatic Control, IEEE Transactions on*, 33(12):1106 –1115, 1988.

[31] W. Favoreel, B.D Moor, P. Overschee, and M. Gevers. Model-free subspace-based lqg-design. In *American Control Conference, 1999. Proceedings of the 1999*, volume 5, pages 3372–3376, 1999.

[32] W. Favoreel, B.D. Moor, and P. Overschee. Subspace state space system identification for industrial processes. *Journal of Process Control*, 10(2-3):149 – 155, 2000.

[33] F. Felici, J.-W. Wingerden, and M. Verhaegen. Subspace identification of mimo lpv systems using a periodic scheduling sequence. *Automatica*, 43(10):1684 – 1697, 2007.

[34] F. Flehmig and W. Marquardt. Detection of multivariable trends in measured process quantities. *Journal of Process Control*, 16(9):947 – 957, 2006.

[35] P. Frank. Fault diagnosis in dynamic systems using analytical and knowledge-based redundancy: A survey and some new results. *Automatica*, 26(3):459 – 474, 1990.

[36] P. Frank, S. X. Ding, and T. Marcu. Model-based fault diagnosis in technical processes. *Transactions of the Institute of Measurement and Control*, 22(1):57–101, 2000.

[37] P. M. Frank and X. Ding. Survey of robust residual generation and evaluation methods in observer-based fault detection systems. *Journal of Process Control*, 7(6):403 – 424, 1997.

[38] Z. Ge and Z. Song. Process monitoring based on independent component analysis-principal component analysis (ica-pca) and similarity factors. *Industrial and Engineering Chemistry Research*, 46(7):2054–2063, 2007.

[39] P. Geladi and B. Kowalski. An example of 2-block predictive partial least-squares regression with simulated data. *Analytica Chimica Acta*, 185:19 – 32, 1986.

[40] J. Gertler, editor. *Fault Detection and Diagnosis in Engineering Systems*. Marcel Dekker Inc., 1998.

[41] J. Gertler and Q. Luo. Robust isolable models for failure diagnosis. *AIChE Journal*, 35(11):1856 – 1868, 1989.

[42] J. Gertler and R. Monajemy. Generating directional residuals with dynamic parity relations. *Automatica*, 31(4):627 – 635, 1995.

[43] J. Gertler and D. Singer. A new structural framework for parity equation-based failure detection and isolation. *Automatica*, 26(2):381 – 388, 1990.

[44] G. Golub and C. Van Loan. *Matrix Computations (Johns Hopkins Studies in Mathematical Sciences)*. The Johns Hopkins University Press, 1996.

[45] T. Gustaffson and C. MacInnes. A class of subspace tracking algorithm based on approximation of noise subspace. *IEEE Transaction on Signal Processing*, 48:3231–3235, 2000.

[46] H. Hao. *Study on independent component analysis based process monitoring*. Master Thesis, University of Duisburg-Essen, 2010.

[47] D. Himmelblau. *Fault detection and diagnosis in chemical and petro-chemical processes.* Elsevier Scientific Pub. Co., New York, 1978.

[48] A. Hoeskuldsson. Pls regression methods. *Journal of Chemometrics*, 2 (3):211 – 228, 1988.

[49] H. Hotelling. Relations between two sets of variables. *Biometrika*, 26: 321–377, 1936.

[50] B. Huang, S. X. Ding, and S. J. Qin. Closed-loop subspace identification: an orthogonal projection approach. *Journal of process control*, 15:53–66, 2005.

[51] R. Isermann. *Identifikation dynamischer Systeme.* Springer Verlag, 1992.

[52] R. Isermann. Fault diagnosis of machines via parameter estimation and knowledge processing: tutorial paper. *Automatica*, 29(4):815–835, 1993. ISSN 0005-1098.

[53] R. Isermann. Supervision, fault-detection and fault-diagnosis methods - an introduction. *Control Engineering Practice*, 5(5):639–652, 1997.

[54] R. Isermann, editor. *Fault diagnosis systems.* Springer Verlag, 2006.

[55] J. Jackson and G. Mudholkar. Control procedures for residuals associated with principal component analysis. *Technometrics*, 21(3):341–349, 1979.

[56] S.-L. Jamsa-Jounela. Future trends in process automation. *Annual Reviews in Control*, 31(2):211 – 220, 2007.

[57] S.-L. Jamsa-Jounela, M. Vermasvuori, P. Enden, and S. Haavisto. A process monitoring system based on the kohonen self-organizing maps. *Control Engineering Practice*, 11(1):83 – 92, 2003.

[58] M. Jia, F. Chu, F. Wang, and W. Wang. On-line batch process monitoring using batch dynamic kernel principal component analysis. *Chemometrics and Intelligent Laboratory Systems*, 101(2):110 – 122, 2010.

[59] H. Jones. *Failure detection in linear systems.* PhD dissertation, MIT, U.S.A., 1973.

[60] B. Juricek, D. Seborg, and W. Larimore. Identification of the tennessee eastman challenge process with subspace methods. *Control Engineering Practice*, 9:1337–1351, 2001.

[61] K. Kameyama and A. Ohsumi. Subspace-based prediction of linear time-varying stochastic systems. *Automatica*, 43(12):2009 – 2021, 2007.

[62] M. Kano, K. Nagao, S. Hasebe, I. Hashimoto, H. Ohno, R. Strauss, and B. Bakshi. Comparison of multivariate statistical process monitoring methods with applications to the eastman challenge problem. *Computers and Chemical Engineering*, 26(2):161 – 174, 2002.

[63] B. Koeppen-Seliger. *Fehlerdiagnose mit kuenstlichen neuronalen Netzen.* PhD dissertation, VDI Verlag, Duesseldorf, Germany, 1997.

[64] T. Komulainen, M. Sourander, and J. Sirkka-Liisa. An online application of dynamic pls to a dearomatization process. *Computers and Chemical Engineering*, 28(12):2611 – 2619, 2004.

[65] T. Kourti and J. MacGregor. Process analysis, monitoring and diagnosis, using multivariate projection methods. *Chemometrics and Intelligent Laboratory Systems*, 28:3, 1995.

[66] W. Ku, R. Storer, and C. Georgakis. Disturbance detection and isolation by dynamic principal component analysis. *Chemometrics and intelligent laboratory systems*, 30:179–196, 1995.

[67] W. Larimore. Statistical optimality and canonical variate analysis system identification. *Signal Processing*, 52(2):131 – 144, 1996.

[68] C. Lee, S. Choi, and I.-B. Lee. Sensor fault identification based on time-lagged pca in dynamic processes. *Chemometrics and Intelligent Laboratory Systems*, 70(2):165 – 178, 2004.

[69] J.-M. Lee, C. Yoo, and I.-B. Lee. Statistical process monitoring with independent component analysis. *Journal of Process Control*, 14(5): 467 – 485, 2004.

[70] H. Li, Y. Liang, and Q. Xu. Support vector machines and its applications in chemistry. *Chemometrics and Intelligent Laboratory Systems*, 95(2):188 – 198, 2009.

[71] W. Li. *Observer-based fault detection of technical systems over networks.* PhD dissertation, VDI Verlag, Duesseldorf, Germany, 2009.

[72] W. Li and S. J. Qin. Consistent dynamic pca based on errors-invariables subspace identification. *Journal of Process Control*, 11(6): 661 – 678, 2001.

[73] W. Li, H. Yue, S. Valle-Cervantes, and S. J. Qin. Recursive pca for adaptive process monitoring. *Journal of Process Control*, 10(5):471–486, 2000.

[74] K. Liu. Identification of linear time-varying systems. *Journal of Sound and Vibration*, 206(4):487 – 505, 1997.

[75] L. Ljung. *System identification: Theory for the user*. Prentice Hall, Englewood Cliffs, New Jersey, 1987.

[76] X.C. Lou, A. Willsky, and G. Verghese. Optimally robust redundancy relations for failure detection in uncertain systems. *Automatica*, 22(3): 333 – 344, 1986.

[77] M. Lovera, T. Gustaffson, and M. Verhaegen. Recursive subspace identification of linear and non-linear wiener state-space models. *Automatica*, 36:1639–1650, 2000.

[78] P. Lyman and C. Georgakis. Plant-wide control of the tennessee eastman problem. *Computers and Chemical Engineering*, 19:321–331, 1995.

[79] J. MacGregor. Statistical process control of multivariate processes. In *In Proc. of IFAC International symposium on Advanced Control of Chemical Processes, New York*, 1994.

[80] R. Manne. Analysis of two partial-least-squares algorithms for multivariate calibration. *Chemometrics and Intelligent Laboratory Systems*, 2(1-3):187 – 197, 1987.

[81] G. Mercere, S. Lecoeuche, and M. Lovera. Recursive subspace identification based on instrument variable unconstrained quadratic optimization. *International Journal of Adaptive control and Signal Processing*, 18:771–797, 2006.

[82] G. Mercere, L. Bako, and S. Lecoeuche. Propagator-based methods for recursive subspace model identification. *Signal Processing*, 88(3):468 – 491, 2008.

[83] A. S. Naik. *Direct identification of model-based fault detection systems in a dearomatization process*. Master Thesis, University of Duisburg-Essen, 2007.

[84] A. S. Naik, S. X. Ding, and S. Yin. Recursive algorithm for parity space based fault detection systems. In *Proceedings of 7th IFAC Symposium*

on Fault Detection and Supervision and Safety of Technical Processes, 2009.

[85] A. S. Naik, S. Yin, S. X. Ding, and P. Zhang. Recursive identification algorithms to design fault detection systems. *Journal of Process Control*, 20:957–965, 2010.

[86] A. Negiz. Statistical monitoring of multivariable dynamic processes with state-space models. *AIChE Journal*, 43(8).

[87] I. Nimmo. Adequately address abnormal situation operations. *Chemical Engineering Progress*, 91(1):1361 – 1375, 1995.

[88] P. Van Overschee and B. De Moor. *Subspace Identification for Linear Systems*. Kluwer Academic Press, Dordrecht, 1996.

[89] E. Page. Control charts for the mean of normal population. *Journal of Royal Statistical Society*, 1954.

[90] R. Patton, P. Frank, and R. Clarke, editors. *Fault diagnosis in dynamic systems: theory and application*. Prentice-Hall, Inc., Upper Saddle River, NJ, USA, 1989.

[91] R. Pearson. Data cleaning for dynamic modeling and control. In *In Proc. of IFAC European Control Conference, Karlsruhe, Germany*, 1999.

[92] K. Peternell, W. Scherrer, and M. Deistler. Statistical analysis of novel subspace identification methods. *Signal Process*, 52(2):161–177, 1996.

[93] S. J. Qin. Statistical process monitoring: Basics and beyond. *Journal of Chemometrics*, 17:480–502, 2003.

[94] S. J. Qin and W. Li. Detection and identification of faulty sensors in dynamic processes. *AIChE Journal*, 47(7):1581 – 1593, 2001.

[95] A. Raich and A. Cinar. Statistical process monitoring and disturbance diagnosis in multivariable continuous processes. *AIChE Journal*, 42(4): 995 – 1009, 1996.

[96] F. Rellich. *Perturbation theory of Eigenvalue problems*. Gordon and Breach, New York, USA, 1969.

[97] E. Russell, L. Chiang, and R. Braatz. *Data-Driven Techniques for Fault Detection and Diagnosis in Chemical Processes*. Springer-Verlag, London, 2000.

[98] W. Shewhart. *Statistical method from the viewpoint of quality control.* Dover publications, 1939.

[99] G. Stewart and J. Sun. *Matrix perturbation theory.* CA: Academic, San Diego, 1990.

[100] N. Thornhill, S. Patwardhan, and S. Shah. A continuous stirred tank reactor simulation model with applications. *Journal of process control,* 18:347–360, 2008.

[101] R. Treasure, U. Kruger, and J. Cooper. Dynamic multivariate statistical process control using subspace identification. *Journal of Process Control,* 14(3):279 – 292, 2004.

[102] S. Valle, W. Li, and S. J. Qin. Selection of the number of principal components: The variance of the reconstruction error criterion with a comparison to other methods. *Industrial and Engineering Chemistry Research,* 38(11):4389–4401, 1999.

[103] V. Venkatasubramanian, R. Rengaswamy, K. Yin, and S.N. Kavuri. Review of process fault detection and diagnosis part i: Quantitative model-based methods. *Computers and Chemical Engineering,* 27:293–311, 2003.

[104] V. Venkatasubramanian, R. Rengaswamy, K. Yin, and S.N. Kavuri. Review of process fault detection and diagnosis part ii: Qualitative models and search engines. *Computers and Chemical Engineering,* 27: 313–326, 2003.

[105] V. Venkatasubramanian, R. Rengaswamy, K. Yin, and S.N. Kavuri. Review of process fault detection and diagnosis part ii: Process history based methods. *Computers and Chemical Engineering,* 27:327–346, 2003.

[106] M. Verhaegen and X. Yu. A class of subspace model identification algorithms to identify periodically and arbitrarily time-varying systems. *Automatica,* 31(2):201–216, 1995.

[107] M. Viberg, B. Ottersten, B. Wahlberg, and L. Ljung. A statistical perspective on state-space modeling using subspace methods. In *Decision and Control, 1991., Proceedings of the 30th IEEE Conference on,* volume 2, 11-13 1991.

[108] M. Viberg, B. Wahlberg, and B. Ottersten. Analysis of state space system identification methods based on instrumental variables and subspace fitting. *Automatica*, 33(9):1603–1616, 1997.

[109] J. Wang and S. J. Qin. A new subspace identification approach based on principal component analysis. *Journal of process control*, 12:841–855, 2002.

[110] J. Wang and S. J. Qin. Closed-loop subspace identification using the parity space. *Automatica*, 42:315–320, 2006.

[111] T. Wang, X. Wang, Y. Zhang, and H. Zhou. Fault detection of nonlinear dynamic processes using dynamic kernel principal component analysis. In *Intelligent Control and Automation, 2008. WCICA 2008. 7th World Congress on*, pages 3009 –3014, 25-27 2008.

[112] T. Willink. Efficient adaptive svd algorithm for mimo applications. *Signal Processing, IEEE Transactions on*, 56(2):615 –622, 2008.

[113] J. Wuennenberg. *Observer-based fault detection in dynamic systems.* PhD dissertation by VDI Verlag, Duesseldorf, 1990.

[114] B. Yang. Projection approximation subspace tracking. *IEEE Transactions on Signal Processing*, 43:95–107, 1995.

[115] J.-F. Yang and M. Kaveh. Adaptive eigensubspace algorithms for direction or frequency estimation and tracking. *Acoustics, Speech and Signal Processing, IEEE Transactions on*, 36(2):241 –251, 1988.

[116] S. Yin, A. S. Naik, and S. X. Ding. Adaptive process monitoring based on parity space method. In *Proceedings of 7th IFAC Symposium on Fault Detection and Supervision and Safety of Technical Processes*, 2009.

[117] S. Yoon and J. MacGregor. Statistical and causal model-based approaches to fault detection and isolation. *AIChE Journal*, 46(9):1813 – 1824, 2000.